Director

FSUF MRTI RAS

V.V.Vetrov

ISTC #2429p

Date: 2005

Final Technical Report on Project ISTC #2429p (017024)

The study of possibility of the ignition of a combustible gas mix by the undercritical MW streamer gas discharge

(01 August, 2002 – 31 July, 2005)

Project Manager Igor Ivanovich Esakov

Federal State Unitary Firm
"Moscow Radio-Technical Institute RAS"
(FSUF "MRTI RAS")

Moscow

This work was supported financially by European Office of Aerospace Research and Development (EOARD) and performed under the contract with the International Science and Technology Center (ISTC)

REPORT DOCUMENTATION PAGE

Form Approved OMB No. 0704-0188

1. REPORT DATE *(DD-MM-YYYY)*	2. REPORT TYPE	3. DATES COVERED *(From – To)*
10-08-2005	Final Report	01-Aug-02 - 25-Oct-05

4. TITLE AND SUBTITLE

The Study Of Possibility Of The Ignition Of A Combustible Gas Mix By The Undercritical Microwave Streamer Gas Discharge

5a. CONTRACT NUMBER
ISTC Registration No: 2429

5b. GRANT NUMBER

5c. PROGRAM ELEMENT NUMBER

6. AUTHOR(S)

Dr. Igor Esakov

5d. PROJECT NUMBER

5d. TASK NUMBER

5e. WORK UNIT NUMBER

7. PERFORMING ORGANIZATION NAME(S) AND ADDRESS(ES)

Federal State Unitary Firm Moscow Radio-Technical Institute RAS (FSUF MRTI RAS)
Warshavskoe Shosse 132
Moscow 117519
Russia

8. PERFORMING ORGANIZATION REPORT NUMBER

N/A

9. SPONSORING/MONITORING AGENCY NAME(S) AND ADDRESS(ES)

EOARD
PSC 821 BOX 14
FPO 09421-0014

10. SPONSOR/MONITOR'S ACRONYM(S)

11. SPONSOR/MONITOR'S REPORT NUMBER(S)
ISTC 01-7024

12. DISTRIBUTION/AVAILABILITY STATEMENT

Approved for public release; distribution is unlimited.

13. SUPPLEMENTARY NOTES

14. ABSTRACT

This report results from a contract tasking Federal State Unitary Firm Moscow Radio-Technical Institute RAS (FSUF MRTI RAS) as follows: The physics of the initiated undercritical streamer microwave discharge can be used for creation of the principally new system of ignition of the fuel-mixture. It represents the system of the spark filaments-that is streamers, that uniformly fill the volume of a microwave radiation beam. The velocity of the discharge front propagation becomes more than 1 km/s. The temperature inside the streamer channels reaches several thousands of Kelvin. These properties of the streamer discharge guarantee quick ignition of the fuel-mixture over the whole cross-section of the discharge even at high flow velocities.
Experimental and theoretical investigations will be carried out in the frame of the project and will allow acquisition of data about parameters of microwave radiation needed for ignition of the model fuel mix by example of butane-propane mixture and data about application of microwave discharge for mixing of fuel and air at speedy flow and catalysis of the combustion. Demonstration of the ignition of the butane-propane mixture in a speedy flow will be made.

15. SUBJECT TERMS
EOARD, Physics, Plasma Physics and Magnetohydrodynamics

16. SECURITY CLASSIFICATION OF:			17. LIMITATION OF ABSTRACT	18, NUMBER OF PAGES	19a. NAME OF RESPONSIBLE PERSON
a. REPORT	b. ABSTRACT	c. THIS PAGE			SURYA SURAMPUDI
UNCLAS	UNCLAS	UNCLAS	UL	64	19b. TELEPHONE NUMBER *(Include area code)* +44 (0)20 7514 4299

List of main authors

Kirill V. Khodataev, scientific Head of Project
Igor I.Esakov, Project Manager
Lev P. Grachev, Chief Experimenter

Content

1. Introduction

This work was executed during the period from August to July 2005. It is the final stage of works in frames of three year ISTC Project #2429p, Ref.[1,2] and ISTC project #1840p, Ref.[3]. These works are devoted to investigation of a possibility of flammable propane –air mixture ignition in high-speed supersonic (SS) airflow with a help of electrical deeply undercritical microwave (MW) discharge initiated by linear electrical vibrator. The fuel in main experiments is delivered to the discharge area through the internal vibrator's region.

Following experimental and theoretical works were to be executed in correspondence with Technical task:

- Experimental determination of maximum diameter and of corresponding length of MW vibrator, at which burning of MW discharge in the vibrator base part is still insured in SS airflow.
- Investigation of multiple MW discharge initiation possibility over vibrator's perimeter in its base.
- Experimental development of propane injection to the stagnant airflow and its mixing with air in required proportion.
- Investigation of head vibrator area form insuring airflow stagnation in internal vibrator's channel.
- Measurements of stagnation pressure and temperature distributions $\mathbf{p_{stag}}$ and $\mathbf{T_{stag}}$ in the trail of the vibrator initiating MW discharge in different conditions:
  - at presence of SS flow only;
  - at presence of SS and MW discharge;
  - at presence of SS, MW discharge and clean air injection to the discharge;
  - at presence of SS, MW discharge and propane –air mixture combustion in the discharge area.
- Processing of measurement data for determining of MW beam electrical energy putted to the discharge and of flammable mixture combustion efficiency.
- Modeling of deeply undercritical MW discharge attached to the initiator in SS flow at injection of flammable mixture into its area and varying of the mixture characteristics, determination of MW energy discharge absorption efficiency and of longitudinal distribution of this energy, determination of combustion influence on flow.

In the next section we will demonstrate logical connection of reported stage works with investigations made during previous stages. In Conclusions we will shortly enumerate main results of present investigations and possible their continuation.

2. Previous stage results and this stage investigation target

Quasi - optical gaseous electrical discharge in quasi - optical beam of EM waves of centimeter range is investigated and possibility of flammable gaseous mixture ignition in high-speed air flow including SS velocity is investigated in frames of presented works.

Principle scheme of this MW discharge realization is represented in Fig.2.1.

In Fig.2.1 one can see that EM wave of $\lambda \approx 1 \div 10$ cm length through the waveguide comes to elements forming its quasi- optical beam. The beam usually has TEM field structure. Electrical discharge is ignited in this beam.

The discharge in motionless air is realized in different forms with respect to air pressure p and value of electrical component E of EM field as it is conditionally shown in Fig.2.2.

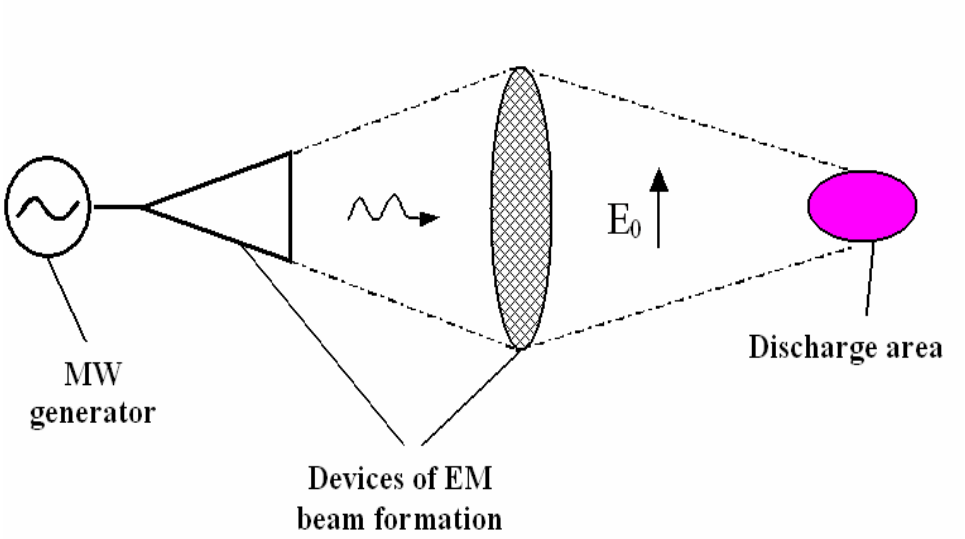

Fig.2.1 Principle scheme of electrical gaseous discharge in quasi-optical beam of EM centimeter range waves realization

Fig.2.2 corresponds to linearly polarized EM field with λ = 8.9 cm and EM pulse duration τ_{pul} = 40 μs. **E** field vector is vertical in photos and radiation propagates from left to the right. One can see In Fig.2.2. that the discharge has diffuse for at low pressure **p** to the left from the curve **I**, and the streamer form to the right from it. Self consistent air electrical breakdown is possible above the line **II**, which is conditional Paschen curve in MW EM field range, here **E** is larger than the minimum breakdown critical field $\mathbf{E_{cr}}$.

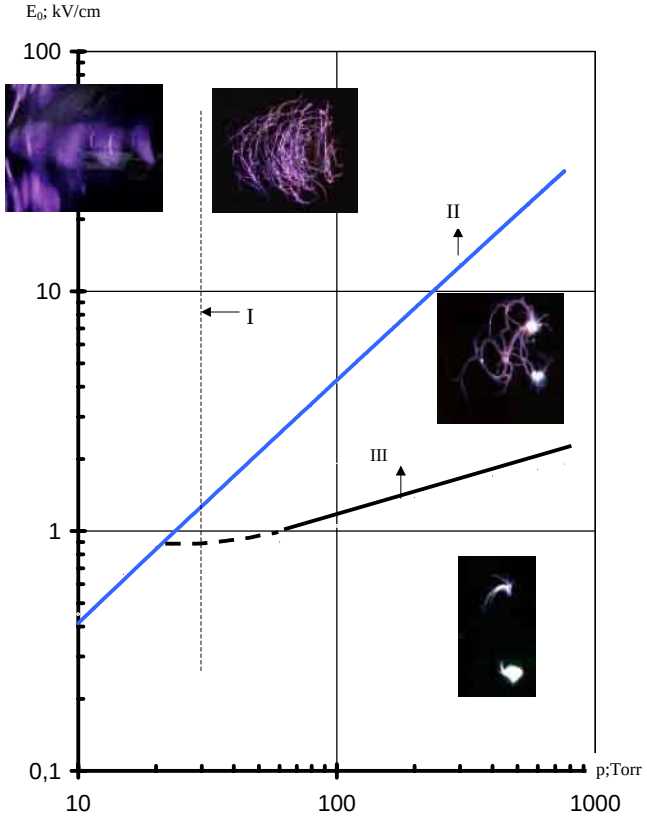

Fig.2.2. Existence regions of different forms of MW discharges

Air breakdown has to be initiated by some way below it. Linear cylindrical metallic MW vibrator is used for this purpose in our experiments, its length is $2L \approx (\lambda/2)$. In so doing increased inductive electrical field near its ends can be larger than $\mathbf{E_{cr}}$. Plasma streamer channels of undercritical initiated discharge are capable to go out of the increase field area near vibrators ends to EM beam area with $E < E_{cr}$ in some definite range of **E** – above the line **III** in Fig.2.2. MW deeply undercritical discharge stays localized only in the area of the increased field with $\mathbf{E > E_{cr}}$ near the ends of initiating vibrator during the time of EM radiation coming to it at fields smaller than of the line **III**.

In present investigations we study the possibility of flammable gaseous mixture ignition by deeply undercritical streamer MW discharge attached to the initiator, i.e. by the discharge, which is situated in E-p diagram, see Fig.2.2, below the line **III.** Field level necessary for its burning allows to realize this discharge not only in pulse mode but in continuous burning mode as well.

The final goal of works was investigation of ignition possibility of propane-air flammable mixture in SS airflow and insuring of its effective burning out with a help of this discharge.

At the same time in the beginning of works the possibility of fuel ignition realization with a help of this discharge was unclear, so works had several stages. Firstly we realized ignition of model propane-air flammable mixture at very low value of its velocity $\mathbf{v_{fl}}$ of several m/s. Then we realized its ignition in the high-speed air stream at flammable mixture delivery to discharge area through initiator internal region. At that keeping succession we varied $\mathbf{v_{fl}}$ from small velocities of several tens of cm/s to SS values up to $v_{fl} = 500$ cm/s, corresponding to Mach number M = 2. Finally at M = 2 we measured amount of energy putted to discharge area by EM beam exciting the discharge, and efficiency of burning out of flammable mixture injected to this area.

Fig.2.3 illustrates the ignition of propane-air flammable mixture at its velocity of several m/s. The given experiment was undertaken with application of the pulse MW discharge with $\lambda = 8.9$ cm, $\tau_{pul} = 40$ μs, in air of atmospheric pressure p = 760 Torr. Field vector is vertical in photos represented in Fig.2.3. Left photo represents appearance of MW deeply undercritical discharge attached to initiator in motionless air. Right photo shows that this discharge realized ignition of flammable mixture stream coming to it from below from the quartz tube.

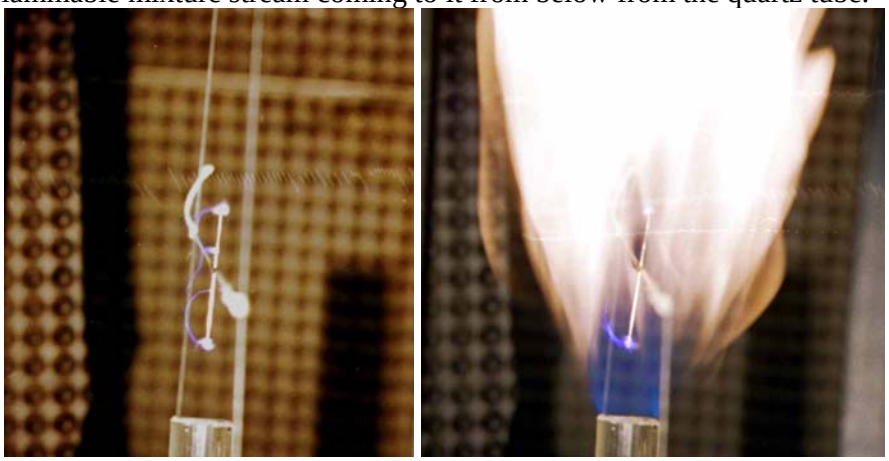

Fig.2.3 Photos of deeply undercritical MW discharge attached to initiator in motionless air (to the left) and in flammable mixture stream (to the right)

It stayed unclear if this discharge could realize ignition of flammable mixture ignition in the high – speed flow. Discharge properties could be considerably changed in this flow. For example, in Fig.2.4 one can see change of deeply undercritical discharge appearance in SS flow. Left photo in it shows the appearance of deeply undercritical pulse MW discharge initiated by the vibrator in motionless air at p = 100 Torr in the field with $\lambda = 8.9$ cm and $\tau_{pul} = 40$ μs. Right photo shows its appearance in SS flow now. The flow is directed down-up along the initiating vibrator and has $v_{fl} = 500$ m/s.

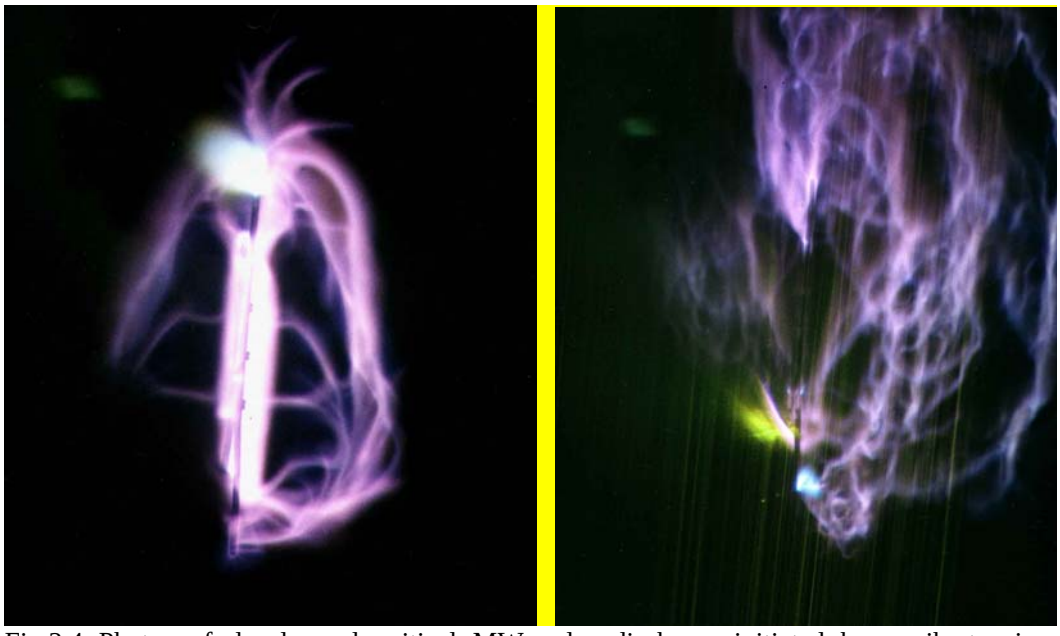

Fig.2.4 Photos of deeply undercritical MW pulse discharge initiated by a vibrator in motionless air at p = 100 Torr (to the left) and in SS stream (to the right). λ = 8.9 cm, τpul = 40 s

MW discharge and air stream mixed with propane were used in the next experiments. Experiments started from known situation, i.e. increase of $\mathbf{v_{fl}}$ to SS started from very small values of $\mathbf{v_{fl}}$, at which experimentally was already demonstrated the possibility of propane-air mixture ignition with a help of this discharge. In Fig.2.5 one can see a set of photos illustrating propane-air mixture combustion, when the mixture is ignited by MW deeply undercritical discharge at different velocities vfl of air stream blowing around the vibrator initiating the discharge. This experiment was undertaken with MW discharge at λ = 12.5 cm in quasi-optical mode of its combustion with τ_{dis} = 0.4 s. The stream in photos has vfl velocity collinear to vibrator axis and directed from left to the right. **E** vector of linearly polarized EM beam is also parallel to the vibrator axis. MW radiation in photos comes from above to the vibrator. Propane in these experiments was injected directly to the discharge area coming out from a hole in the vibrator base end. One can see in photos that there is burning propane tail area in the vibrator trail in the stream blowing around the vibrator. Its length decreases with increase of $\mathbf{v_{fl}}$. From the photos it is unclear if propane-air mixture combustion is realized at $\mathbf{v_{fl}}$ = 200-500 m/s.

The fact of propane combustion at supersonic $\mathbf{v_{fl}}$ was detected by measurements of stagnation pressure and temperature – $\mathbf{p_{stag}}$ and $\mathbf{T_{stag}}$ in the vibrator trail. Typical corresponding waveforms from Pitot pipe and thermocouple are represented in Fig.2.6a and Fig.2.6b, respectively. Initial vertical rise of the oscilloscope beam in Fig.2.6a corresponds to the moment of switching on of SS flow, and its final drop corresponds to the flow shut down. Signal drop on the upper part of the upper waveform in its center characterizes decrease of $\mathbf{p_{stag}}$ during burning of only MW in SS flow. It is connected only with air heating in the discharge; this is illustrated by the lower waveform in Fig.2.6b. Additional decrease of $\mathbf{p_{stag}}$ in the lower waveform in Fig.2.6a takes place at propane injection to the discharge. It is connected not only with heating air by the discharge but with propane combustion as well; this is illustrated by the upper waveform in Fig.2.6b. We have to note that this method of propane combustion detection in SS flow by measurements of $\mathbf{p_{stag}}$ and $\mathbf{T_{stag}}$ in the trail is maybe the only convincing direct quantitative means.

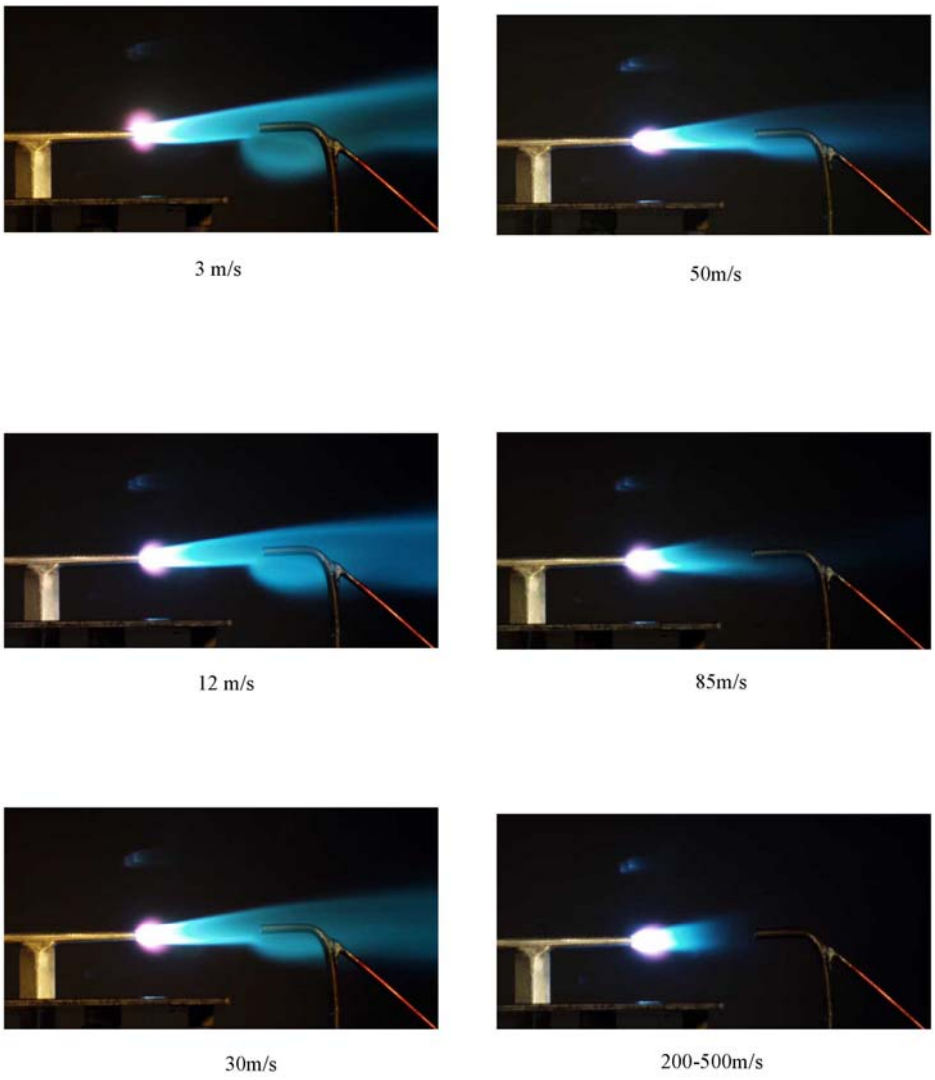

Fig.2.5 Photos illustrating propane-air mixture combustion ignited by deeply undercritical MW discharge at different velocities vfl of air stream blowing a vibrator initiating a discharge

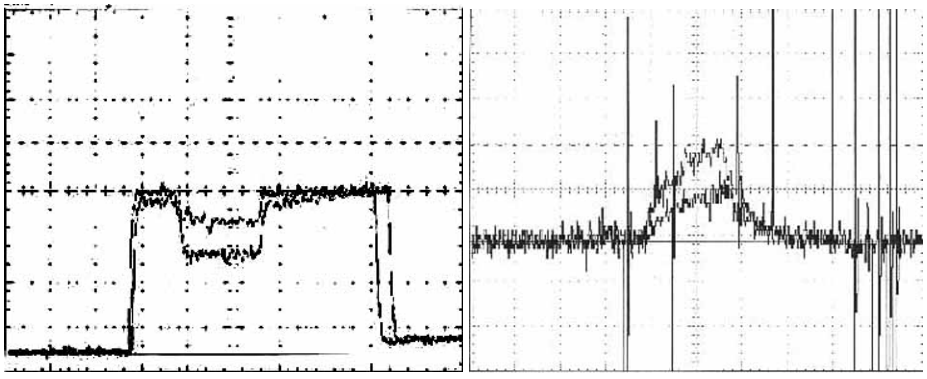

a) b)

Fig.2.6.Waveforms of flow stagnation pressure p_{stag} (a) and stagnation temperature T_{stag} (b) in a vibrator trail at burning of only discharge in SS stream and at discharge burning and propane combustion injected to the trail

For example in Fig.2.6a and Fig.2.6b are represented typical distributions of $\mathbf{T_{stag}}$ in the vibrator trail in the plane perpendicular to SS flow. Fig.2.7a corresponds to burning of only the discharge in SS flow, and Fig.2.7b corresponds to burning of the discharge and combustion of propane injected to its area. They were obtained with a help of EM beam power of P_{gen} = 1.5 kW and rate of propane injection $m = 8.6 \cdot 10^{-3}$ g/s. Combustion power of $P_{com\ max}$ = 400 W corresponds to this rate of injection in the case of propane complete burning out.

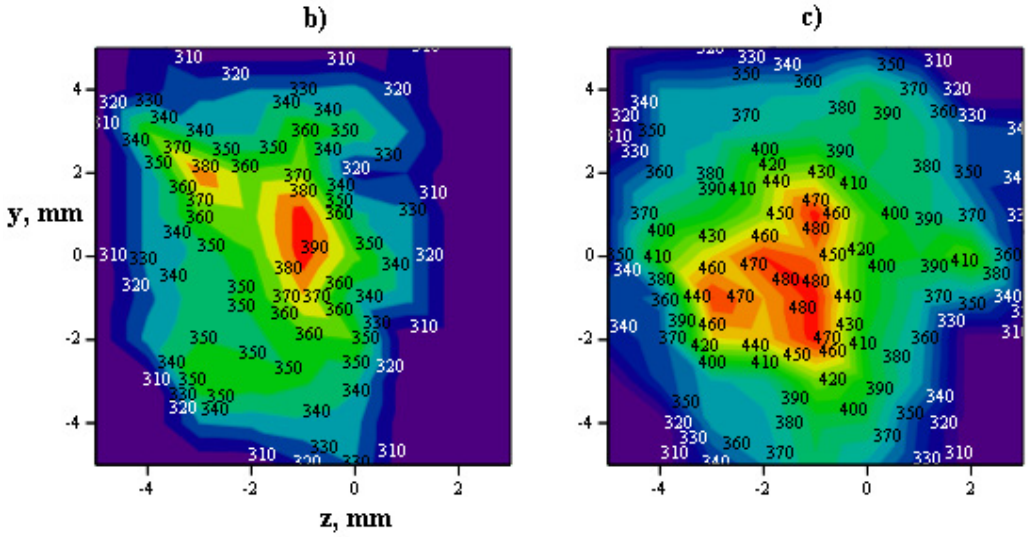

Fig.2.7. Typical distributions of Tstag in vibrator trail in a plane perpendicular to SS stream

The corresponding processing of experimentally obtained distributions of $\mathbf{p_{stag}}$ and $\mathbf{T_{stag}}$ showed, that $P_{MW} \approx 160$ W is putted by MW beam energy to air heating in the discharge. It is about 10 % of the generator power $\mathbf{P_{gen}}$. Energy additionally putted to the flow heating due to propane burning out corresponds to the power of $P_{com} \approx 280$ W. This shows that about 70 % of propane burn out in the discharge in this experimental formulation. We emphasize once again that applied experimental method is maybe the only direct measuring method of energy efficiency of EM beam energy putting to the area of MW gaseous electrical discharge, and of burning out of the fuel ignited by it.

However the experiment in this experimental formulation showed that $\mathbf{P_{com}}$ practically did not change at propane injection rate increase for about an order of magnitude. It means that amount of the burnt out propane was constant, and hence, efficiency of its burning drops down. Uncontrolled processes of propane-air mixing, flammable mixture ignition and combustion take place in this experimental formulation in the base area of the vibrator ionizing the discharge, in the area of MW discharge burning.

The goal of executed works during this stage was development of the scheme, which in principle could allow to burn out preliminary given propane amount in SS airflow with the application of deeply undercritical MW discharge initiated by the vibrator excited by quasi-optical EM beam. At that we suppose to spatially separate the process of propane-air mixing in internal vibrator area, its ignition and combustion already in its base area. Air at that has to come to the mixing area directly from the SS flow coming on the vibrator. The illustrating scheme of this experimental formulation is represented in Fig.2.8.

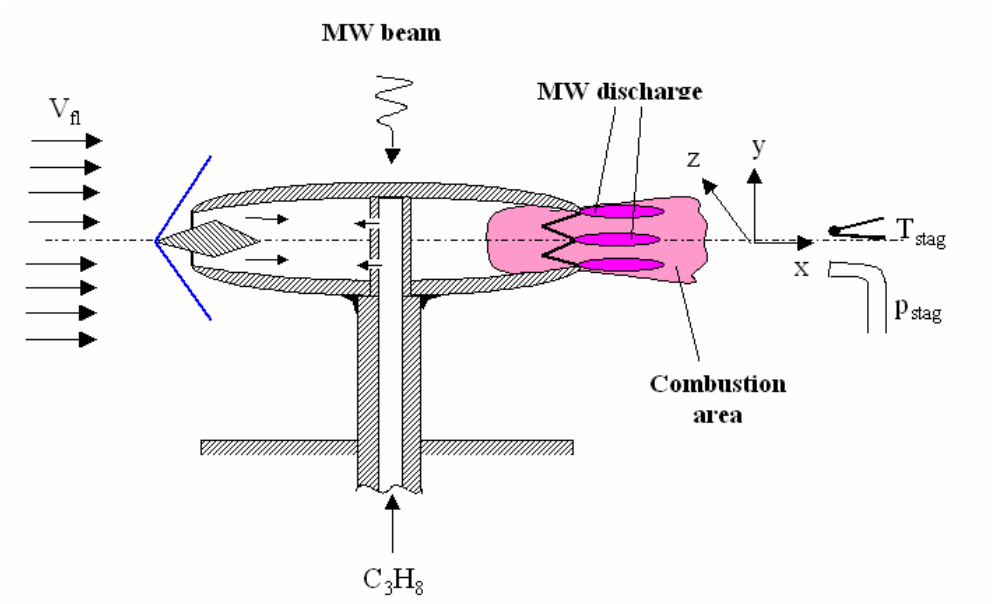

Fig.2.8 Scheme of experimental formulation.

3. Experimental setup

Experimental setup was in details described in previous Reports on this Project. In the present report we will represent only main its parameters. Scheme of the setup is represented in Fig.3.1, its appearance is represented in Fig..3.2, and in Fig.3.3 one can see a photo of its working area in one of definite experiments. The setup includes the vacuum part; the aerodynamic part forming SS flow; MW part forming EM beam; elements of discharge initiation; propane injection line, and measuring equipment.

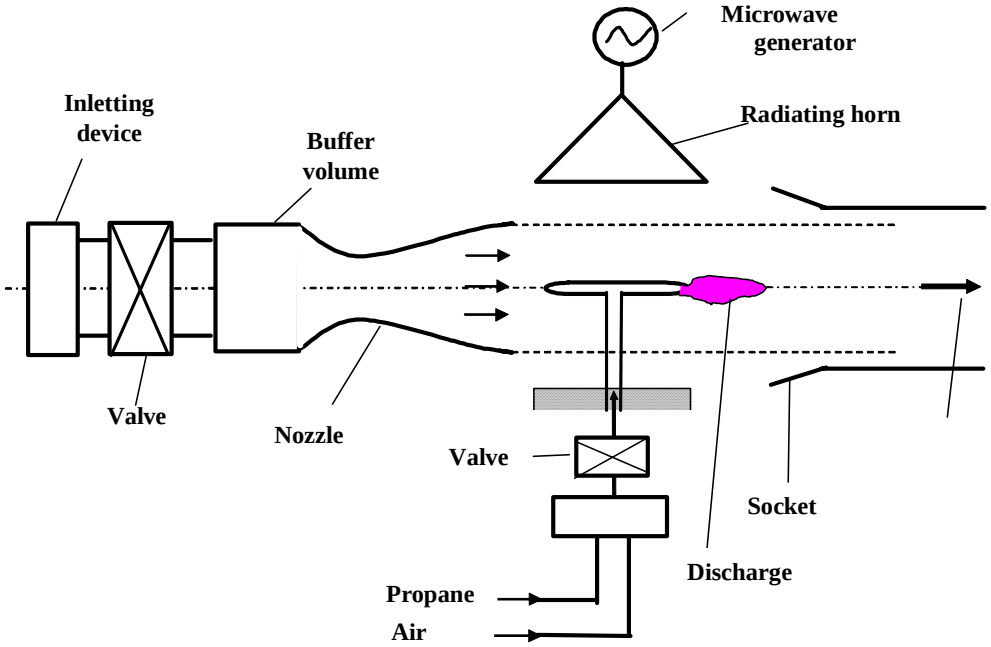

Fig.3.1 Scheme of experimental setup .

3.1. Gas-dynamic part of the setup

Vacuum part of the setup consists of the working chamber and large hermetic tank connected with it. The working chamber is a cylinder with window on its side surface placed horizontally, its diameter is 70 cm and length is 100 cm. It is connected with relatively large tank of the volume $V_r = 4{,}2\ m^3$. Pressure in range $p_{c\,0} = 10 \div 760$ Torr can be set in all this hermetic volume. It is measured by static manovacuummeter with accuracy ±1.5 Torr. Temporary air pressure measurements $\mathbf{p_c}$ in the working chamber are detected at the oscilloscope screen from the outlet of electronic measurer of pressure **p** with typical velocity up to 10^5 Torr/s and accuracy ±1.5 Torr.

Aerodynamic part of the setup forms high-speed submerged air stream in the working part of the setup along its axis as it is schematically shown in Fig.3.4.

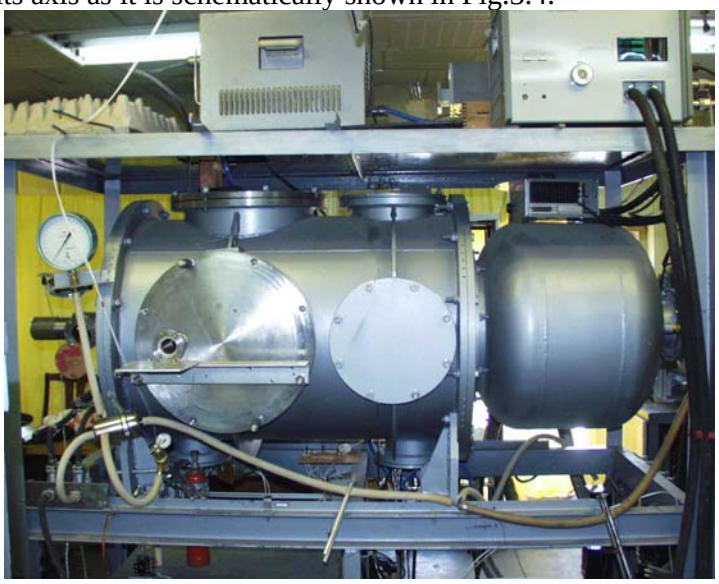

Fig.3.2 Appearance of experimental setup

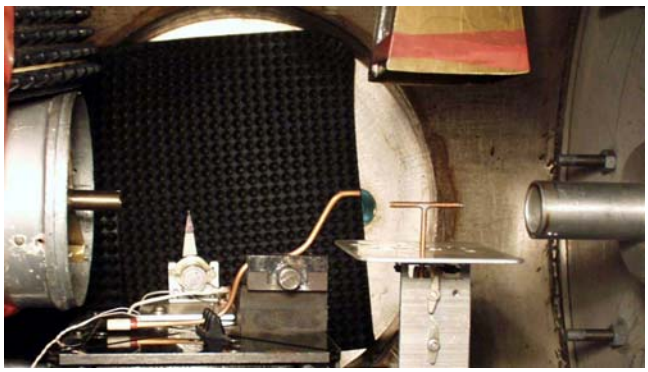

Fig.3.3 Experimental setup working area photo in one of definite experiments

The stream with SS value of velocity $\mathbf{v_{fl}}$ is formed by the axially symmetric Laval nozzle. Electromechanical valve is located at its inlet, its typical response time is about of hundred of a second.

Air flow to the chamber takes place through the nozzle from the atmosphere at $p \approx 760$ Torr. Submerged air stream with velocity $v_{fl} = 500$ m/s is formed at pressure in the chamber $p_c < 400$ Torr after opening of the valve at the outlet of the Laval nozzle at gas temperature $T = 150$ K, for example with Mach number $M = 2$ at pressure $p = 97$ Torr. It is evident that the stream formed by the Laval nozzle at gas pressure in the chamber $p_c = 97$ Torr is comparably long. Experiments showed that in this case there is still a core of SS stream with diameter of 1.8 cm at 12 cm from the nozzle outlet. The stream is intercepted by a convergent tube (confuzer) in the working chamber, connecting it with relatively large hermetic tank –

receiver. The experiment showed that aerodynamic pumping out of the working chamber takes place in this case. So if initial pressure in the chamber and receiver is $p_{c\,0}$ = 114 Torr then the pressure p_c= 97 Torr in the chamber is established after approximately 0.2 s. This pressure is maintained practically constant during approximately 1 s, and then it starts to grow. Our experiments are carried out approximately during this second.

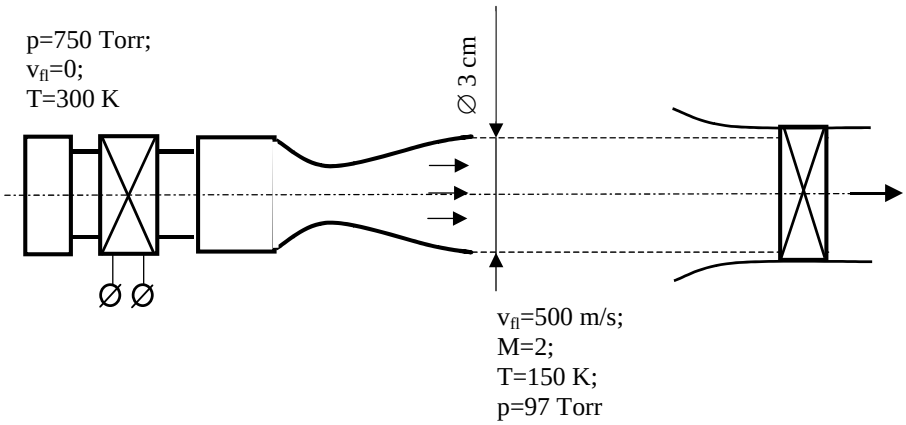

Fig.3.4 Scheme of aerodynamic part of the setup .

3.2. MW system

EM wave is generated by a magnetron with outlet power of P_{gen} = 1.5 kW and λ = 12.5 cm. Linearly polarized EM beam formed in the working chamber is perpendicular to SS stream velocity, and it has typical sizes 9x9 cm in its area as it is shown in Fig.3.5. **E** vector of EM field electrical component is parallel to $\mathbf{v_{fl}}$ and has a value E ≈ 120 V/cm. Applied magnetron can in principle generate EM wave continuously. The generation time in the experiments was set by the modulation of its anode feeding.

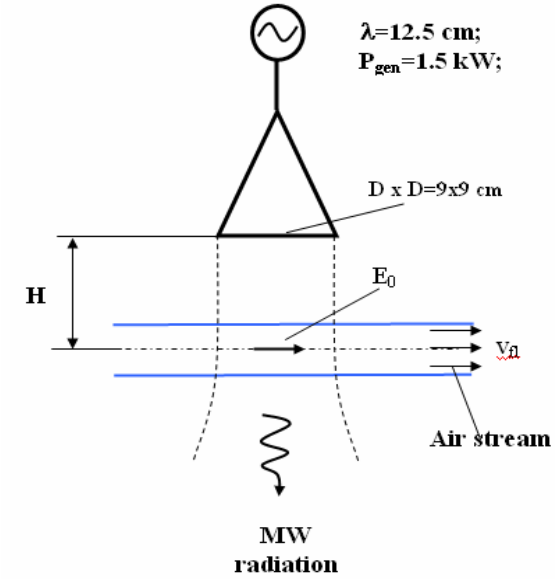

Fig.3.5 Scheme of MW radiation formation

In Fig.3.6 one can see schematics of the vibrator initiating a discharge location in the working chamber. The vibrator was placed horizontally over SS air stream axis along $\mathbf{v_{fl}}$ and symmetrically with respect to MW beam along the field **E**. MW radiation comes to the vibrator from above. The vibrator is located over flat conducting screen. The vibrator design and its fastening post are depicted conditionally. They will be described in details below in

corresponding parts of the report. The distance H from the vibrator axis to the screen was experimentally selected.

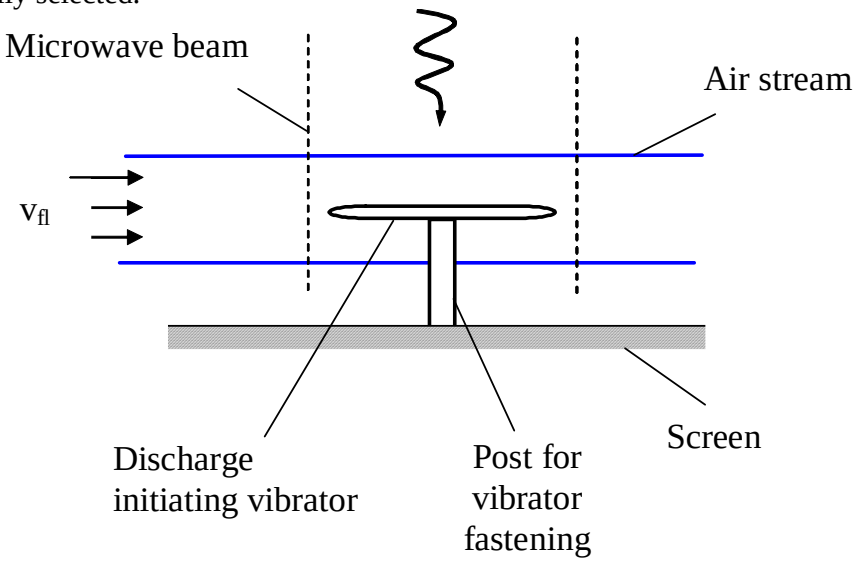

Fig.3.6. Scheme of the vibrator location with respect to the stream and radiation flux.

3.3. System of injection

Propane in this experimental series was delivered to internal vibrator area through the hole in its fixing post over special injection line. The injection line scheme is represented in Fig.3.7. In includes initial tank with the volume $V_\Sigma = 500$ cm^3, which can be filled either by pure propane or its mixture with air in required proportion up to pressure $\mathbf{p_\Sigma}$. Controlled electromechanical valve is placed at the exit from this tank; it allows to deliver a fuel through a pipe to the post fastening the vibrator (that initiates the discharge). The final part of the injection line has through hole diameter 2 mm; it is a copper pipe with the outer diameter 4 mm and length 70 mm, the vibrator is fastened to it. The last part of the line with length of about 1 m has internal diameter of 4÷10 mm. Decrease of fuel pressure in its initial tank $\mathbf{\Delta_{p\Sigma}}$ can be detected in experiments during the injection time $\boldsymbol{\tau_{inj}}$.

Using this value one can determine experimental injection rate of a fuel:

$$m= (V_\Sigma \cdot \rho_{760} \cdot \Delta p_\Sigma)/(\tau_{inj} \cdot 760)\text{-}m'; \text{ g/s}, \qquad (3.1)$$

here $\mathbf{V_\Sigma}$ - in cm^3 , $\boldsymbol{\rho_{760}}$ – in g/cm^3 – is a density of propane or of its mixture with air at normal conditions, $\mathbf{\Delta p_\Sigma}$ - in Torr m'- the amendment which is taking into account processes on a site of a path of injection from the valve up to hole.

Let us represent some reference data for air and propane at normal conditions:

Air: adiabatic exponent $\gamma = 1.4$;

Molecular weight $m_a = 4.8 \cdot 10^{-23}$ g;

Density $\rho_{760} = 1.23 \cdot 10^{-3}$ g/cm^3;

Sound velocity $v_s = 3.4 \cdot 10^4$ cm/s.

Propane: chemical formulae– C_3H_8;

adiabatic exponent $\gamma = 1.14$;

Molecular weight $m_a = 8 \cdot 10^{-23}$ g;

Density $\rho_{760} = 1.9 \cdot 10^{-3}$ g/cm^3;

Sound velocity $v_s = 2.5 \cdot 10^4$ cm/s;

Combustion heat $Q = 4.64 \cdot 10^4$ J/g.

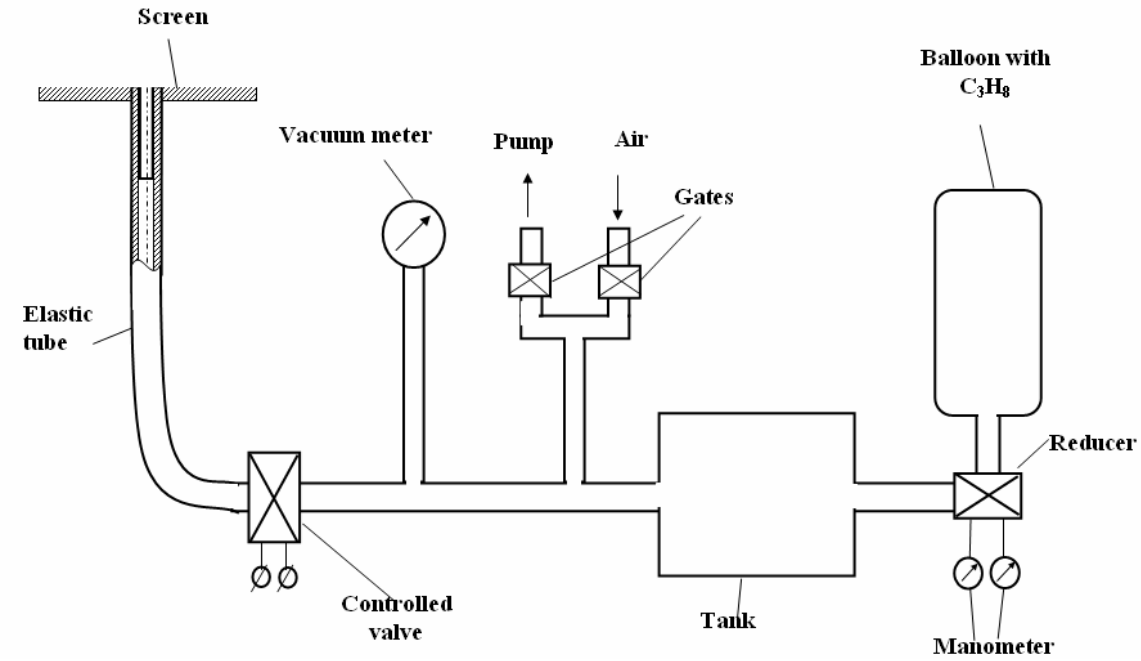

Fig.3.7 Scheme of mixture injection line.

3.4. Means of diagnostics

Manovacuummeters are included into the composition of main measuring equipment, they measure static pressure pc in the working chamber and $\mathbf{p_\Sigma}$ in the initial tank with a fuel; high-speed electronic sensor measuring pressure variation pc in the working chamber; Pitot pipe with corresponding electronic scheme that measures stagnation pressure of the flow $\mathbf{p_{stag}}$; and thermocouple flow temperature $\mathbf{T_{stag}}$ measurer.

In Fig.3.8 one can see a waveform from the sensor measuring $\mathbf{p_c}$. The horizontal scale in is is 0.2 s/div as in all following waveforms. Initial horizontal part of the waveform corresponds to $p_{c\,0} = 114$ Torr. The oscilloscope beam drop starts from the moment of the valve opening at the inlet of the Laval nozzle. The valve is opened during $\tau_{fl} = 1.1$ s. Decrease of pressure pc in the chamber takes place in the result of aerodynamic pumping out of the working chamber by SS stream, as it was indicated above. The drop process lasts approximately 0.2 s. Then pc begins to grow slowly staying practically the same during 0.7 s. The grow rate becomes quicker only during last 0.2 s. Final horizontal waveform part corresponds to pc with accounting of air leak in to the vacuum volume during the time $\boldsymbol{\tau_{fl}}$. Manovacuummeter shows that it corresponds to $p_{c\,end} = 132$ Torr. Vertical difference between the initial and the final parts of the waveform equal to 18 Torr gives its absolute vertical scale.

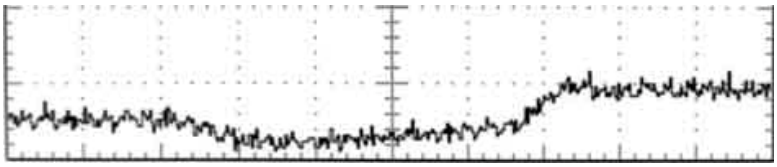

Fig.3.8 Waveform from the sensor measuring pc

Metallic Pitot pipe with outer diameter of 2.8 mm and internal diameter of 2.2 mm (or diameters 1 and 0.5 mm, respectively) is placed in SS flow with its open end towards $\mathbf{v_{fl}}$. In Fig.3.9 one can see the typical waveform of $\mathbf{p_{stag}}$ in some point of the vibrator trail. Its initial part still corresponds to $p_{c\,0} = 114$ Torr and final to $p_{c\,end} = 132$ Torr, the horizontal, upper, beam part

corresponds to the time τ_{fl}. In Fig.3.10 is represented the waveform of $\mathbf{p_{stag}}$ as another example, it was measured by Pitot pipe in free stream (without a vibrator) along its axis at the distance of 110 mm from the outlet cross section of the Laval Nozzle. The vertical scale in it also is given by the difference ($p_{c\,end}$ - $p_{c\,0}$). Accounting it one obtains the signal amplitude Δp_{stag} = 386 Torr, or with accounting of $\mathbf{p_{c\,0}}$ one gets the stagnation pressure in this point to be p_{stag} = 500 Torr. Ratio of this value and static pressure in the stream give equal to pressure in the chamber gives Mach number M = 1.9 on the represented graph in Fig.3.11.

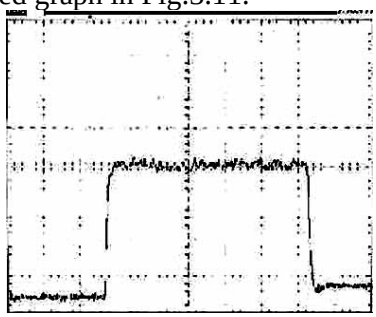

Fig..3.9 Typical waveform of pstag in the vibrator trail

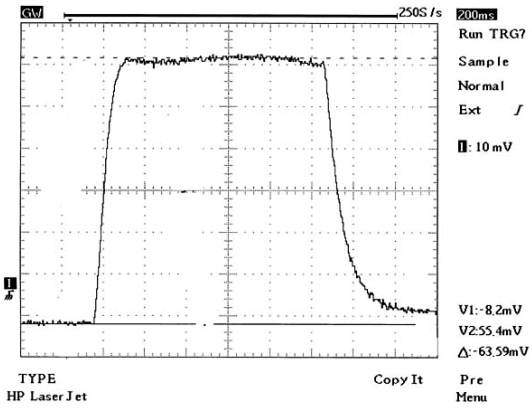

Fig.3.10 Waveform of pstag measured by Pitot pipe at the axis of free stream without the vibrator at the distance of 110 mm from Laval outlet cross section.

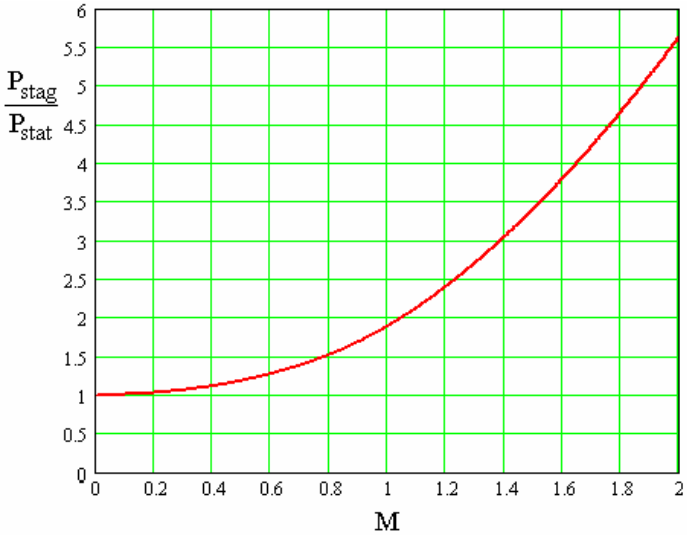

Fig.3.11 Graph of stagnation pressure and static pressure ratio via Mach number calculated by Rayleigh formulae (γ = 1.4).

$\mathbf{T_{stag}}$ temperature is measured by Ahromel - Allimel thermocouple. Its average sensitivity equals to α=24.5 K/mV in the range ΔT = (100÷1400) K where $\mathbf{\Delta T}$ is difference of temperature

of warm and hot thermojunctions. Hot thermojunction end are isolated correspondingly, they go inside the metal pipe, which external diameter is 2.8 mm, and internal is 2.2 mm.

Thermojunction goes out of the open face of this pipe directed towards the flow for about of 1 mm. $\mathbf{T_{stag}}$ measuring scheme is comparably inertial, as, for example, it follows from Fig.2.5b, above. The time of discharge burning was set usually τdis = 0.4 s in the experiments. Warm thermojunction temperature does not have time to be heated up to $\mathbf{T_{stag}}$ during this time. This temperature corresponds to air temperature heated by the discharge in the flow.

Method developed in previous Report on the Project allows to calculate $\mathbf{T_{stag}}$ using the form and amplitude $\mathbf{U_{max}}$ of the waveform from the thermocouple. For this purpose one determine with a help of the waveform, for example, the ratio $\mathbf{U_{1/2}}$ /$\mathbf{U_{max}}$, where $\mathbf{U_{1/2}}$ is the signal value in the time moment $\boldsymbol{\tau_{dis}}$/2, and the corresponding coefficient is determined with a help of the graph in Fig.3.12, which is used at calculations of $\mathbf{T_{stag}}$:

$$T_{stag} = 300 + U_{max} \cdot \alpha \cdot k; \text{ K.} \qquad (3.2)$$

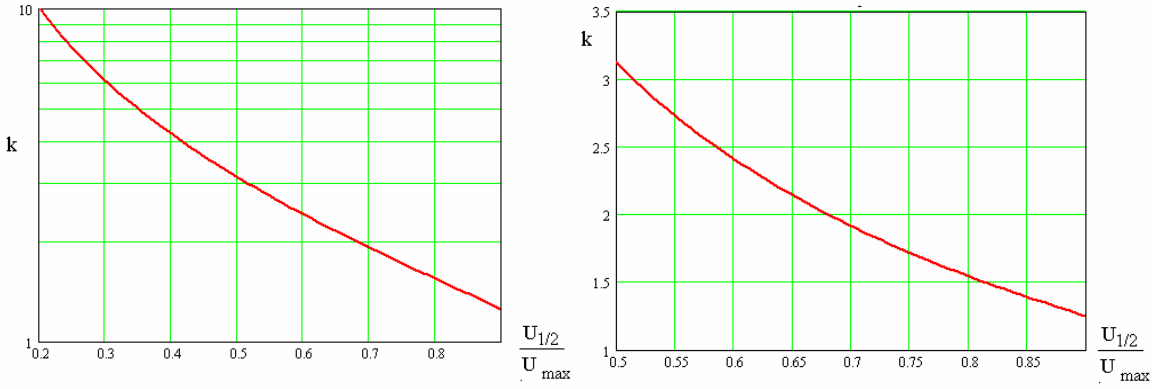

Fig.3.12 Accounting coefficient of thermocouple sensor

Measured $\mathbf{T_{stag}}$ at estimated Mach number with a help of $\mathbf{p_{stag}}$ measured by Pitot pipe and the graph in Fig.313 gives static temperature $\mathbf{T_{stat}}$ in the stream.

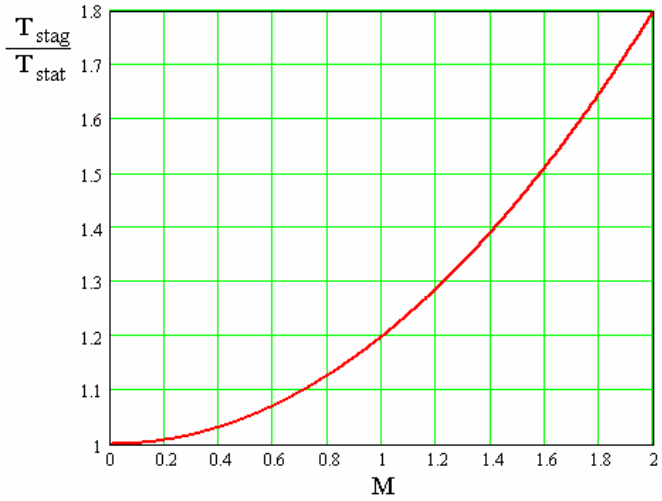

Fig.3.13 Graph of stagnation temperature and static temperature ratio via Mach number (γ = 1.4).

The Pitot pipe and the thermocouple are placed on the electrically controlled coordinate device. It allows to point after point reconstruct fields of $\mathbf{p_{stag}}$ and $\mathbf{T_{stag}}$ in MW discharge trail and in propane combustion area in the plane perpendicular to $\mathbf{v_{fl}}$ without of decompression of the working chamber in the successive series of experiments.

3.5. Temporal program of the equipment work

In Fig.3.14 one can see an illustration of temporary chain of the equipment work of the experimental setup. In it above one can see conditionally shown $\mathbf{p_{stag}}$ waveform, and of $\mathbf{T_{stag}}$ below; they are measured in the trail of the vibrator initiating the discharge. Under them intervals of temporary SS stream existence, of MW discharge burning and of fuel injection are shown

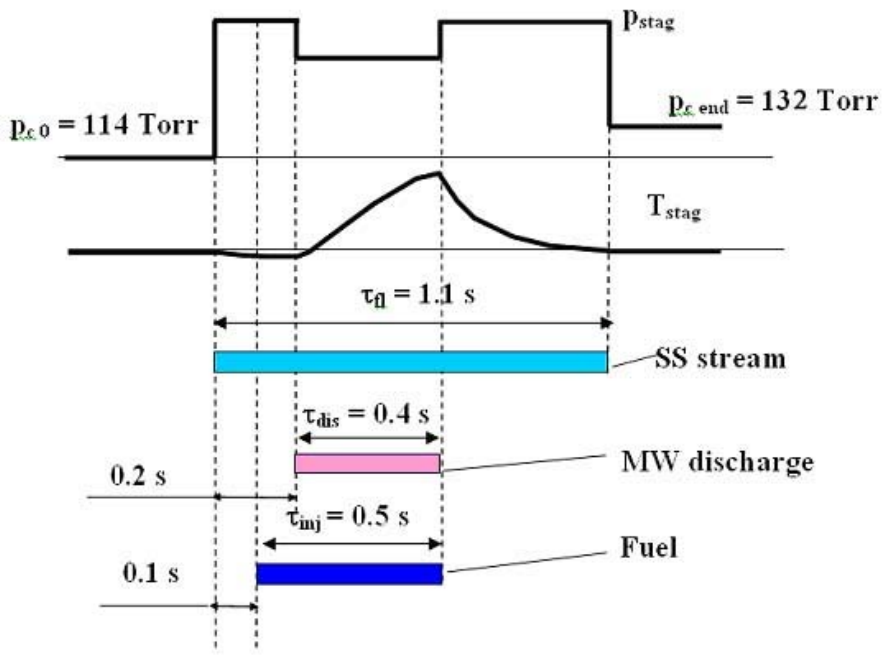

Fig.3.14 Temporary sequence of experimental setup equipment work.

As it was noted initial part of the waveform pstag corresponds to initial pressure $p_{c\,0}$ = 114 Torr in the chamber, and the final part corresponds to the pressure $p_{c\,end}$ = 132 Torr established in the chamber after finishing of air leak into the chamber process through the Laval nozzle. On the upper part of this waveform of duration τ_{fl} = 1.1 s one can see "undershoot" of duration τ_{dis} = 0.4 s in the case of MW discharge burning connected with gas heating in the discharge area. Its beginning is delayed for 0.2 s with respect to valve response at the inlet of the Laval nozzle. The controlled valve in the fuel injection line to the discharge area responds with advance of 0.1 s with respect to MW discharge start of burning. This advance insures stabilization of fuel flow process over the line of its injection. Naturally that $\mathbf{p_{stag}}$ stays the same during this time because the fuel is ignited namely by the discharge.

Thermocouple sensor of Tstag is comparably inertial in difference with the measurer pstag as it was already noted. So its reading smoothly limit to the established value at switching of different devices of the setup, and this value some times can not be reached during their work. Initial part of this waveform corresponds to the room temperature $T \approx 300$ K, because the difference of warm and cold thermojunctions in initial state is $\Delta T = 0$. The temperature of warm thermojunction limits to the temperature $T \approx 300$ K also at the final part of the waveform after finishing of MW discharge burning. $\mathbf{T_{stag}}$ has not to be changed in ideal case at switching on of SS stream because the flow through the Laval nozzle takes place from the atmosphere at T = 300 K. The sensor in realty is not ideal, and its warm thermojunction temperature decreases by several degrees. Air temperature in the stream sharply grows at switching of MW discharge if the stream propagated through the discharge area. So the temperature of the warm thermojunction begins to rise up to new value of $\mathbf{T_{stag}}$. So the waveform traces this process.

4. Vibrator diameter and length influence on the possibility of MW discharge realization

The final goal of present investigation is mixing of propane with air in required proportion and effective combustion of this flammable mixture in the stagnant flow. Air in experiments has to come to the mixing area from SS stream and to be dragged in the internal volume of the vibrator initiating the discharge. At that air drag the more effective at constant cross section of inletting hole in the nose part of the vibrator the larger is a diameter of the vibrator internal cross section. The discharge and the fuel will be burning in the base area of the vibrator. This burning will take place in shadow area in the case of its large external size, i.e. in the dragged flow. In experiments described in this part we determined how enlargement of vibrator diameter **2a** (at corresponding change of its length **2L**) influences MW discharge ignition possibility in SS stream. In the experiments we also developed vibrator base end form so that it could insure sufficiently large size of the discharge area (with respect to vfl) or initiation of discharge channels multitude located round the base vibrator perimeter.

4.1. Experiments in motionless air

Vibrators in experiments were made of copper pipes with flat faces and outer diameter **2a**, equal to 4, 6, 10, 12 and 18 mm. At that in the case of each vibrator we varied its length 2**L** and the distance H from the vibrator axis and the screen.

In Fig.4.1.1 for example one can see a photo of deeply undercritical MW discharge initiated by the vibrator with 2a = 4 mm, 2L = 50 mm and H = 32 mm in motionless air at p = 200 Torr. We notice, that discharges areas are localized to the ends of the initiator.

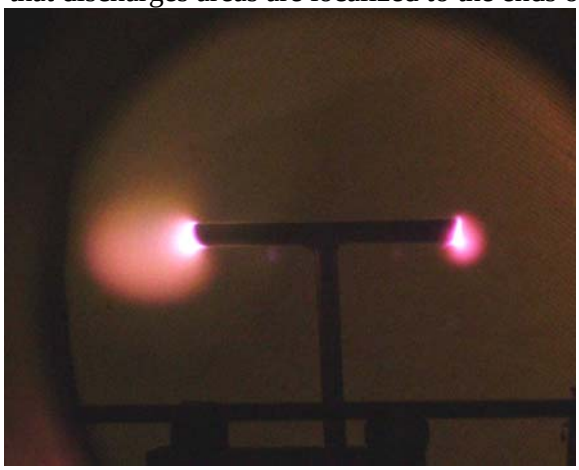

Fig.4.1.1 Photos of deeply undercritical MW discharge initiated by the vibrator with 2a = 4 mm, 2L = 50 mm and H = 32 mm in motionless air at p = 200 Torr.

For each vibrator in Fig.4.1.2 one can see experimental dependencies of maximum pressure in the working chamber at which MW discharge was still realized at definite vibrator length, – $p_{br}(2L)$. It follows fFrom these dependencies that resonance vibrator length **2L** decreases with increase of **2a**, and resonance itself becomes not so implicit. So it is not practically observed at 2a = 18 mm.

Experiments showed that optimal size of **H** decreases with growth of **2a** . So $H \approx \lambda/4$ at small 2a = 4 mm , but, for example, it equals to 28 mm at 2a = 12 mm, at it is smaller than $\boldsymbol{\lambda/4}$.

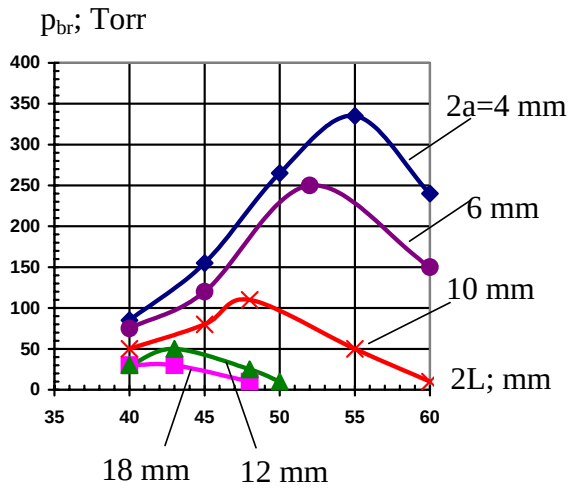

Fig.4.1.2 Experimental dependencies of maximum pressure in the working chamber, at which MW discharge was still realized

4.2. Experiments in supersonic flow

Air is cold in experiments at static pressure of p_{st} ≈100 Torr in SS stream. Its static temperature is T_{st} ≈ 150 K. It means that a concentration of molecules in air, of which breakdown field is dependent, corresponds to motionless air pressure of p = 200 Torr. It follows from Fig.4.1.2 that air breakdown in experimental conditions in SS flow (without accounting flow disturbances in the vibrator vicinity) is possible only with vibrators, which have 2a < 10 mm. At the same time there can be formed the decompression area in the face area of the vibrator pipe in the case of the closed hole of the vibrator pipe by the dielectric fairing, so air breakdown can be realized in the decompression area. This supposition was tested in experiments.

As it was shown earlier SS submerged stream used in the experiment has SS core at M≈2 only at the diameter 18 mm in the vibrator location area. So, experiments in SS stream were undertaken with vibrators having a diameter 2a ≤ 12 mm.

In Fig.4.2.1 one can see a photo of deeply undercritical MW discharge initiated by the vibrator with sharpened base end in SS stream. Such a vibrator with the diameter in the central area 2a = 4 mm and a pylon of flown around form was used in experiments of the previous stage of this Project. In the photo one can see that the discharge burns only near the base vibrator end.

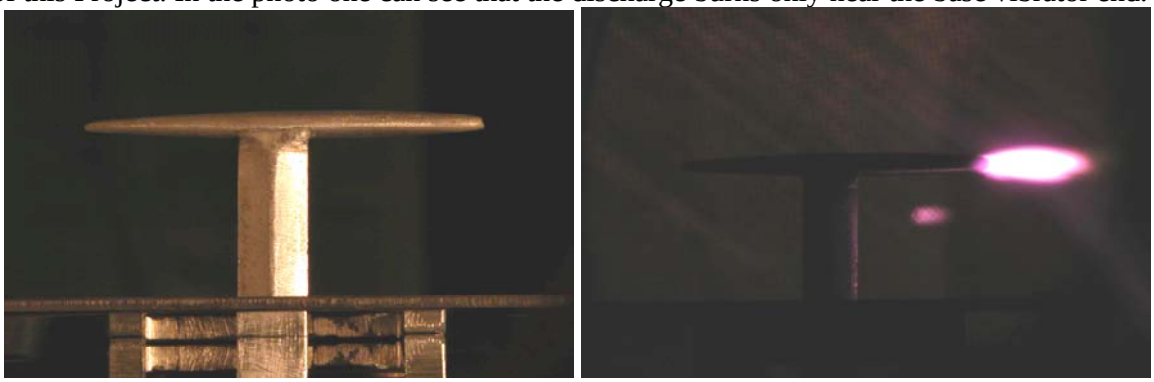

Fig.4.2.1 A photo of a vibrator with sharpened base end (to the left) and deeply undercritical MW discharge in SS stream initiated by this discharge (to the right).

Experiments with vibrators made of pipes with closed nose hole by the dielectric fairing and flatly cut base show that the discharge burns in their base only at 2a ≤ 6 mm. Photos of these discharges at 2a = 4 mm and 2a = 6 mm are represented in Fig.4.2.2 and Fig.4.2.3, respectively. The discharge in this case burns over the whole base face pipe perimeter.

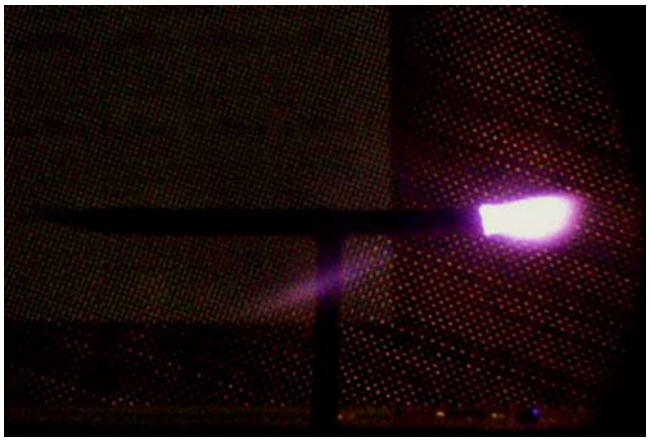

Fig.4.2.2 A photo of a discharge in the vibrator base part with closed nose hole and flatly cut base at 2a = 4 mm

The discharge is not initiated at this initiator design at their large diameters. So the decreasing of air molecules density in the base area of the vibrator placed in SS stream exists but insignificantly.

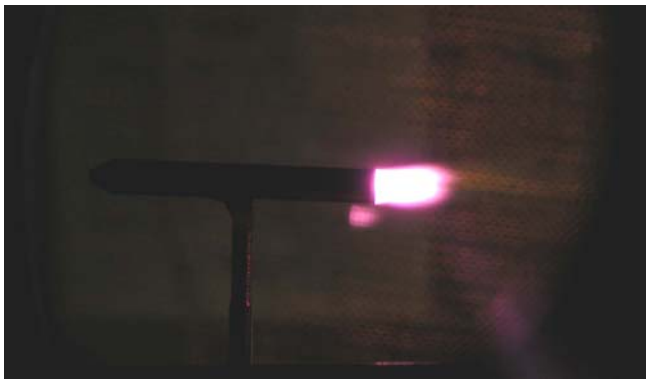

Fig.4.2.3 A photo of a discharge in the vibrator base part with closed nose hole and flatly cut base at 2a = 6 mm

Experiments on base end vibrator form selection with diameters 2a > 6 mm were executed.

In Fig.4.2.4a one can see the base end of the vibrator sharpened in the form of a facet. Vibrators with such end form still did not initiate a discharge.

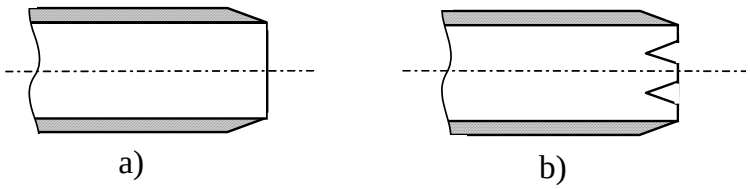

Fig.4.2.4 Base end of the vibrator: a) – with sharpened face, б) - with sharpened face and triangle deepenings

In Fig.4.2.4b one can see a design of the vibrator aft end with sharpened facet and triangular cuts. In Fig.4.2.5 for an example one can see vibrator photo with this base end design at 2a = 12 mm. It is seen from this photo that this vibrator initiates MW discharge. The discharge photo in Fig.4.2.5 corresponds to exposure time τ_{ex}= 1 s. Its photo detection with smaller $\boldsymbol{\tau_{ex}}$ shows that the discharge in this case jumps over base pipe perimeter with typical times of 10^{-2} s. The discharge area at that has maximum transversal size of some millimeters.

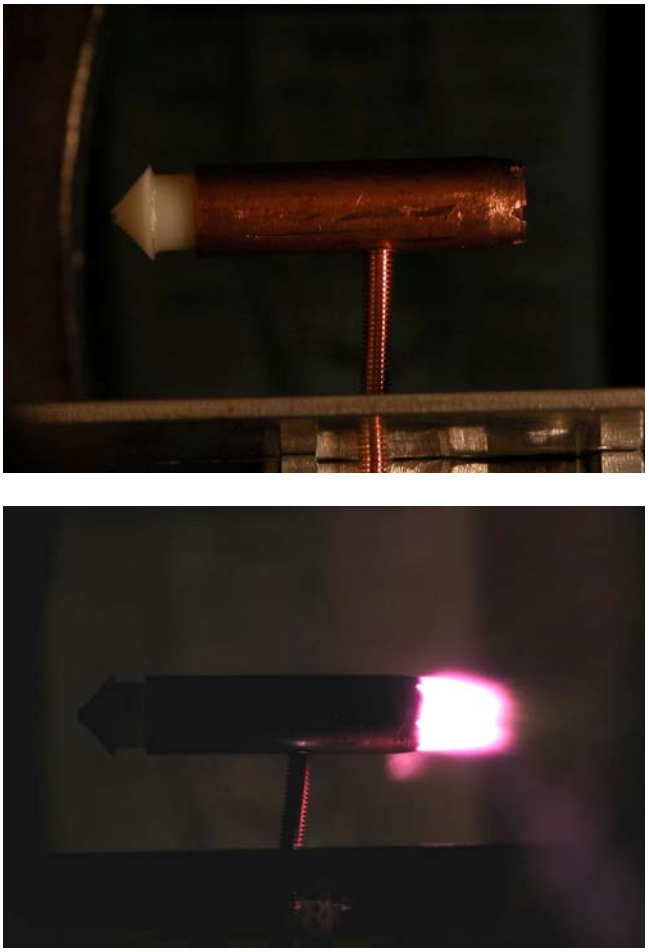

Fig.4.2.5 A vibrator with sharpened face and triangle deepenings - a), Discharge photos in its base part - б).

In the next series of experiments we gave to the vibrator base end the form of six sharpened teeth uniformly placed over the pipe perimeter, their height was 10 mm, as it is shown in the upper photo of Fig.4.2.6. The discharge was initiated also in SS stream in this case. However it was attached either one or two teeth sometimes, as it is shown in Fig.4.2.6.

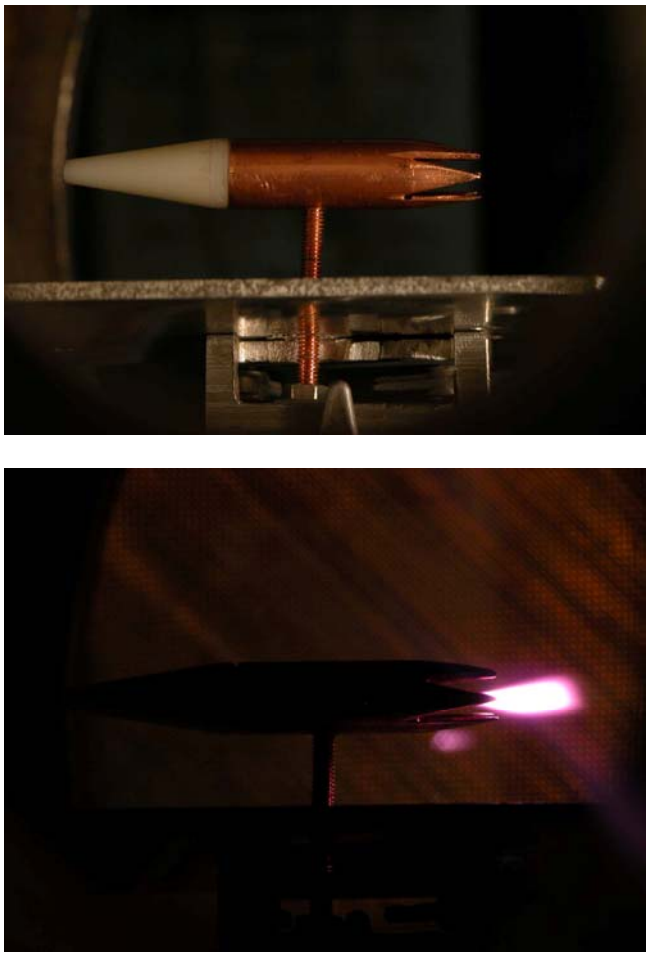

Fig.4.2.6a. A vibrator with edges in its base part

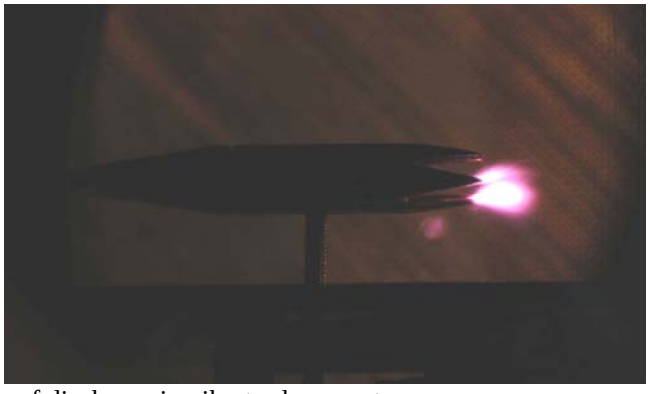

Fig.4.2.6b. Photos of discharge in vibrator base part

This design of the base vibrator end allows decreasing the distance between its sharpened ends and the vibrator axis, i.e. to draw them in. The experiment showed that the discharge begins to burn over ends simultaneously at their location on the diameter with 2c = (6÷7) mm. Photos of the vibrator made in this way and MW discharge burning at τ_{ex} = (1/30) s are represented in Fig.4.2.7.

In Fig.4.2.8 one can see a photo of initiated by this vibrator MW discharge at τ_{ex} = 1 s, and in Fig.5.2.9 - at $\tau_{ex} = 10^{-3}$ s.

The last photo gives grounds to suppose that deeply undercritical MW discharge initiated by this way in SS flow conserves features of the streamer discharge. So one can suppose that iin this case there are only several streamer channels simultaneously with typical duration and origin

period of microsecond units. However this supposition requires special experimental and theoretical understanding.

Fig.4.2.7a Vibrator with drawn in edges.

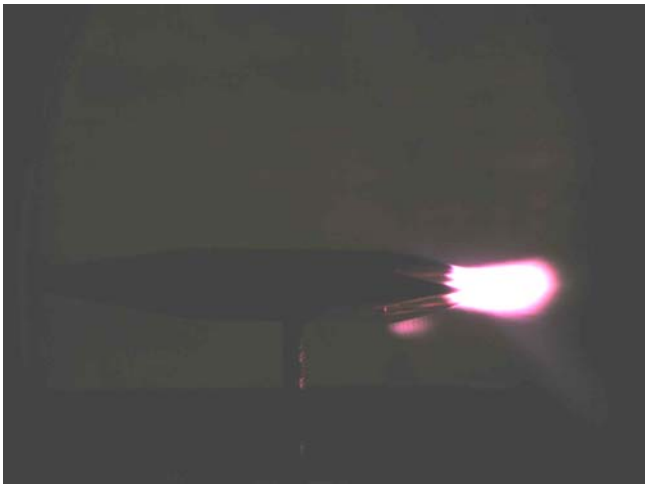

Fig.4.2.7b. Discharge photos in vibrator base part with drawn in edges (b).

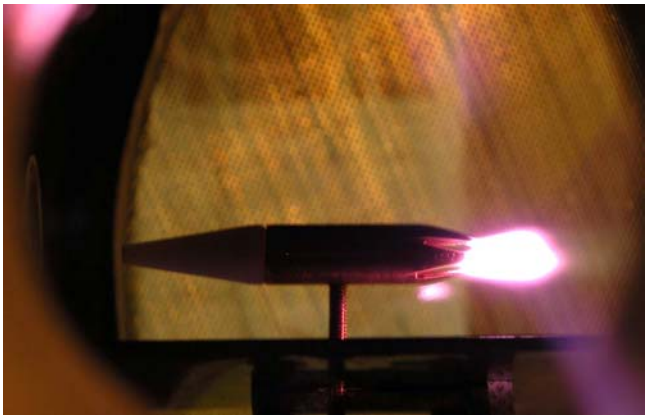

Fig.4.2.8 Discharge photo in vibrator base part with drawn in edges at exposure time τ_{ex}= 1s

Fig.4.2.9 Discharge photo in vibrator base part with drawn in edges at exposure time $\tau_{ex}= 10^{-3}$ s

So experimentally we selected design of the vibrator with rather large diameter that allows to insure combustion in its base area relatively uniform deeply undercritical MW discharge in the transversal to $\mathbf{v_{fl}}$ direction at multitude of initiation centers distributed over the perimeter of the base vibrator end.

Generally executed experimental search and its results are represented in Fig.4.2.10.

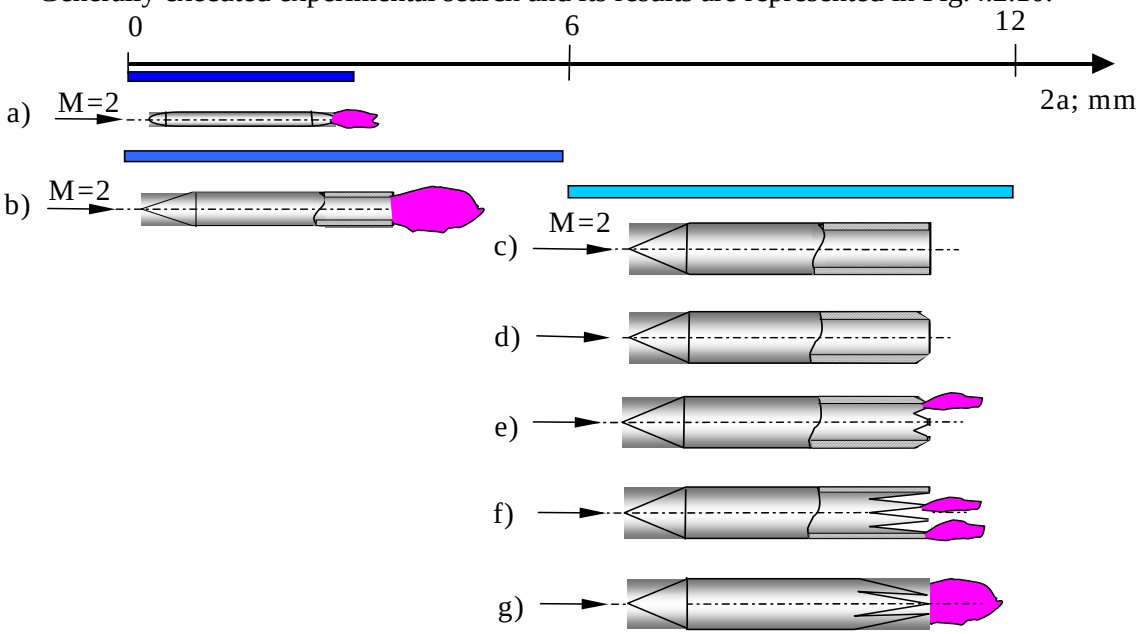

Fig.4.2.10 Scheme of initiating vibrator optimal form search for mixture ignition

5. Finishing of propane-air flammable mixture combustion process ignited by deeply undercritical MW discharge

During this stage of investigations we experimentally developed construction scheme of propane-air flammable mixture with a help of deeply undercritical MW discharge initiated in the base of electrical vibrator that insures effective combustion of the mixture in the discharge area. The vibrator at that is located in SS stream, and the flammable mixture is delivered to the discharge area through internal region of the vibrator. We used vibrators in experiments, which developed design is described in preceding part of the Report. We used the vibrator made of copper pipe with 2a = 12 mm, internal diameter 2b = 10 mm, the diameter for sharpened base ends 2c = 6.5 mm, with length 2L = 42 mm and the distance from the axis to the screen H = 28 mm.

5.1. Stages of experimental program execution

Works were executed in the following sequence. Firstly we developed the aerodynamic design of the base vibrator region that insures most effective combustion of the flammable mixture ignited by the discharge. At that propane-air mixture was injected to the internal region of the vibrator, it was preliminary prepared in initial tank include to the injection line. After the development of the combustion area design we injected now pure propane to the internal region of the vibrator, and air went there from SS stream through a small hole in the nose area of initiator dielectric fairing. Then the size of the hole for air inletting was increased, and respectively increased the amount of injected propane, i.e. we tested the principle possibility of increase of combusting out fuel.

5.2. Experiments with preliminary prepared flammable mixture in the injection line with "natural" combustion area

In present part of the Report we describe experiments with injection of preliminary prepared flammable mixture into internal vibrator region when the mixture was prepared in the tank included into the injection line. The mixture was prepared with the given weight proportion of air and propane **r**. At that there is no a hole in the dielectric nose fairing of the MW initiating vibrator for air inletting to its internal volume from SS stream. Schematically design of internal initiator area is

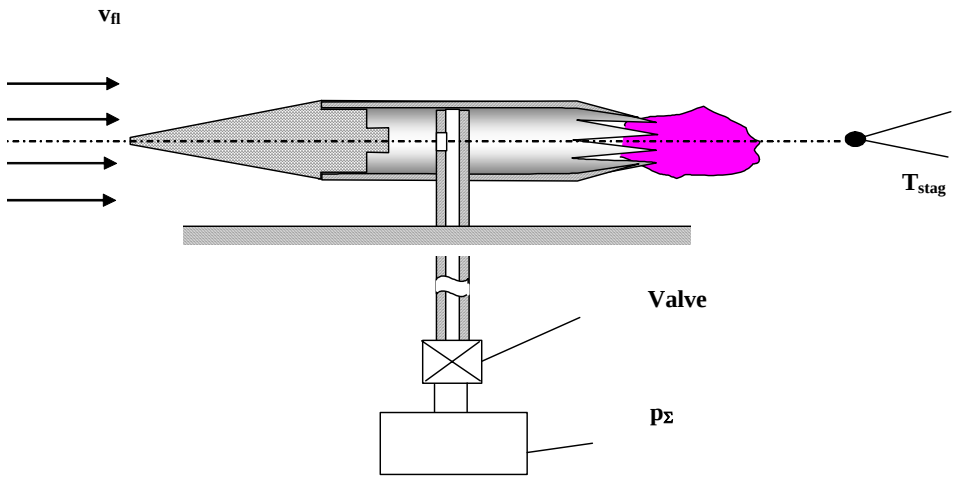

Fig.5.2.1. Scheme of internal initiator area design.

Let us firstly describe several preliminary experiments.

It is evident that area of aerodynamic shadow is formed behind the vibrator located in SS stream in the near field. Its characteristics were estimated by measurements of pstag over the vibrator's axis.

In Fig.5.2.2 one can see most typical waveforms. Near each waveform we indicate the distance (in millimeters) between measuring Pitot pipe and base cut of the vibrator. This distance we denote as **x**, it has the sign «+» at Pitot pipe moving away from this cut, and «-» at its deepening inside the vibrator. From the waveforms follows that aerodynamics decompression is realized in the internal vibrator area and in its near trail at distances below $x \le 5$ mm. Then $\mathbf{p_{stag}}$ gradually rises.

In Fig.5.2.3a one can see the graph of $\mathbf{p_{stag}(x)}$ made on a basis of experimental waveforms. Axis x goes along the initiator axis from the vibrator. For «**0**» in it we took location of its base cut. In Fig.5.2.3b is represented calculated dependence $\mathbf{v_{fl}(x)}$ calculated with a help of $\mathbf{p_{stag}(x)}$.

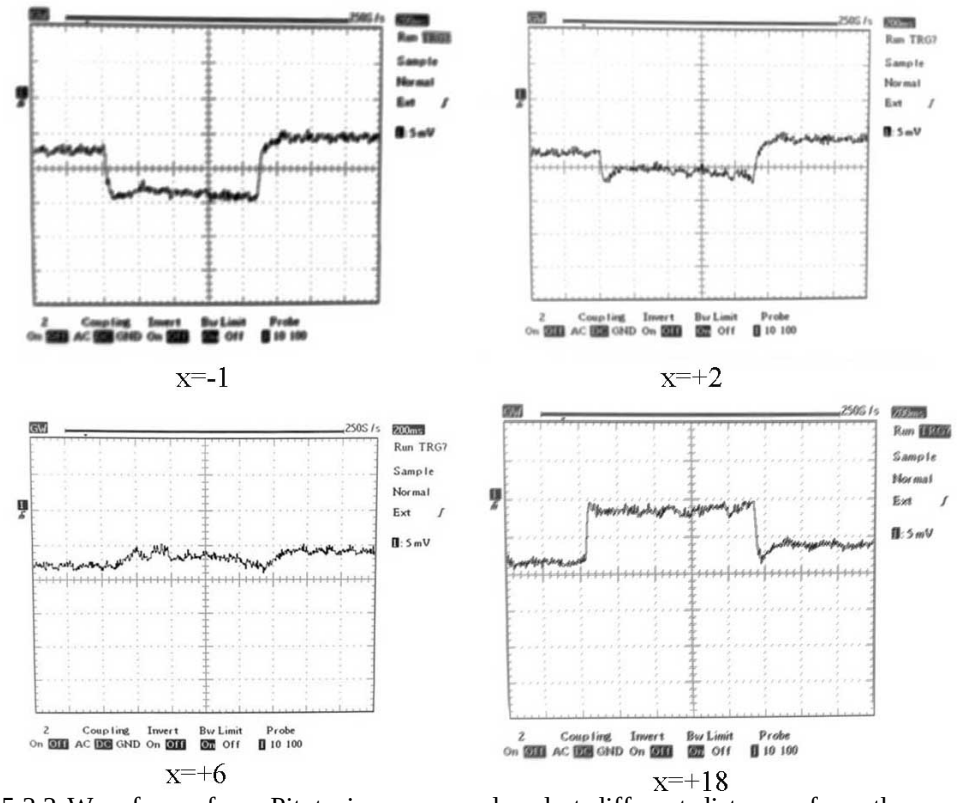

Fig.5.2.2 Waveforms from Pitot pipe sensor, placed at different distances from the nozzle exit

Calculations of $\mathbf{v_{fl}}$ were made according the following algorithm. Let us assume that static pressure pstat in the stream at p_{stag}>97 Torr equals to pressure in the chamber $p_{stat} = p_c = 97$ Torr. Knowing ratio $\mathbf{p_{stag}/p_{stat}}$ for each value of **x** one can determine Mach number **M** with a help of the graph in Fig.3.11 in this point of the flow and the static air temperature $\mathbf{T_{stat}}$ in it with a help of Fig.3.13. At that it is naturally supposed that the stream temperature $T_{stag} = 300$ K without external energy put. $\mathbf{v_{fl}}$ is calculated using these data with a help of the formulae

$$v_{fl} = M \cdot 340 \cdot \sqrt{T_{stat} / 300}; \text{ m/s}, \qquad (5.2.1)$$

where $\boldsymbol{T_{stat}}$ is in K.

In Fig.5.2.3 one can see, that pressure $\mathbf{p_{stag}}$ and stream velocity $\mathbf{v_{fl}}$ are still smaller then their undisturbed values $p_{stag} \approx 500$ Torr and $v_{fl} = 500$ m/s in the vibrator trail up to measured $x \le 25$ mm.

In the next experiment we measured pressure drop $\mathbf{\Delta_{p\Sigma}}$ in the initial tank in the injection line during injection time $\boldsymbol{\tau_{inj}}$ with respect to initial pressure in this volume $\mathbf{p_\Sigma}$**.** The experiment was carried out with filling of this tank with air, constant injection time $\tau_{inj} = 0.5$ s, and at vibrator blowing around by SS stream. In Fig.5.2.4 is represented the corresponding experimental graph.

It follows from the experiment, as it should be, the injection rate has to be zero at $\mathbf{p_\Sigma}$ smaller than pressure established in internal vibrator volume. Injection has unstable character at small $\mathbf{p_\Sigma}$, and its rate grows approximately linearly starting from $p_\Sigma \approx 120$ Torr.

Experiments were carried out with air because of two reasons. First, MW discharge was not switched on during them and hermetic volume of the setup (including the working chamber and receiver) in experiments with propane would be “contaminated” by propane and could become explosive. Second, stoichiometric ratio of air-propane mixture is $r \approx 16 >> 1$, so gasdynamic characteristics of this mixture are mainly determined by air.

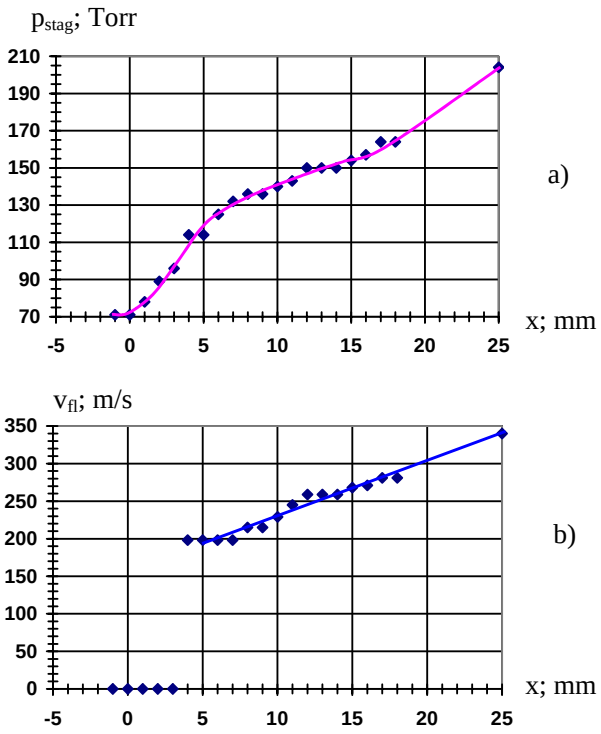

Fig.5.2.3 Graphs of experimental dependencies: $\mathbf{p_{stag}(x)}$ - a), $\mathbf{V_{fl}(x)}$ - b).

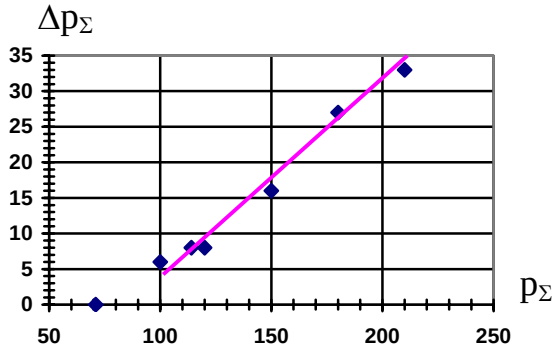

Fig.5.2.4 Pressure p drop in initial tank dependence during injection time via initial pressure p в in it.

One can estimate flammable mixture flow out velocity $\mathbf{v_{in}}$ from the vibrator base hole using measured Δp_Σ. For example at Δp_Σ = 33 Torr one has m = $5.3 \cdot 10^{-2}$ g/s according with (3.1) and from the equation

$$m = v_{in} \cdot \rho_{760} \cdot (p_c / 760) \cdot (\pi \cdot b^2) , \qquad (5.2.2)$$

where $p_c \approx 100$ Torr, v_{in} = 4.5 m/s.

In next experimental series we measured $\mathbf{p_{stag}}$ and $\mathbf{T_{stag}}$ in the vibrator trail in some point **x** along its axis at discharge burning and flammable mixture injected to it. Ratio $\mathbf{r = m_{air}/m_{pr}}$ at that was varied from infinity (at injection of pure air) to zero (at injection of pure propane). The experiment showed that waveforms of $\mathbf{T_{stag}}$, for example, at p_Σ = 210 Torr, to which corresponds Δp_Σ = 33 Torr in the graph in Fig.5.2.4, began to significantly differ only at approach to r = 4 in the case of burning of only the discharge or combustion of the mixture injected to it. Propane pressure of p_{pr} = 30 Torr corresponds to this r value in initial injection line tank at total pressure of the mixture p_Σ = 210 Torr. Appearance of waveforms for $\mathbf{T_{stag}}$ practically did not change with decrease of r ($r \le 4$) up to injection of pure propane.

In Fig.5.2.5a and Fig.5.2.5b one can see discharge photos and $\mathbf{T_{stag}}$ waveforms illustrating said above at injection to the discharge of pure air and of propane-air mixture with r = 4 from the initial tank with p_Σ = 210 Torr. Sizes of discharge areas can be estimated by the size 2c = 6.5 mm. Waveforms were obtained at warm thermojunction of thermocouple measurer in the point x = 19 mm. Vertical scale in the waveforms is– 2 mV/div. So the voltage is U_{max} ≈ 3 mV at $U_{1/2}$ ≈ 2.4 mV for the waveform in Fig.5.2.5a, and U_{max} ≈ 3.8 mV at $U_{1/2}$ ≈ 2.8 mV for the waveform in Fig.5.2.5b . Values k = 1.55 and k = 1.8To correspond to the ratios $U_{1/2}/U_{max}$ on the graph in Fig.3.12. So one has T_{stag} = 414 K using Eq.(3.2) at discharge switching on in the measuring point, i.e. the gas temperature grew for ΔT_{dis}= 114 K. T_{stag} = 468 K at injection of propane-air mixture, i.e. the gas temperature additionally grew for only ΔT_{com} = 54 K.

Results of energy interaction of EM beam with discharge area were represented in previous report on the Project. There was shown that about of P_{MW} = 160 W was putted to air heating in the discharge at the beam power of P_{gen} = 1.5 kW , and air was heated at that for ΔT_{dis} ≈70 K. $\mathbf{\Delta T_{dis}}$ became about two times greater at application of the vibrator in these investigations. But additional maximum air heating due to propane combustion was ΔT_{com} = 130 K in previous experiments, and this is about three times smaller of this value in the present experiments. This demonstrates rather ineffective propane combustion organization in the present experiments. Really, total power of propane combustion was estimated as P_{com} = 400 W in previous experiments at minimum rate of propane injection. rate of propane delivery to the discharge area in present experiments at Δp_Σ = 33 Torr and r = 4 can be estimated as $m_{pr} \approx 10^{-2}$ g/s, this gives P_{com} ≈ 600 W with accounting of its combustion heat.

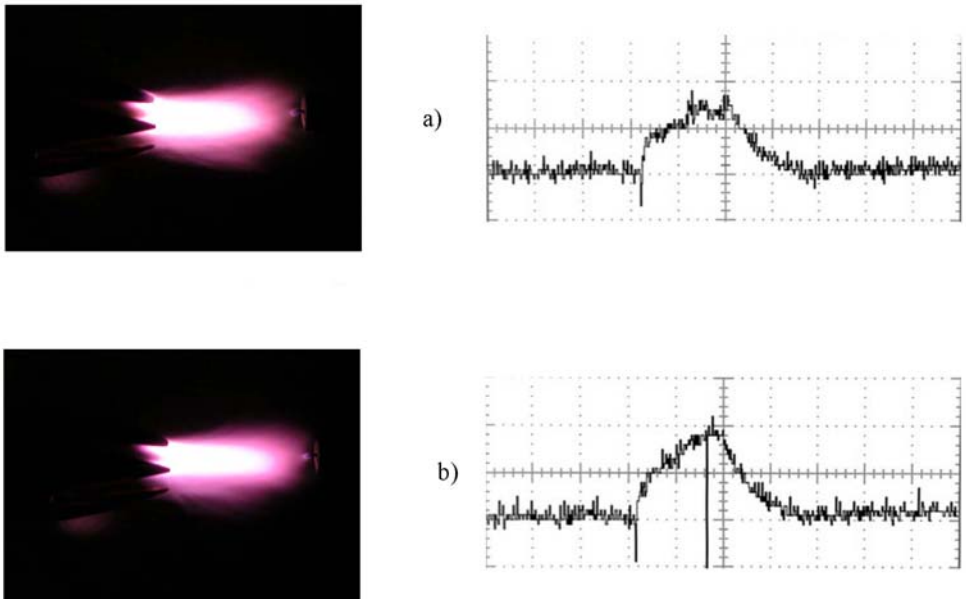

Fig.5.2.5 Two discharge realizations and corresponding waveforms from stagnation temperature sensor at p = 210 Torr.

For example in Fig.5.2.6 are represented superimposed waveforms of pstag at x = 25 mm for the same cases, i.e. with r = ∞ and r = 4. One can see in it that additional energy put of propane combustion is not traced in the waveforms of $\mathbf{p_{stag}}$. In this connection in this experimental series we applied only thermocouple measurer of $\mathbf{T_{stag}}$ more sensitive for this experimental formulation.

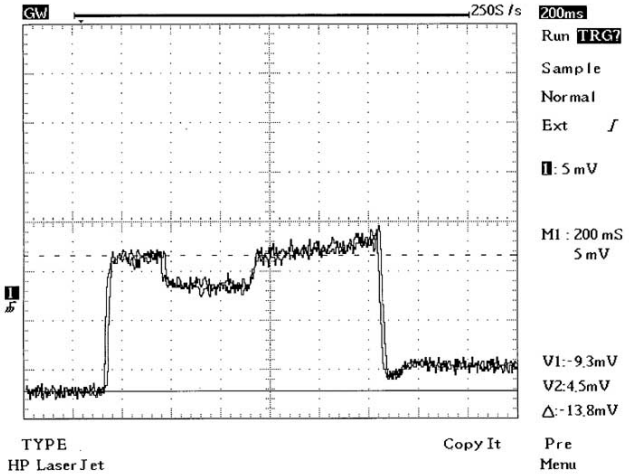

Fig.5.2.6 Superimposed waveforms of p_{stag} at x = 25 mm for r =∞ and r = 4.

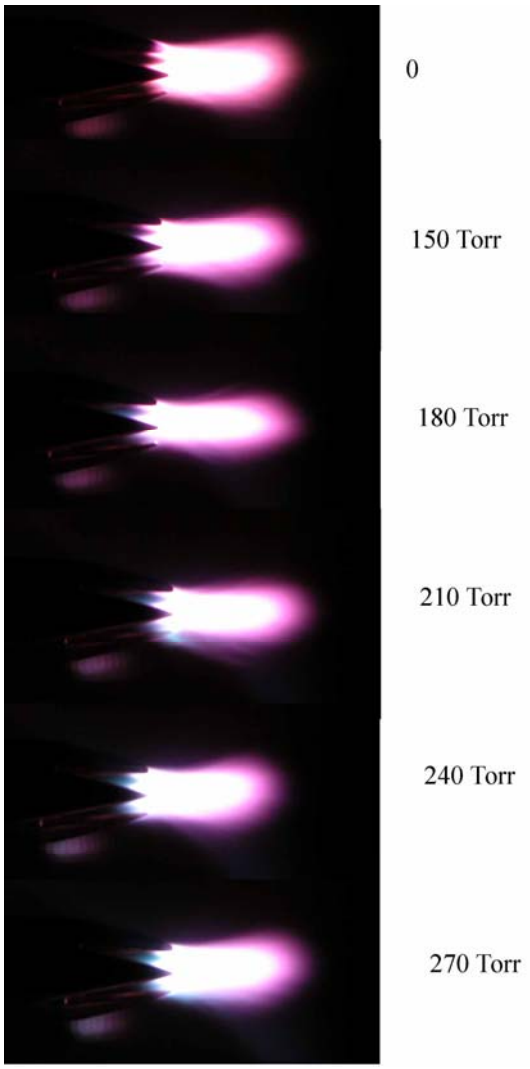

Fig.5.2.7 Discharge appearance photos at absence of propane injection to its area (upper photo) and at pure propane injection at varying of p.

In Fig.5.2.7 for additional example is represented a set of discharge appearance photos at propane injection absence – the upper photo, and at pure propane injection at variation $\mathbf{p_\Sigma}$,

starting from p_Σ = 150 Torr to p_Σ = 270 Torr. It can be seen that discharge appearance in this changes weakly.

5.3. Experiments with flammable mixture preliminary prepared in the injection line with formed "combustion chamber"

The base vibrator part in this experimental series was added by the nozzle in the form of radio transparent PVC tube, as it is shown in Fig.5.3.1. Internal diameter of this tube is 2b = 10 mm, and external is 12 mm. PVC tube is rather elastic, so it is densely covers the base vibrator end.

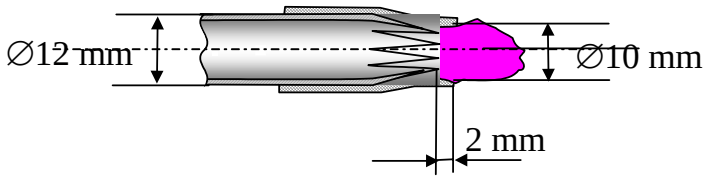

Fig.5.3.1 A vibrator with a nozzle

The base cut of the nozzle in the described experiments goes beyond vibrator's teeth h = 2 mm, as if it forms the combustion chamber. Flammable mixture pressure in initial tank in the injection line was constant p_Σ = 210 Torr, and propane percentage was changed. Remind that there was decrease of $\mathbf{p_\Sigma}$ for Δp_Σ = 33 Torr during $\boldsymbol{\tau_{inj}}$. Initial tank in each definite experiment of this series firstly was filled by propane up to chosen pressure $\mathbf{p_{pr} \le p_\Sigma}$, and then was filled by air additionally up to $\mathbf{p_\Sigma}$.

In Fig.5.3.2 one can see a set of photos of discharge region in this experimental series. There is a value of ratio $p_{pr}/(p_\Sigma - p_{pr})$ near each of them, this allows to estimate relative weight air content to those of propane r in flammable mixture injected to the discharge area. Calculated values of r in initial mixture are also represented near photos. Left upper photo in the set corresponds to injection of pure propane, right second from below corresponds to injection of pure air, and right bottom corresponds to the discharge at presence of SS stream and at absence of injection, i.e. without valve opening in the injection line. From photos it follows that discharge region color in propane and air is significantly different. It is blue in propane, and it is pink in air. It follows from the photos that the color of the discharge area gradually transforms from blew to pink at decrease of propane amount in the mixture. PVC tube used in experiments was not thermally proof, so its edge was slightly burnt in the course of experiments.

In Fig.5.3.3 one can see a set of waveforms $\mathbf{T_{stag}}$ corresponding to the experimental sequence represented in Fig.5.3.2, vertical sensitivity in them is 2 mV/div. It follows from them that amplitudes $\mathbf{U_{max}}$ practically coincide at injection of pure propane and pure air, i.e. injected pure propane does not combust in this experimental formulation. The amplitude $\mathbf{U_{max}}$ grows with gradual increase of air amount in initial mixture up to the value of $r \approx 4$. It stays constant up to $r \approx 11$. This value is slightly smaller of stoichiometric ratio of air and propane. Then $\mathbf{U_{max}}$ begins to drop down. So one can suppose that the same amount of propane combusts in the range from r = 4 to r = 11, i.e. it combusts totally at $r \ge 11$. At that at r = 11 the mixture in the combustion area becomes stoichiometric with $r \approx 16$ due to addition of air from the external flow, and at greater **r** propane combusts in excess of air.

Comparison of Fig.5.3.3 and Fig.5.3.2 shows that propane blue color remains at propane incomplete combustion in the discharge area. Blue propane color is practically absent starting from r = 11, i.e. at complete propane combustion.

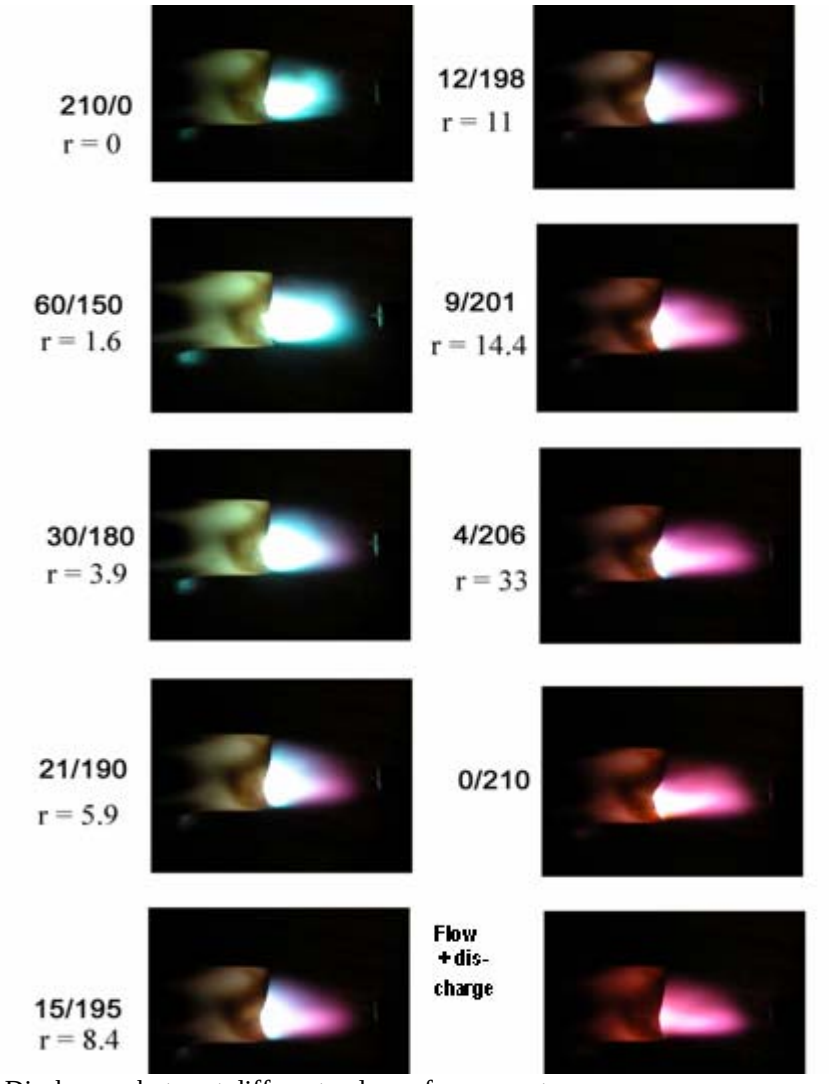

Fig.5.3.2 Discharge photos at different values of **r** parameter

From photos one can see that the discharge area is deposed below especially at air excess in initial mixture. It can be explained by the following: badly flown around vibrator fastening "foot" shadows SS stream namely from below.

Quantitative analysis of waveforms gives the scale of air heating $\Delta T_{dis} \approx 86$ K due to only MW discharge burning in it and additional maximum its heating $\Delta T_{com} \approx 170$ K. due to propane combustion. Hence increase of air temperature **T** in these experimental conditions is by two times greater due to propane combustion than due to only MW discharge. Presented values are close to analogous data obtained at previous stage of works on this Project $\Delta T_{dis} \approx 70$ K and $\Delta T_{com} \approx 130$ K. These results allowed to coming to experiments on this scheme with air intake for its mixing with propane and SS stream.

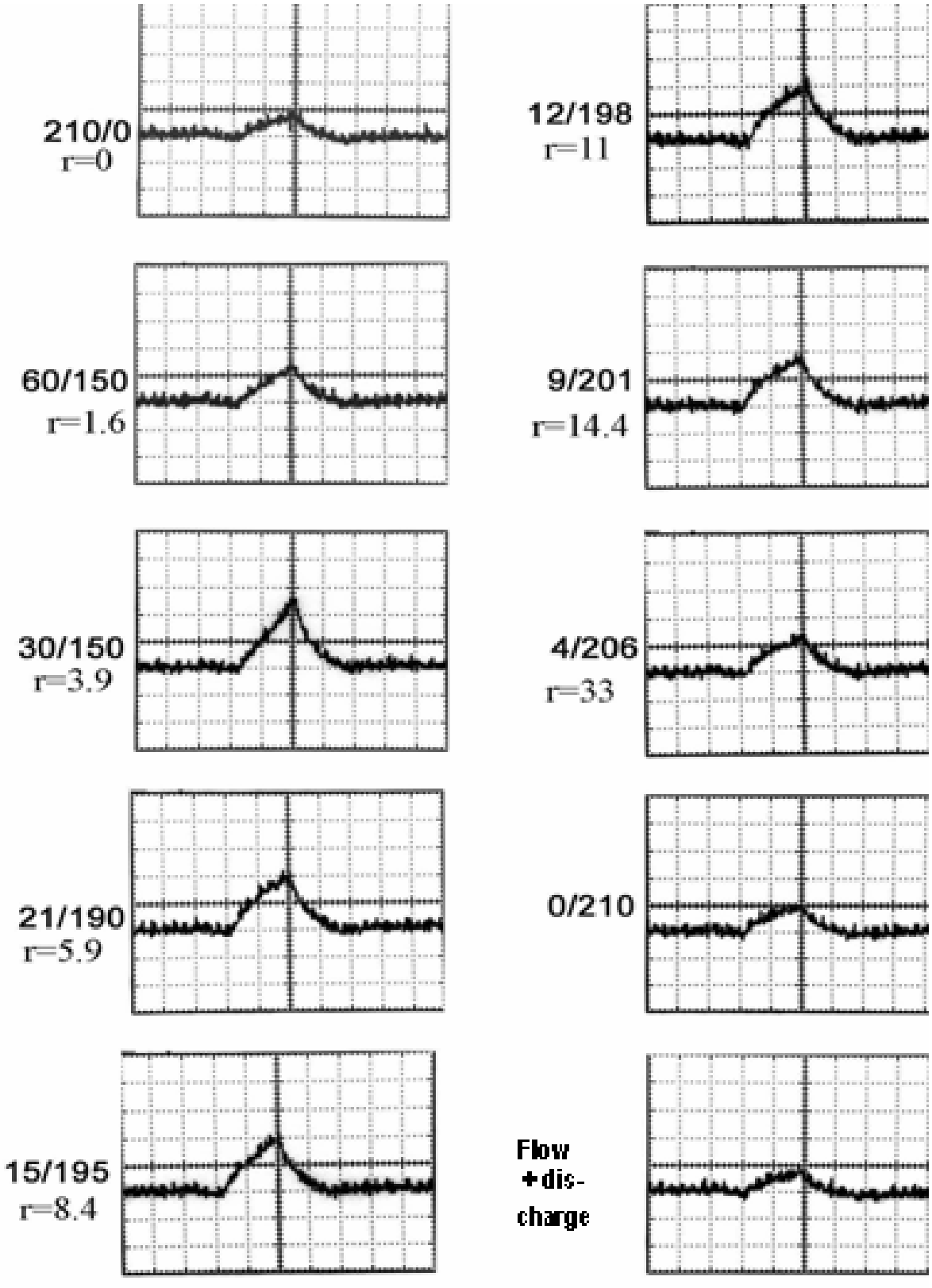

Fig.5.3.3 Waveforms from stagnation temperature sensor at different values of **r** parameter

5.4. Experiments with air delivery from the SS stream to the area of its mixing with propane

In this experimental series there was combustion chamber in the vibrator base part. Air was delivered to the internal volume of the initiator from SS flow, and pure propane was delivered to the chamber from the hole of diameter 2d = 0.6 mm through the injection line.

In initial experiments of this series there was made the axial hole of diameter with 2e = 1 mm in the nose dielectric fairing of the vibrator. Experiments showed that the signal amplitude of the signal $\mathbf{T_{stag}}$ from the thermocouple sensor firstly increases and then decreases with increase of propane delivery to the region of its mixing with air. In the end it almost approaches the waveform T_{stag}, which the sensor detects at MW discharge burning only in air. At that the color of the discharge area gradually changes from pink to blue with increase of propane delivery. Maximum amplitude $\mathbf{T_{stag}}$ is detected and propane delivery when Δp_Σ = 9 Torr is in initial tank of its injection line.

In Fig.5.4.1 one can see a photo of tested design in the working position, and in Fig.5.4.2. are for example represented discharge area photos at different propane delivery to the mixing area: In Fig.5.4.2a at zero propane delivery, in Fig.5.4.2b – at Δp_Σ = 9 Torr (p_Σ = 210 Torr), and in Fig.5.4.2c - at Δp_Σ = 18 Torr (p_Σ = 270 Torr). There are also represented the corresponding waveforms $\mathbf{T_{stag}}$. Lower beam in each waveform shows for reference variation of pressure $\mathbf{p_c}$ in the chamber at presence of SS stream.

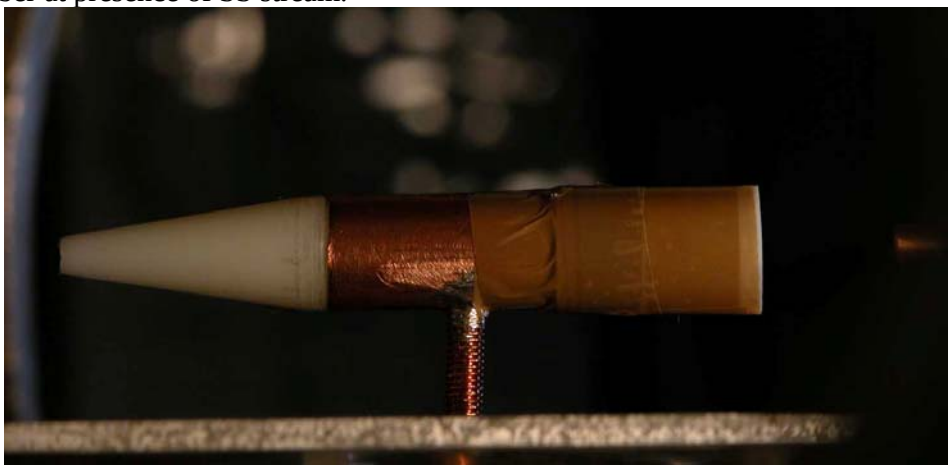

Fig.5.4.1 A photo of testing construction in working position.

Analysis of the waveform at optimal propane injection gives practically the same combustion power $\boldsymbol{P_{comb}}$ as it was in earlier described tests with preliminary prepared flammable mixture in initial tank of injection line.

Air inletting hole diameter in the nose vibrator fairing was increased up to 2e = 1.5 mm in the next series of experiments. Character of measured $\boldsymbol{T_{stag}}$ behavior with $\mathbf{\Delta p_\Sigma}$ increase was analogous to those of the previous series, but the signal amplitude from the thermocouple sensor was significantly greater at optimal injection. For example, in Fig.5.4.3 is represented a photo of the discharge area at optimal $\mathbf{\Delta_{p\Sigma}}$ and the waveforms $\boldsymbol{T_{stag}}$.

The lower waveform in it corresponds to discharge burning in air at absence of propane injection. The tube-type post fastening the vibrator was located in dielectric fairing during this experimental series, as one can see in Fig.5.4.3. The area of discharge burning and propane combustion became more symmetric over the height.

It follows from the waveforms in Fig.5.4.3 that $\Delta T_{dis}\approx$140 K and $\Delta T_{com}\approx$550 K are in these experimental conditions. Hence, increase of air temperature **T** in these conditions was by 4 times greater due to combusted propane than its temperature rise due to MW discharge.

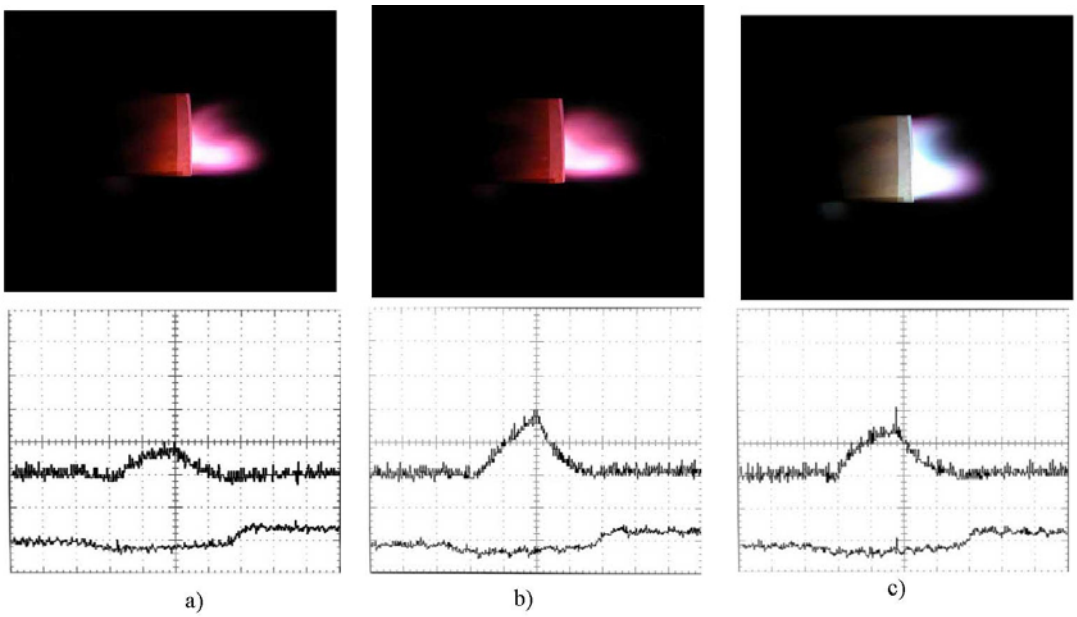

Fig.5.4.2 Discharge area photos at different propane delivery to mixing area: a) – at zero propane delivery, b) - at p = 9 Torr (p = 210 Torr) and c) - at p = 18 Torr (p = 270 Torr).

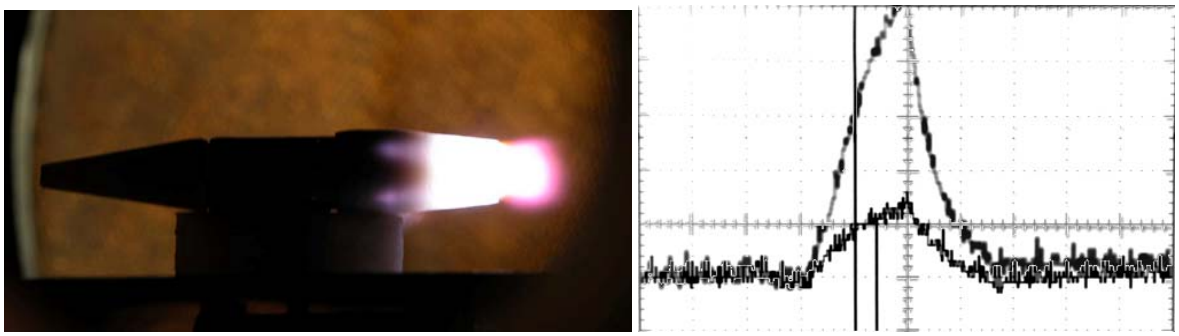

Fig.5.4.3 A discharge in the base part of the vibrator fixed to a post with aerodynamic shape (to the left) and waveforms from the stagnation temperature sensor for air-propane mixture and pure air.

So experiments showed that present scheme allows in principle to set amount of burning out propane proportionally increasing delivery of the fuel and air into discharge area.

6. Comprehensive experiment

In previous section we described experiments devoted to search of propane-air mixture optimal ignition scheme with a help of deeply undercritical MW discharge. The scheme in principle had to allow burning out required amount of the mixture. Design of separate elements of the device were changed during this search so obtained quantitative dependences were not sometimes mutually matched. In this section we describe experiments on measuring of “through” quantitative dependences set without principle change of the chosen design. Last experimental target was obtaining of data allowing evaluating the interaction energy efficiency of EM field exciting the discharge and the discharge plasma and propane combustion efficiency as well.

In Fig.6.1 one can see testing device design. In this device we use a vibrator made of a copper pipe 2 L = 42 mm length, outer diameter of 2a = 12 mm, internal diameter 2b = 10 mm and a circle diameter of 2c = 5.5 mm created by ends of the vibrator sharpened base teeth. A distance between the vibrator axis and the screen is H = 24 mm. The vibrator is fixed to a copper pipe located in a dielectric fairing, which is perpendicular to the vibrator. This pipe is a post with an outer diameter of 4 mm and internal diameter of 2 mm. Outlet hole diameter of propane injection line to internal vibrator area was 2d = 0.6 mm.

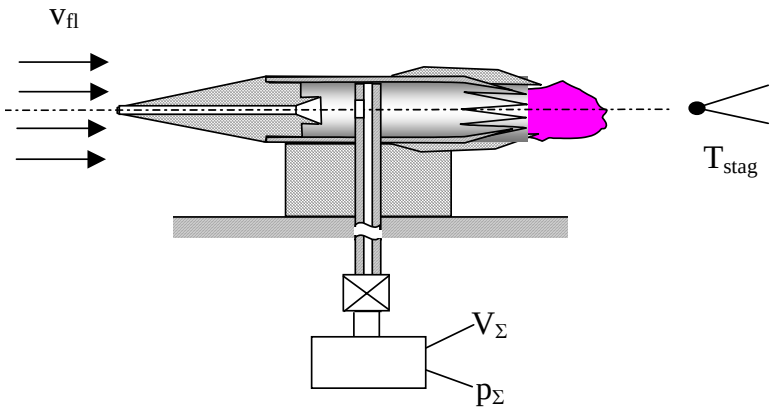

Fig.6.1. Sketch of device for ignition of air-propane mix by attached undercritical MW discharge in SS flow

Axial diameter of a hole in the nose dielectric fairing of the initiator is 2e = 1.5 mm. Air from SS flow comes to internal vibrator area through this hole. Base radio transparent dielectric nozzle over the initiator was made of glass fiber plastic in present experiments. It is more heat-resistant material than poly vinyl chloride used earlier. Internal outlet nozzle diameter was 2f = 8 mm. Its base cut comes out of sharpened vibrator's teeth for a distance of h = 5 mm.

6.1. Mass flow rate of injected propane

In Fig.6.1.1a one can see experimental graph of the absolute value of Δp_Σ dependence on p_Σ: $|\Delta p_\Sigma| = f(p_\Sigma)$ - at constant injection time при τ_{inj} = 0.5 s. This experiment was undertaken with switching on of SS stream. It was executed without MW discharge burning. In order not to load up the setup vacuum volume by propane we undertook this experiment with air. Experimental data for air are represented in the graph in a form of bold points. Then the pressure drop was measured in the injection tank with propane only at several values of Δp_Σ. These experimental data are represented in the graph in a form of crosses; they are also connected by approximation curve.

The experiment has shown that the pressure in the buffer volume of the injection line rose during the time τ_{inj} in experiments in air at p_Σ < 225 Torr. The gas began to flow out of this volume only at p_Σ > 225 Torr. The pressure drop Δp_Σ in this volume at that gradually rose at following rise of p_Σ. So air injected to internal volume of the vibrator (through its nose hole) creates a pressure p_Σ = 225 Torr in the region of the outlet hole of the injection line in the presence of SS stream. Let us suppose that this value p_Σ is a stagnation pressure of air flowing around the injection tube of propane and injected to internal area of the initiator. A ratio of this value and static pressure in this volume, $p_{stat} = p_c$ = 105 Torr, is the Mach number of airflow in the internal area of the initiator at the section from the inlet hole up to the tube of propane injection, which can be determined with a help of the graph in Fig.3.11, and it equals to M = 1.1.

There are experimental points for the case of injection line buffer volume filled by pure propane in this graph $|\Delta p_\Sigma| = f(p_\Sigma)$, as it was indicated before. In Fig.6.1.1a one can see that $|\Delta p_\Sigma| = f(p_\Sigma)$ dependences are similar for air and propane. At the same time the mass flow rate of propane is slightly smaller than the mass flow rate of air at the same p_Σ. Propane begins to be injected to the internal vibrator area also at p_Σ > 225 Torr. Foe example decreasing Δp_Σ = 3 Torr corresponds to p_Σ = 250 Torr.

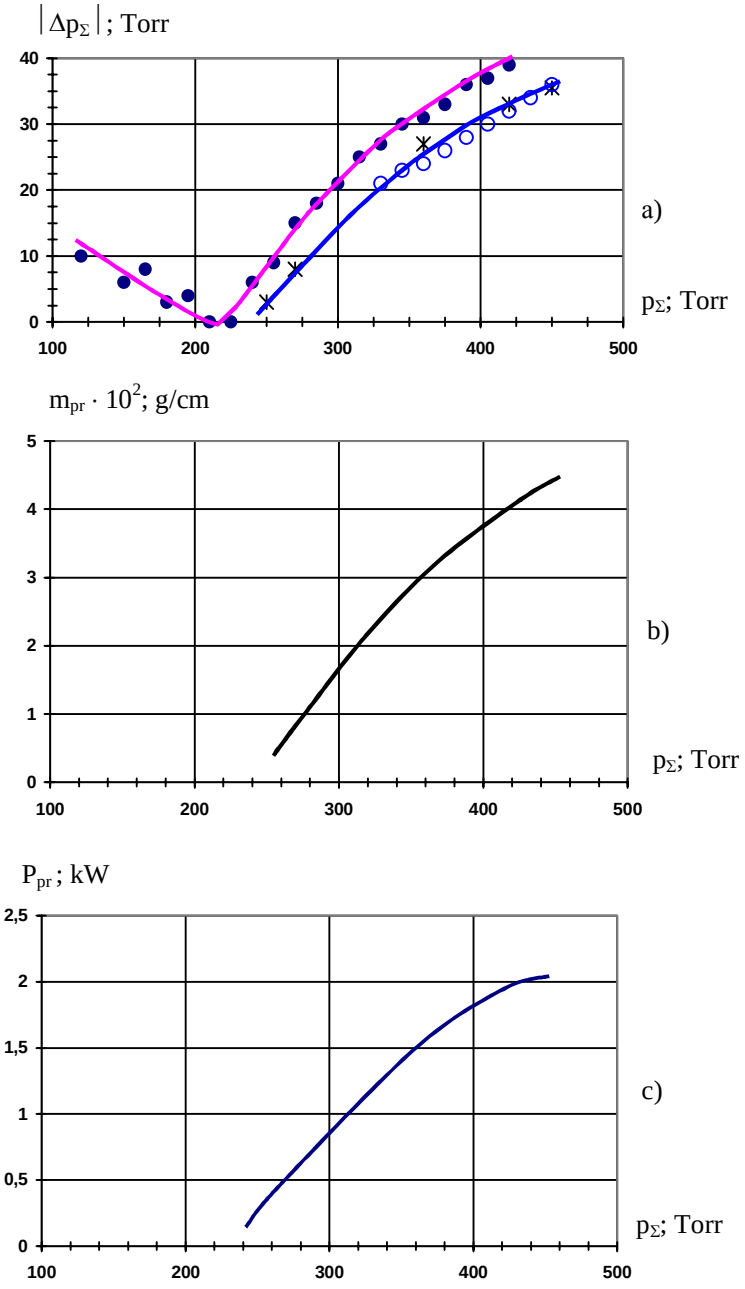

Fig.6.1.1.Dependence on initial pressure in the tank with propane: a) – of the pressure change during time of the valve switch on, б) – of the average mass flux of propane, c) – of burning power of propane in supposition of its full oxidation.

In Fig.6.1.1a data represented by circles characterize propane injection rate already at combustion of propane and MW discharge burning in the base part of the vibrator. These data is taken from the following parts of the Report.

For references in Fig.6.1.1 are represented calculated data of injected propane mass flow rate $\boldsymbol{m_{pr}(p_\Sigma)}$ (Fig.6.1.1b) and propane combustion power at its complete combustion $\boldsymbol{P_{pr}(p_\Sigma)}$ (Fig.6.1.1c) obtained with a help of the Eq.(3.1) and experimental data.

6.2. Calibration of p_{stag} measurer

Clarification absolute calibration of stagnation pressure $\boldsymbol{p_{stag}}$ measurer and check up of its linearity with respect to measured pressure value was made during these experiments. The

measurer was made on a basis of Pitot tube. For this purpose fixed pressure $\boldsymbol{p_c}$ is set in the working chamber , this pressure is measured by a calibrated pressure-vacuum gage. A signal from the Pitot tube located in the working chamber is given to an inlet of an oscilloscope with memory, and the signal level is identified with pressure-vacuum gage results.

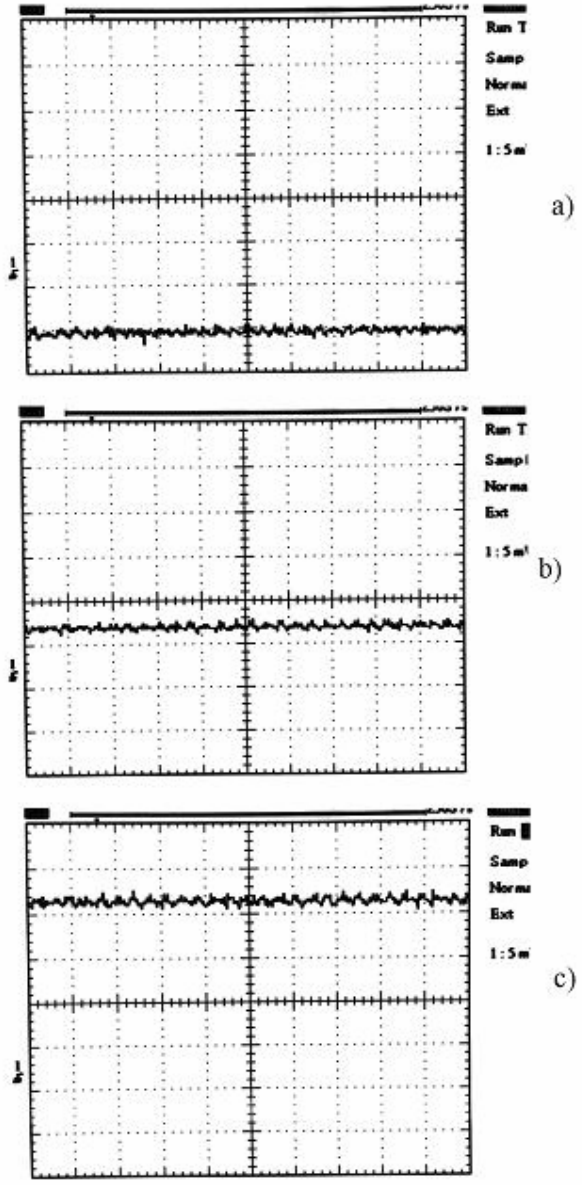

Fig.6.2.1. The waveforms of gauge of tube Pitot at: p_c = 114 Torr - a), p_c = 200 Torr - 1b), p_c = 300 Torr - c)

In Fig.6.2.1 one can see waveforms at p_c = 114 Torr (рис.6.2.1a), p_c = 200 Torr (Fig.6.2.1b) and p_c = 300 Torr (Fig.6.2.1c). A horizontal scale in the waveforms is 0.2 s/div as in all other analogous waveforms, a vertical scale is 5 mV/div. One can see in the waveforms that gas pressure detection scheme including Pitot tube and electronic part has a scheme noise even at measurements of static pressure. Mutual analysis of the waveforms gives absolute vertical sensitivity of the stagnation measurer scheme S = 7.1 Torr/mV. At that linearity of this measurer with respect to pressure was confirmed.

In Fig.6.2.2 one can see additional fragment of the waveform $\boldsymbol{p_{stag}}$ at switching of SS stream obtained with a help of this measurer. A vertical scale in it is also equals to 5 mV/div, initial and final parts are still $p_{c\,0}$ = 114 Torr and $p_{c\,end}$ = 132 Torr. A difference between them equal to 18 Torr also corresponds to S = 7.1 Torr/mV.

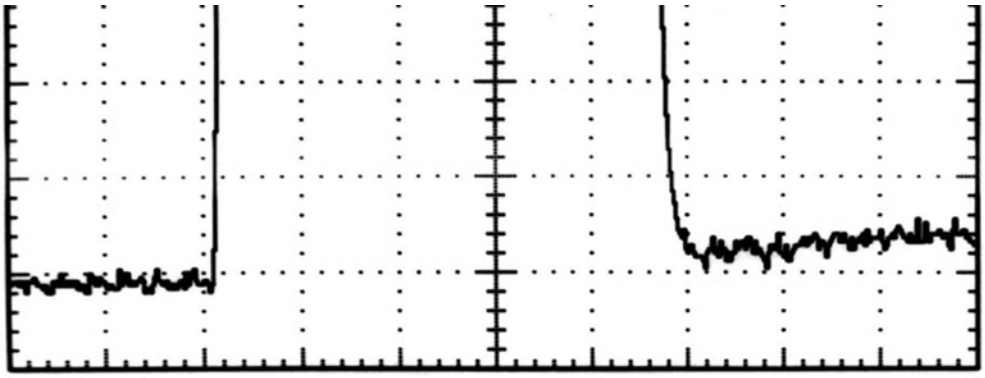

Fig.6.2.2. Fragment of waveform $\boldsymbol{p_{stag}}$ at SS flow switching

6.3. Aerodynamic airflow parameters in near wake of the vibrator

We determined parameters of aerodynamic flow in the near wake of the given vibrator also as in the section 5.2. $\boldsymbol{p_{stag}}$ is measured for this purpose in several points $\boldsymbol{x}$ over the vibrator axis. During these measurements we did not close a nose hole of the vibrator. A valve is opened in the injection line during the experiments, its volume is filled with air at initial pressure p_Σ = 420 Torr. Axis $\boldsymbol{x}$ is still counted out from the base of a nozzle put on the vibrator. In Fig.6.3.1 one can see a photo of testing device at one of measuring Pitot tube positions.

Fig.6.3.1. Photo of the tested device at some location of Pitot tube

In Fig.6.3.2 one can see typical waveforms with indicated coordinate $\boldsymbol{x}$ in them. Pulses tops in the waveforms have complicated temporary character. Noise fluctuations amplitude raises on the tops, the fluctuations exist also at pressure measurements in flow absence. Relatively smooth variation of a signal level on the pulse top principally repeats pressure variation character in the chamber $\boldsymbol{p_c}$ at SS stream switched on (see Fig.3.8). The amplitude of these changes rises at the same time. Several measurements were made at each $\boldsymbol{x}$ value in the range $x < 8$ mm. This allowed to evaluated their repeatability. For example in Fig.6.3.2 we represent two waveforms at $x = -2$ mm and $x = -1$ mm. Their comparison shows high stability of aerodynamic processes at different switching on of the set up.

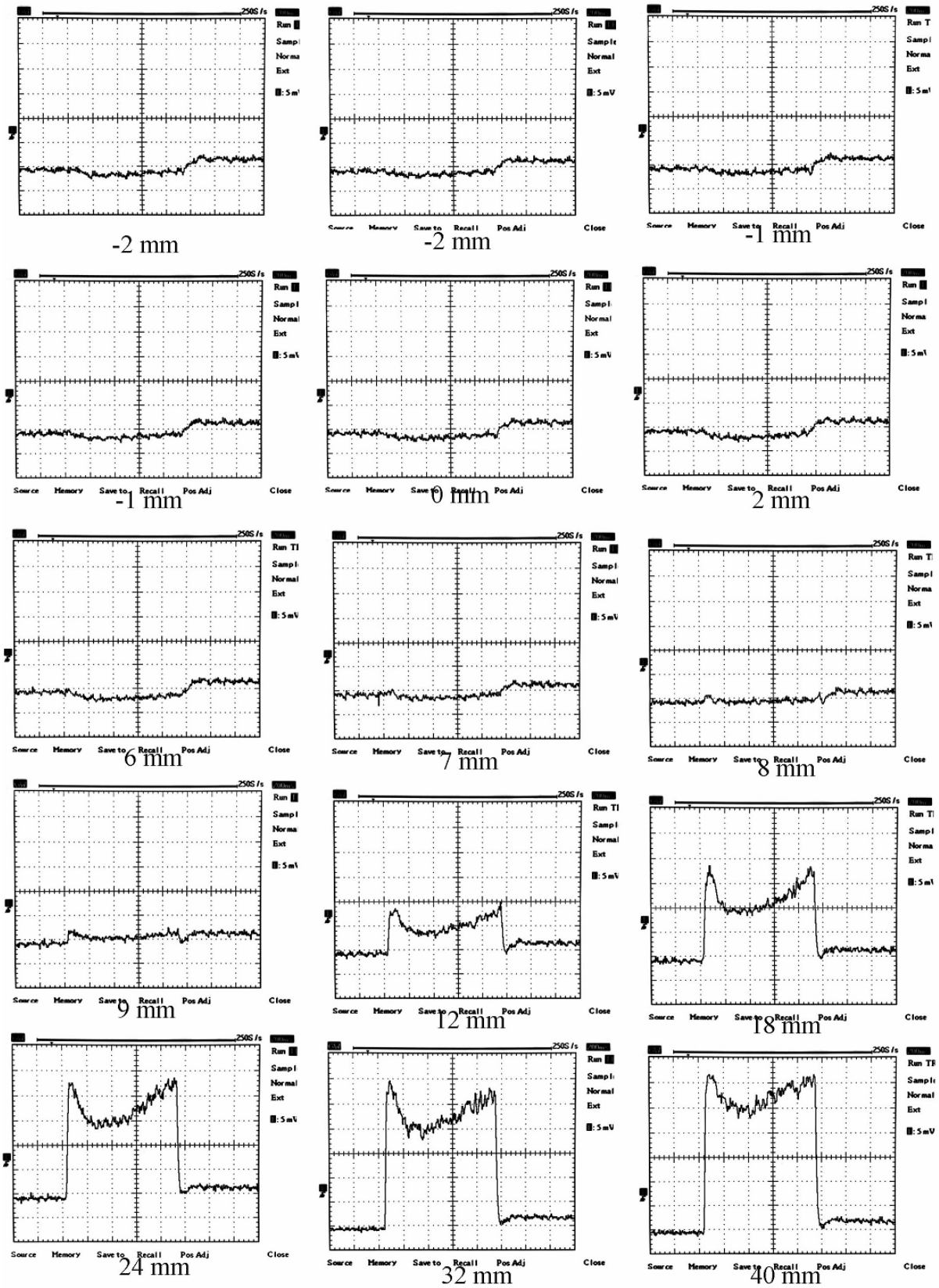

Fig.6.3.2. The waveformes of gauge $\mathbf{p_{stag}}$ at different locations on the system axis at the air injection through mixer without MW discharge.

In Fig.6.3.3a is represented an experimental graph of $p_{stag}(x)$ dependence obtained with a help of the represented waveforms. p_{stag} value was determined during approximately 0.4 s,

measurements were made 0.2 s after the valve opening at the inlet of the Laval nozzle to the flow. p_{stag} is minimal and approximately constant during these 0.4 s. One can see in the graph that measured stagnation pressure practically does not change in the range –1 mm ≤ x ≤ 7 mm and equals to p_{stag} = 108 Torr. Then it starts to rise, but at x = 40 mm it is still below p_{stag} ≈ 500 Torr, which is a parameter of the free stream.

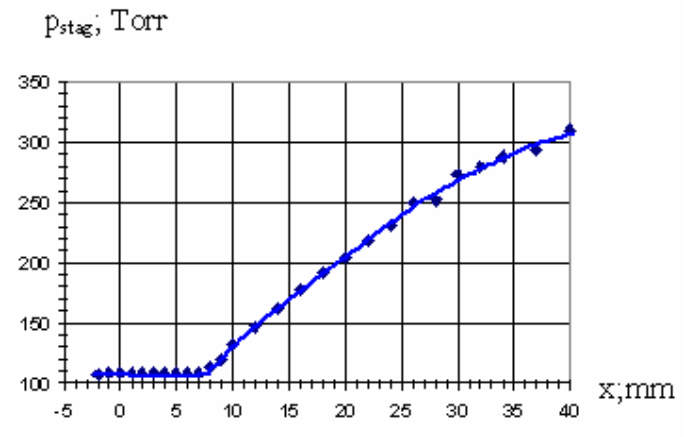

Fig.6.3.3.a. Measured dependence $p_{stag}(x)$

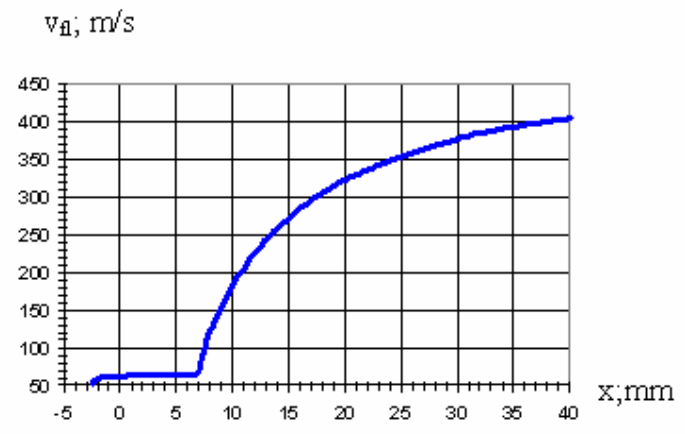

Fig.6.3.3б. Dependence $\mathbf{v_{fl}}(x)$, calculated from Fig.7.3.3a

In Fig.6.3.3b one can see $\mathbf{v_{fl}}(x)$ depe4ndence calculated with a help of the graph in Fig.6.3.3a. We accepted p_{stat} = 105 Torr = const in the calculations. It was determined with a help of the waveform represented in Fig.3.8.

$\mathbf{v_{fl}}$ calculation scheme for Fig.6.3.3b was the following. Firstly we determined a ratio of measured p_{stag} in some definite point x and p_{stat} . Then the corresponding flow Mach number in this point was determined with a help of the graph in Fig.3.11. Using determined Mach number we obtained T_{stag}/T_{stat} with a help of the graph in Fig.3.13. T_{stag} equals to room temperature in this experimental formulation, so obtained ratio T_{stag}/T_{stat} determines also T_{stat} in this point. In its turn it determines a local value of a sound velocity, which product with M gives $\mathbf{v_{fl}}$.

It follows from Fig.6.3.3b that the flow velocity is constant and is v_{fl} = 68 m/s in the range–1 mm ≤ x ≤ 7 mm, i.e. in the near wake of the vibrator. Then v_{fl} begins to rise. It gradually approaches a velocity of undisturbed flow v_{fl} = 500 m/s.

6.4. A rate of air delivery to an area of its mixing with propane

One can suppose that v_{fl} value calculated with a help of experimental data and represented in Fig.6.3.3b ($v_{fl} = 6.8 \cdot 10^3$ cm/s at the distance (–3) ≤ x ≤ 7mm) is determined by a rate of air delivery to an internal vibrator area through a hole in its nose fairing. This supposition allows to determine a rate of air delivery:

$m_{air} = v_{fl} \cdot \rho_{in}$. S; g/s. (6.4.1)

This is the estimate since an accuracy of obtained $\mathbf{v_{fl}}$ value used in this formula is not high. $\mathbf{p_{stag}}$ is insignificantly different from $\mathbf{p_{stat}}$ in this range of **x**. Determination accuracy of a cross section ***S*** through which air flows out of the base vibrator region is not high in measuring points in the given range of ***x***. Remember that this area has a complicated geometry of six draw in teeth. Pitot tube measuring end is located in this area, its outer diameter is 2g = 4 mm. Let us accept that $S \approx \pi \cdot (e^2 - g^2) = 3.8 \cdot 10^{-1}$ cm^2. Air density is $\rho_{air} = \rho_{760} \cdot (p_{stat} / 760)$ in the Eq.(6.4.1), here $\rho_{760} = 1.23 \cdot 10^{-3}$ g/cm^3 and p_{stat} = 105 Torr. The Eq.(6.4.1) gives $m_{air} = 4.4 \cdot 10^{-1}$ g/s accounting this values.

Air delivery rate to the mixing zone can be also determined with a help of well known aerodynamic formulas of air flowing out of the nose hole of the vibrator fairing at an inlet and an outlet of this hole.

Earlier we accepted that the pressure inside the vibrator area is maintained equal to the pressure in the chamber p_c = 105 Torr. Air pressure at an inlet of the hole is approximately equal to the flow stagnation pressure. The last depends, in principle, on a form of the nose vibrator fairing. We undertook a special experiment for its determination.

Fig.6.4.1. Photo of the mixer with attached Pitot tube

Measuring Pitot tube in this experiment is hermetically lead to the base vibrator end as it is shown in Fig.6.4.1. The valve in propane injection line is closed at its leading to. The pressure is measured in the internal region of the initiator, and in essence $\boldsymbol{p_{stag\ inter}}$ is measured in the area of the nose hole of the vibrator fairing. In Fig.6.4.2 one can see the corresponding waveform. A vertical scale in it is 10 mV/div and the horizontal scale is 0.2 s/div as usual. From it follows, that $p_{stag\ inter}$ = 476 Torr Remember that $p_{stag} \approx$ 500 Torr in the free stream in this cross section.

Measured $\boldsymbol{p_{stag\ inter}}$ allows to calculate air injection rate $\boldsymbol{m_{air}}$ and to compare obtained value with earlier made estimate.

The ratio $\boldsymbol{p_{stag\ inter}} / \boldsymbol{p_c}$ is larger than 1.9 and hence critical mode of flow with M = 1 is realized in the nose hole of the initiator dielectric fairing. The following formulae is known for air flowing rate through this cross section:

$m_{cr} = m_{air} = \rho_0 \cdot v_{s\,0} \cdot S \cdot (1/1.73)$. (6.4.2)

Here $\rho_0 = \rho_{760} \cdot (p_{stag\ inter}/760)$ is air density and $v_{s\,0} = 3.4 \cdot 10^4$ cm/s is air sound velocity at the inlet of injection hole; $S = \pi \cdot e^2$ is a cross section of this hole, and 1/1.73 is a coefficient accounting air properties. In this case we have $\rho_0 = 7.7 \cdot 10^{-4}$ g/cm^3, $S = 1.77 \cdot 10^{-2}$ cm^2 and the

Eq.(6.4.2) gives $m_{air} = 2.7 \cdot 10^{-1}$ g/s. This value is close to $m_{air} = 4.4 \cdot 10^{-1}$ g/s estimated earlier. We will use $m_{air} = 3 \cdot 10^{-1}$ g/s in the following estimates.

Measured $\mathbf{p_{stag\ inter}}$ allows also to count Mach number of air flow in internal volume of the fairing, this air flows around propane injection tube. We use well known formulae

$$M = \sqrt{5 \cdot \left[\left(p_{stag\ inter} / p_c \right)^{(1/3.5)} - 1 \right]} . \qquad (6.4.3)$$

At p_c= 105 Torr it gives M = 1.1.

This experimental scheme of Pitot tube hermetic connection with the internal volume of the initiator allows to measure air leak in rate to a volume of propane injection line. Its results give additional information about this line parameters. Initial air pressure p_Σ = 105 Torr was set in the volume of the injection line during the present experiment, and this pressure increase was measured in presence of SS flow around the initiator and at opened valve during τ_{inj} = 0.5 s in the injection line. The experiment gave Δp_Σ = 24 Torr.

6.5. Selection of optimal r

$\boldsymbol{T_{stag}}$ is measured in this experiment at increasing of $\boldsymbol{p_\Sigma}$ in propane injection line during successive tests, i.e. by a variation of its injection rate $\mathbf{m_{pr}}$ to the internal vibrator zone where propane is mixed with air. Measurements are made in the same point, x = 14.5 mm, in the vibrator wake along its axis. In Fig.6.5.1 one can see a set of corresponding waveforms. A vertical scale in them is 2 mV/div, and a horizontal scale is a 0.2 s/div. MW discharge ignition time is τ_{dis} = 0.4 s. $\boldsymbol{p_\Sigma}$ value and nearby $\boldsymbol{\Delta p_\Sigma}$ (in Torr) in brackets are represented near each of the waveforms. There is a corresponding photo near a waveform. In photos to the left one can see the base end of the vibrator and an area of MW discharge and of propane combustion stretched out along the flow.

In the waveforms one can see that the signal amplitude $\boldsymbol{U_{max}}$ and its form change with $\boldsymbol{\Delta p_\Sigma}$ variation, i.e. the ratio $\boldsymbol{U_{1/2}/U_{max}}$ is changed. The amplitude of $\boldsymbol{U_{max}}$ firstly rises with the rise of $\boldsymbol{\Delta p_\Sigma}$, and then is somewhat drops down. In Fig.6.5.2 one can see a graph of $\boldsymbol{\Delta T(p_\Sigma)}$. $\boldsymbol{\Delta T}$ value was counted with a help of the Eq.(3.2) and data from the waveforms. In Fig.6.5.3 one can see the graph $\boldsymbol{\Delta T(m_{pr})}$. At that propane delivery rate $\boldsymbol{m_{pr}}$ to the zone of its mixing with air was calculated using experimental values of $\boldsymbol{\Delta p_\Sigma}$.

One can see from the graphs that there is an optimal propane injection rate, to which corresponds maximum temperature rise in energy release zone wake. It corresponds to $p_\Sigma \approx$ 390 Torr or $m_{pr} = 3.5 \cdot 10^{-2}$ g/s . At that we have the maximum value $\Delta T \approx 750$ K . Air delivery rate to the mixing zone estimated above was $m_{air} = 3 \cdot 10^{-1}$ g/s. So the “optimal” weigh ratio of air and propane in the region of their mixing is $r = m_{air}/ m_{pr} = 9$, i.e. it is at the outlet from the internal vibrator area. The stoichiometric ratio at the same time is $r \approx 16$. So we can suppose that deficient air comes to propane combustion area from external flow.

Let us consider now photos represented In Fig.6.5.1 on the waveforms. One can see that energy release zone changes its color with increase of $\boldsymbol{m_{pr}}$, its brightness and extension along the flow are changed as well.

Energy zone color is pink at small $\boldsymbol{m_{pr}}$ corresponding to p_Σ = 330 Torr. This color is typical for MW discharge in air. Small areas with the bleu color appear at p_Σ = 345 Torr near the base vibrator nozzle cut in the periphery radial regions of energy release zone. This color is typical for MW discharge in propane. These regions appear in more extent at p_Σ = 360 Torr. At that the brightness of energy release central area increases, and its base end continues to have the pink color typical for a discharge in air. Bleu halo practically covers all the central bright area with $\boldsymbol{p_\Sigma}$ rise. At that the pink color at p_Σ = 435 Torr practically disappears in the energy release zone far down the flow.

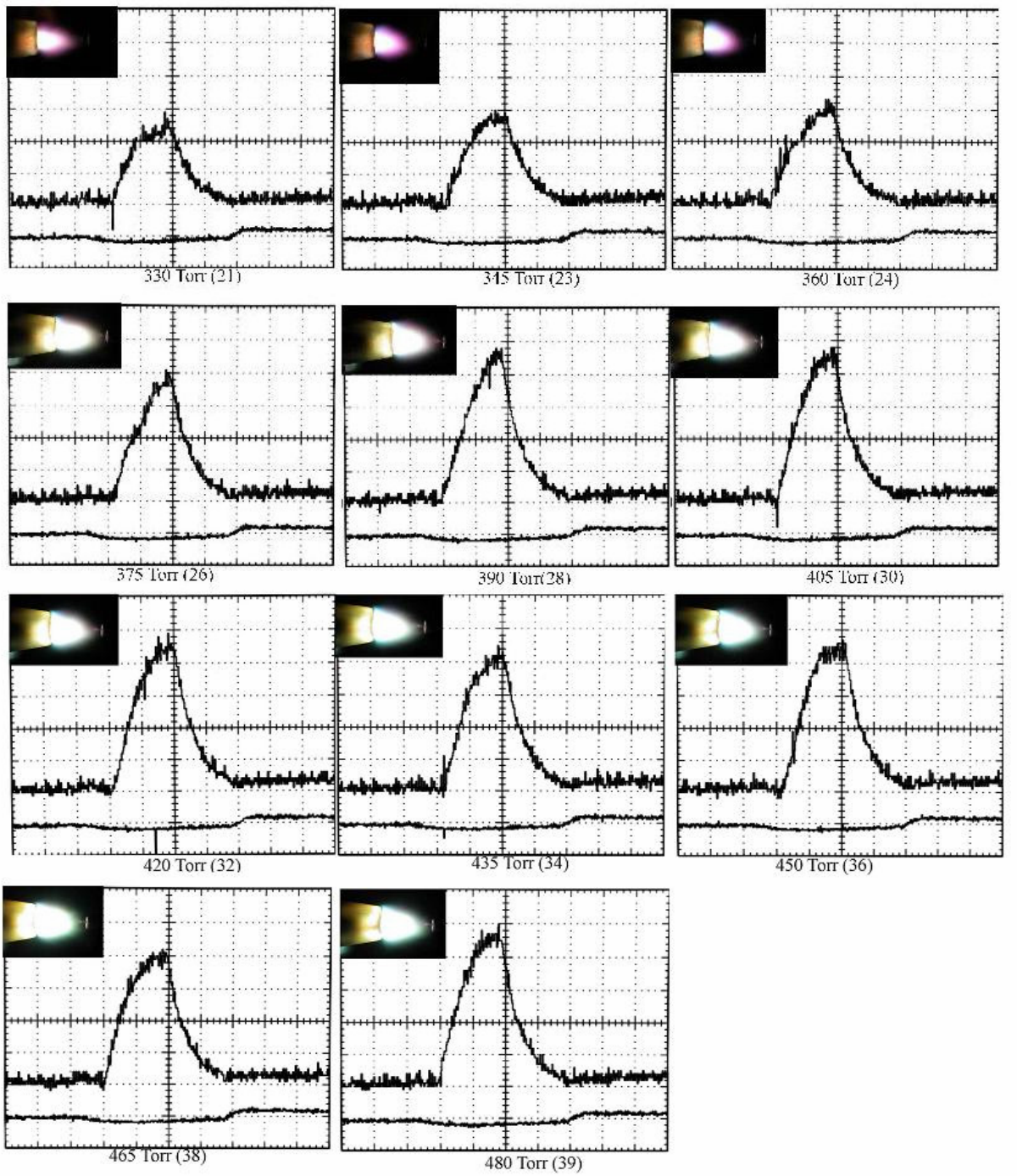

Fig.6.5.1. Waveformes of the temperature gauge at different magnitudes of initial pressure in the propane tank

We can suppose that described character of energy release zone color variation characterizes a level of burning out of propane delivered to the discharge area. It means that propane burns out practically immediately in the internal area of the nozzle at small $\boldsymbol{m_{pr}}$, and considerable its part does not burn out at all at $m_{pr} > 3.5 \cdot 10^{-2}$ g/s.

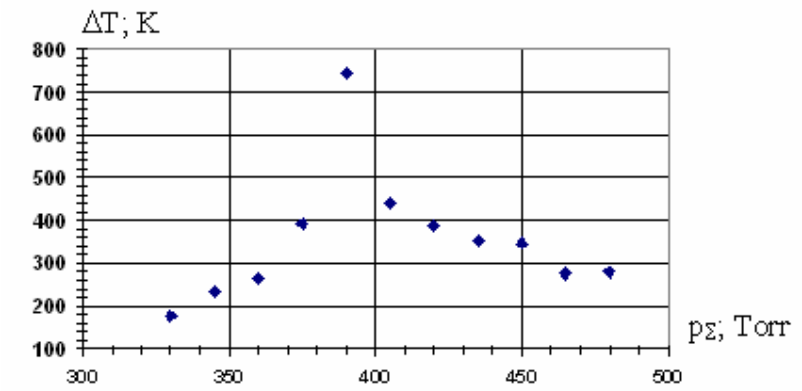

Рис.6.5.2. Dependence $\Delta T(p_\Sigma)$

Extension of energy release zone and increase of its internal area glow brightness leads to the following at $p_\Sigma \geq 375$ Torr : in photos one can already see a measuring end of T_{stag} thermocouple measurer. At that the distance between the far end (with respect to the flow) of the glowing zone and the thermocouple already practically does not change and detected T_{stag} drops down.

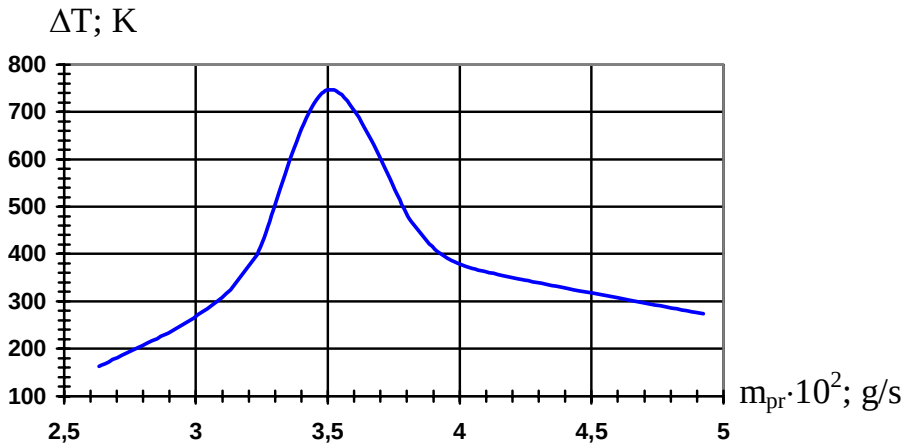

Fig.6.5.3. Dependence $\Delta T(m_{pr})$

6.6. Distributions of T_{stag} and p_{stag} fields

During these experiments we measured distribution fields of T_{stag} and p_{stag} in the vibrator wake in a plane perpendicular to $\mathbf{v_{fl}}$. The thermocouple or the Pitot tube are fixed for this purpose on a coordinate device, and their location is changed along a horizontal axis ***z*** and a vertical axis ***y*** at the same x = 14.5 mm. Experiments were made with a step 2 mm and a range ***y-z*** ±8 mm, where ***y*** and ***z*** are counted from the vibrator axis. The experiment showed that neither the vibrator nor energy release zone practically do not change parameters of initial flow in the stream at larger extension from this axis. Firstly in experiments a working end of a corresponding sensor is let down to the position y = -8mm, and a measurement is made along the horizontal axis. Then the sensor is lifted for 2 mm, and again we make a measurement along the horizontal axis, etc.

In Fig.6.6.1 one can see p_{stag} measuring results at MW discharge burning and injection of air (not propane) from the injection line to the discharge area at $p_\Sigma = 270$ Torr. At that $\Delta p_\Sigma = 9$ Torr during the injection time. Vertical sensitivity in the waveforms is 10 mV/div, a horizontal sensitivity is 0.2 s/div as in all the waveforms of the Report. The lower row of the waveforms in the set corresponds to y = –6 mm, the forth from below- to y = 0 mm, and the upper- to y = 6 mm. The last left column in the set corresponds to z = –8 mm, the fifth- to z = 0 mm, and the last right column -to z = 8 mm.

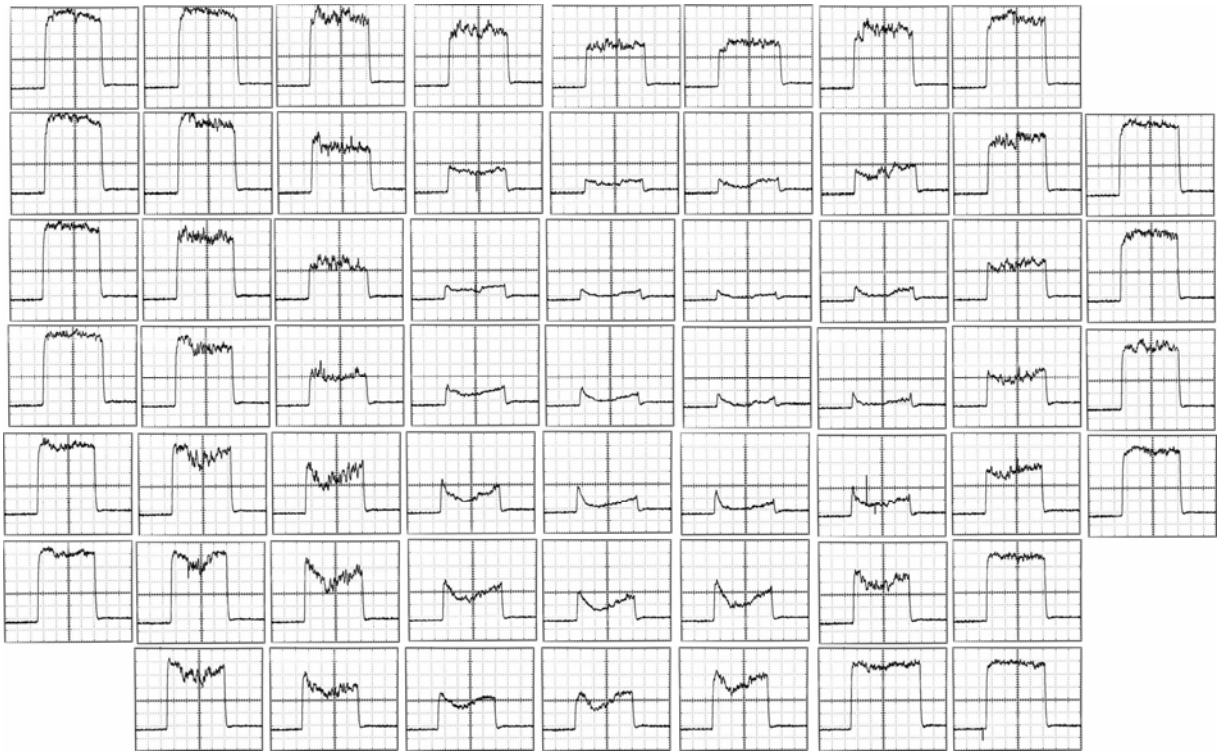

Fig.6.6.1. The measured waveforms $\boldsymbol{p_{stag}}$ in the control crosssection at air injection in the discharge area., p_Σ = 270 Torr.

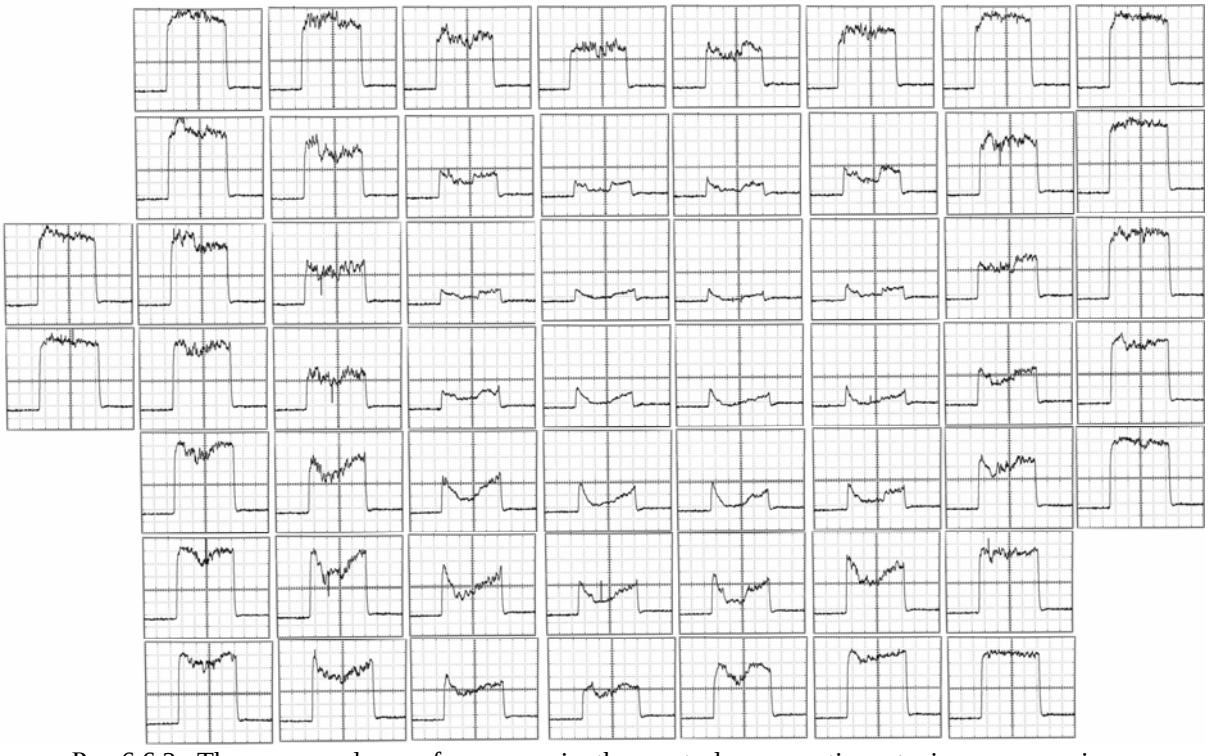

Рис.6.6.2. The measured waveforms $\boldsymbol{p_{stag}}$ in the control crosssection at air-propane mix injection in the discharge area., p_Σ = 390 Torr.

In Fig.6.6.2 one can see results of $\boldsymbol{p_{stag}}$ measurements at MW discharge burning and propane injection the discharge area at p_Σ = 390 Torr. At that Δp_Σ = 28 Torr during the injection time. $\boldsymbol{p_\Sigma}$ is optimal as it was determined earlier. Propane combustion in the MW discharge zone maximally rises air temperature in its velocity flow in experimental conditions at this $\boldsymbol{p_\Sigma}$.

Vertical sensitivity in the waveforms is still equals to 10 mV/div. The lower row of waveforms in the set corresponds to y = –6 mm, the forth -to y = 0 mm, and the upper -to y = 6 mm. The last left column in the set consisting of two waveforms corresponds to z = –8 mm, the fifth -to z = 0 mm, and the last right column -to z = 8 mm.

Fig.6.6.3. The measured waveforms $\boldsymbol{T_{stag}}$ in the control crosssection at air injection in the discharge area., p_Σ = 270 Torr. Upper waveforms - $\boldsymbol{T_{stag}}$, lower waveformes –$\boldsymbol{p_c}$

Data set represented in Fig.6.6.3 corresponds to simultaneous detection of two values. Upper waveforms in the figure give recordings of the thermocouple and the lower show $\boldsymbol{p_c}$ pressure variation in the chamber for each point of the plane $\boldsymbol{y-z}$. The Pitot tube is completely let of air stream at $\boldsymbol{p_c}$ detection. Data were obtained at MW discharge burning and additional air (nor propane) injection to the discharge area from the injection line at p_Σ = 270 Torr. It means that results of these experiments correlate with data for $\boldsymbol{p_{stag}}$ represented in Fig.7.6.1. Vertical sensitivity is 2 mV/div for the upper waveforms and it is 10 mV/div for the lower ones. The lower data row in the set in Fig.6.6.3 corresponds to y = –6 mm, the fourth -to y = 0 mm, and the upper -to y = 6 mm. The last left data column corresponds to z = –6 mm, the fourth -to z = 0 mm, and the last right -to z = 6 mm.

Also two waveforms correspond to each the datum in Fig.6.6.4. Here the upper waveform still corresponds to $\boldsymbol{T_{stag}}$ measurement and the lower waveform - to $\boldsymbol{p_c}$ pressure in the chamber. They were obtained at MW discharge burning and propane injection to the discharge area at $\boldsymbol{p_\Sigma}$ = 390 Torr. It means that all the measuring results correlate with $\boldsymbol{p_{stag}}$ data represented in Fig.6.6.2. Vertical sensitivity is 2 mV/div for the upper waveforms, and it is 10mV/div for the lower ones. The lower waveforms in the set correspond to y = –8 mm, their fifth row- to y = 0 mm, and the upper waveforms – to y = 8 mm. The last left data column in the set corresponds to z = –6 mm, the fourth – to z = 0 mm, and the last to the right-to z = 8 mm.

It follows from represented measuring results that stagnation pressure p_{stag} decreases and gas temperature T rises in the wake of the vibrator and energy release zone. Highest absolute changes of these values are observed in the region of the axial line at y ≈ 0 and z ≈ 0.

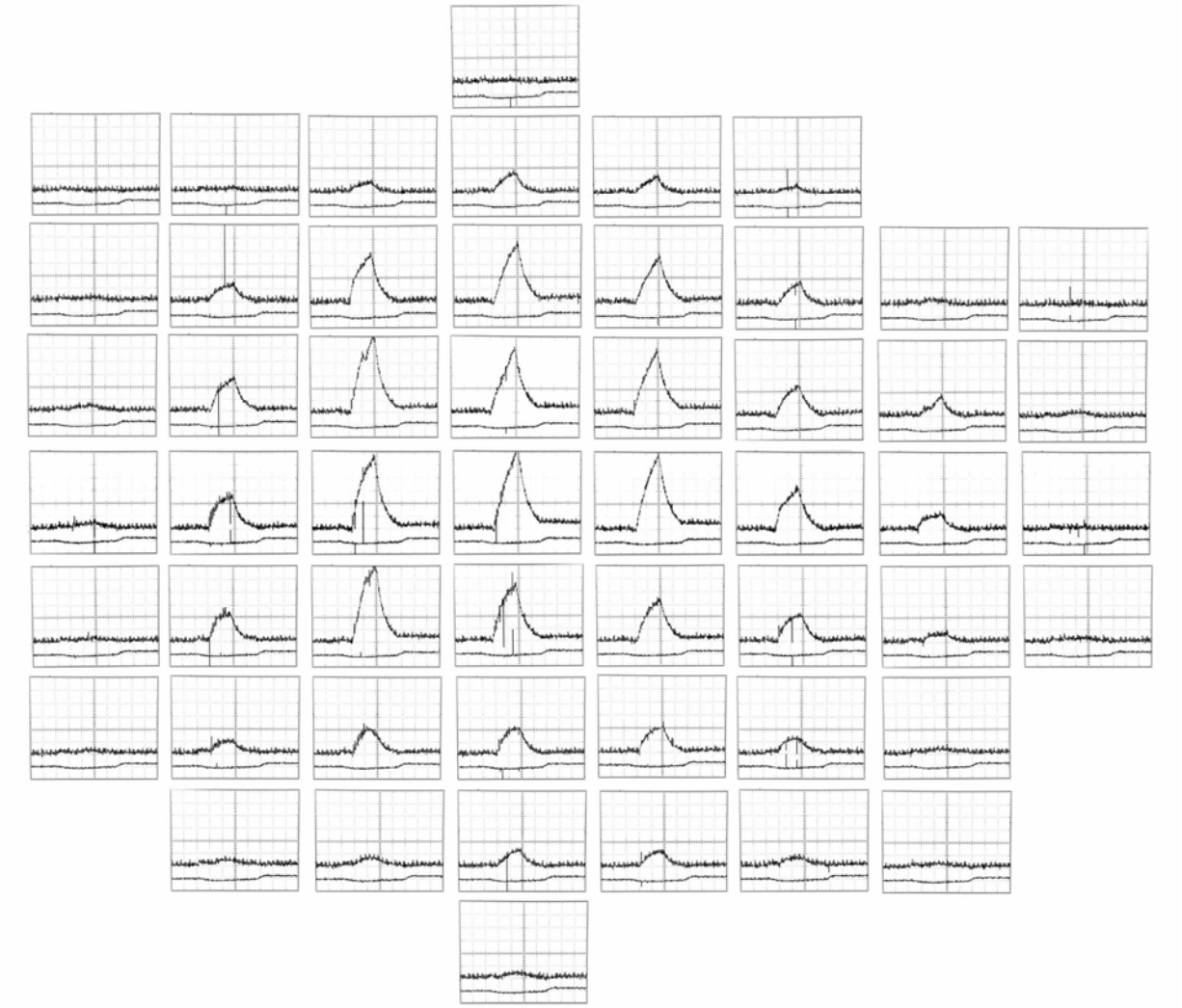

Fig.6.6.4. The measured waveforms T_{stag} in the control crosssection at air-propane mix injection in the discharge area., p_{Σ} = 390 Torr.. Upper waveforms - T_{stag} , lower waveformes – p_c

For example in Fig.6.6.5 we represented T_{stag} dependences along **z** axis at y = 0, they were obtained with a help of experimental data from Fig.6.6.3 and Fig.6.6.4. The lower curve corresponds to burning of only MW discharge, and the upper- to burning of MW discharge and propane combustion. Calculation method is described above in the Report. It accounts both the sensitivity of the thermocouple measurer and the form of the curve detected by it. It follows from the graphs that air heating was detected at the diameter $d_{dis} \approx 12$ mm at only the discharge burning. At that the maximum air temperature increase was 220 K at average increase of its temperature $\Delta T_{dis} = 120$ K. Air heating was detected at the diameter $d_{com} \approx 18$ mm at the discharge burning and propane combustion. At that the maximum air temperature increase was 810 K at average increase of its temperature $\Delta T_{dis+com} = 390$ K. So combusted propane additionally in average increased air temperature for $\Delta T_{com} = 270$ K.

We know from theoretical works that gas velocity in the flow $\mathbf{v_{fl}}$ stays practically constant in the case of isobaric energy supply to the flow. For example in Fig.6.6.6 one can see a graph of $\mathbf{v_{fl}}$ dependence along **z** axis at y = 0, it was made with a help of experimental data for p_{stag} at burning of only MW discharge, i.e. using a data of Fig.6.6.1. Flow Mach number M in required

point was determined with a help of experimental ratio $\boldsymbol{p_{stag}/p_c}$. A temperature in it, which determines local sound velocity value was taken from a graph in Fig.6.6.5. One can see in Fig.6.6.6 that $\mathbf{v_{fl}}$ limits to a value $v_{fl} \approx 500$ m/s characterizing a free stream at radial moving off the vibrator axis, as it should be. $\mathbf{v_{fl}}$ drops down to its minimum value $v_{fl} \approx 230$ m/s in shadow of the vibrator. Using the graph one can estimate average velocity of gas molecules; it is $v_{fl} \approx 340$ m/s at $\boldsymbol{d_{dis}}$ and $v_{fl} \approx 350$ m/s at $\boldsymbol{d_{com}}$.

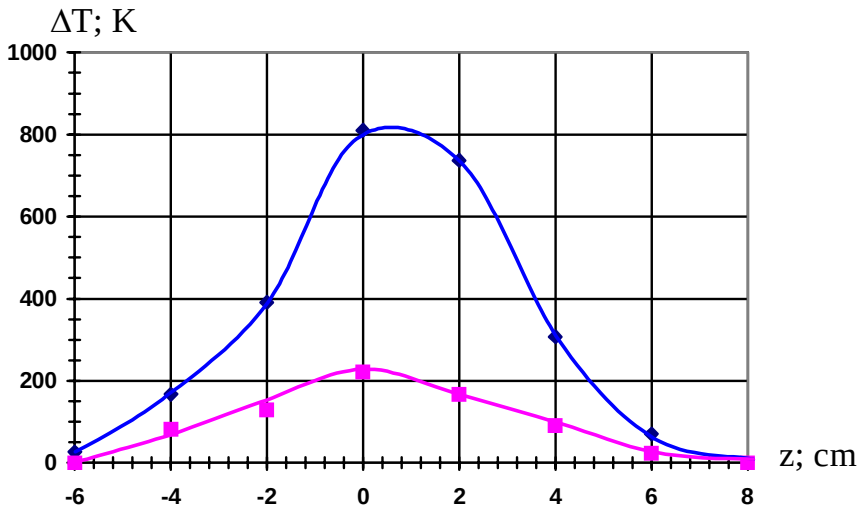

Fig.6.6.5. Dependence $\boldsymbol{T_{stag}}$ (z) at y = 0. The lower curve corresponds to injection of air into discharge, the upper – to air-propane mix injection.

Obtained values allow to estimate a scale of energy power put to heating due to discharge, P_{dis} , and due to propane combustion. In calculations one can use the formulae :

$$P = (7/2)\cdot k\cdot \boldsymbol{\Delta T}\cdot n\cdot S\cdot v;\ W\ . \qquad (6.6.1)$$

Estimated earlier corresponding values of $\boldsymbol{\Delta T}$ in K, $\boldsymbol{S}$ in cm^2, and $\mathbf{v}$ in cm/s are used in this formulae. $k = 1.38\cdot 10^{-23}$ J/K is Boltzmann constant in Eq.(6.6.1), and $\boldsymbol{n}$ in $1/cm^3$ is a concentration of air molecules. It is counted with a help of isobaric condition of processes $p = n\cdot k\cdot T = p_c$ using the corresponding average gas temperature $\boldsymbol{T}$.

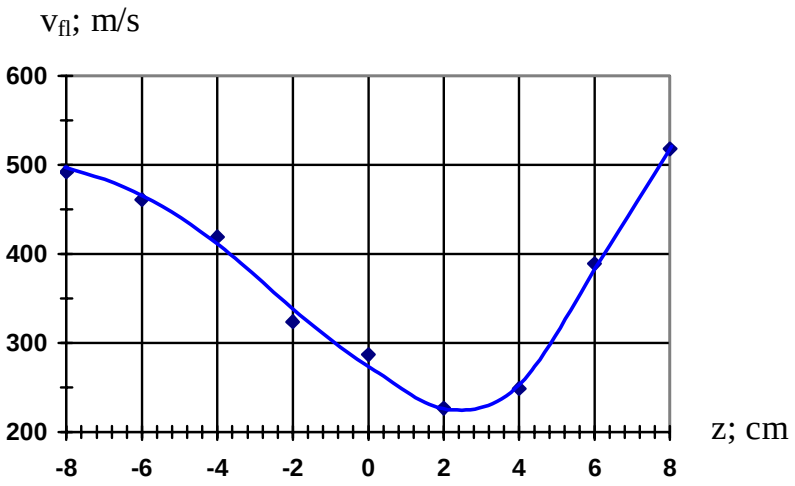

Fig.6.6.6. Dependence $\mathbf{v_{fl}}$ along axis $\boldsymbol{z}$ (y = 0) at burning of MW discharge only

The calculation gives the following scales: $P_{dis} \approx 530$ W and $P_{com} \approx 1.4$ kW. So we put about one third of MW beam of EM waves power to gas heating in the discharge in this

experimental formulation; and about of 50 % of propane injected to the discharge is burned out in the discharge.

7. Measurement results

7.1. Analysis of primary data

In Fig.7.1 one can see results of stagnation pressure and stagnation temperature in a transversal cross of the flow at a distance of 1.4 см from the mixer base cut, they are represented for two cases. The case a) air is injected through the mixer to a discharge area; the case b) – propane-air mixture with optimal relative propane content for given injection conditions is injected to a discharge area. (For units of measurements we use p_1=1 atm, T_1=300 K). A method of real temperature value with accounting of thermocouple time constant is represented in the Report Ref.[2]. Well seen deviation from azimuth symmetry at the foot of stagnation pressure distributions is determined by a mixer mounting influence.

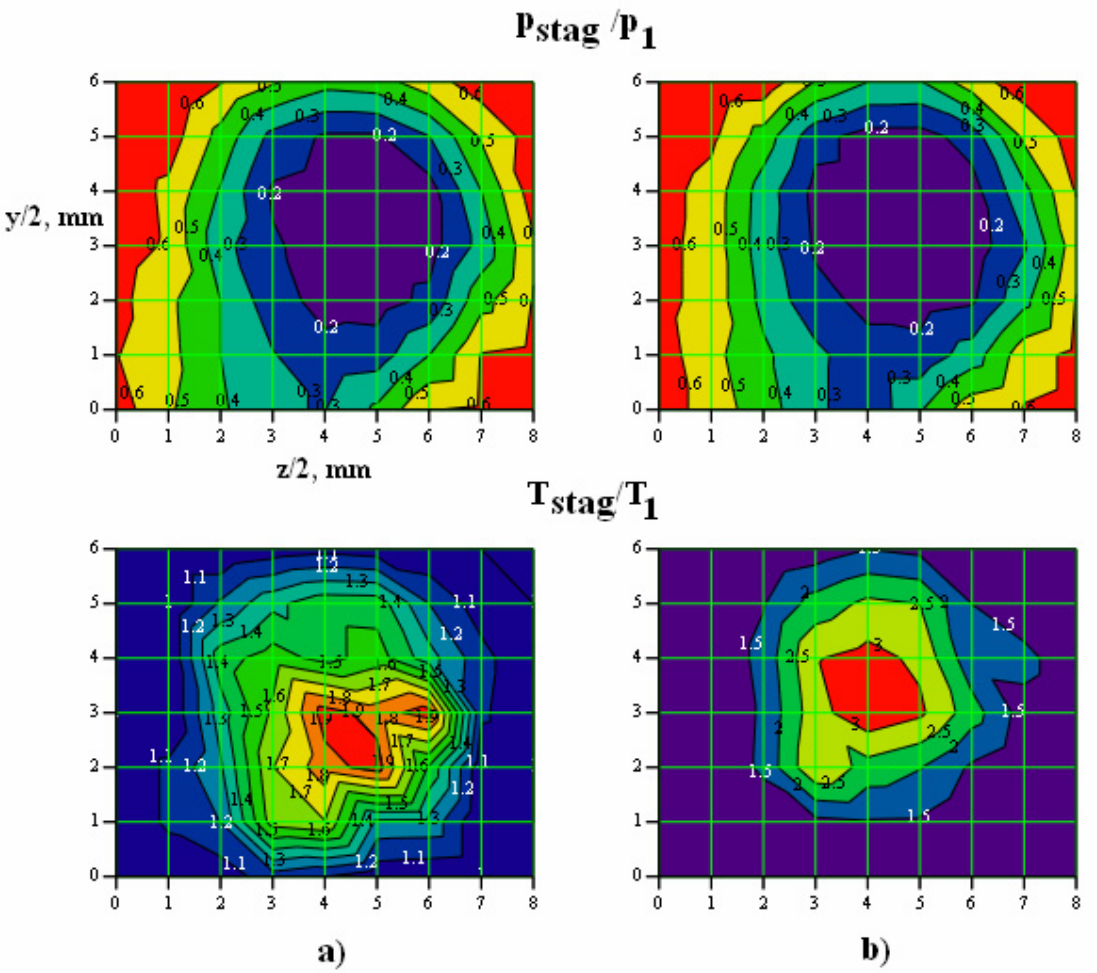

Fig.7.1 Stagnation pressure and stagnation temperature in a transversal cross of the flow at a distance of 1.4 см from the mixer base cut: a) air is injected through the mixer to the discharge area; b) propane-air mixture is injected to the discharge area.

Values of the velocity, density and static temperature could be determined, as it was noted before, Ref.[2], using measured values of stagnation pressure and temperature in a supposition that the static pressure in the submerged stream equals to surrounding gas pressure. An algorithm of calculations is the following. Firstly one determines the Mach number by solution of Rayleigh transcendent equation:

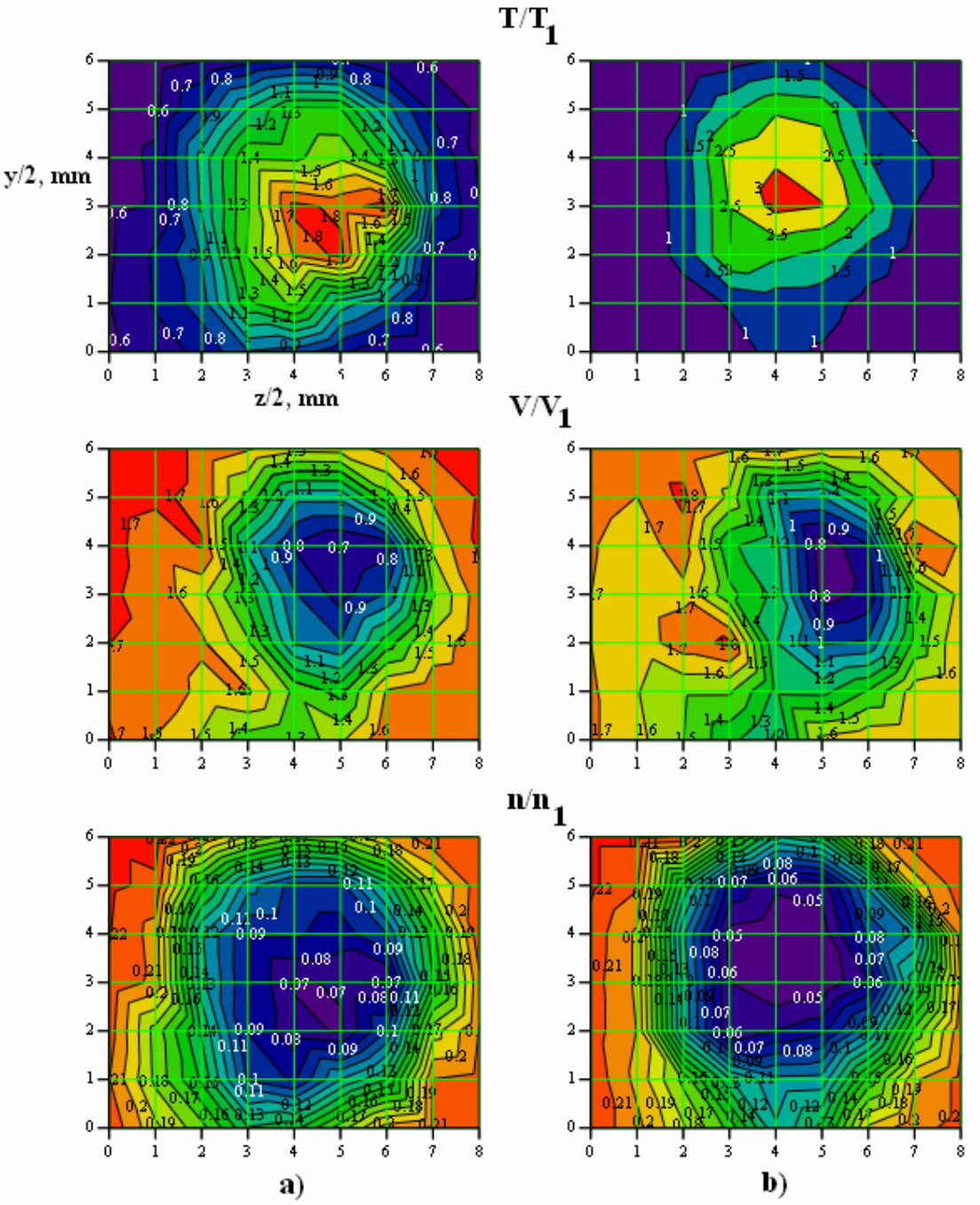

Fig.7.2. Distributions of static temperature, a concentration and a flow velocity calculated with a help of Eq.(7.1) – Eq.(7.5): a) air is injected through the mixer to the discharge area; b propane-air mixture is injected to the discharge area.

$$\left(\frac{\gamma+1}{\gamma}\right)^{\frac{\gamma+1}{\gamma-1}}\cdot\left(\frac{2}{\gamma-1}\right)^{\frac{1}{\gamma-1}}\cdot\frac{M^{\frac{2\gamma}{\gamma-1}}}{\left(\frac{2\cdot\gamma}{\gamma-1}\cdot M^{2}-1\right)^{\frac{1}{\gamma-1}}}=\frac{p_{stag}}{p_{st}}, \tag{7.1}$$

if

$$\frac{p_{stag}}{p_{st}}>\left(\frac{\gamma+1}{2}\right)^{\frac{\gamma}{\gamma-1}},$$

Or in the opposite case

$$M = \sqrt{\left[\left(\frac{p_{stag}}{p_{st}}\right)^{\frac{\gamma-1}{\gamma}} - 1\right] \cdot \frac{2}{\gamma - 1}} \qquad (7.2)$$

(Eq.(7.1)-Eq.(7.2) are shown in Fig.3.11).

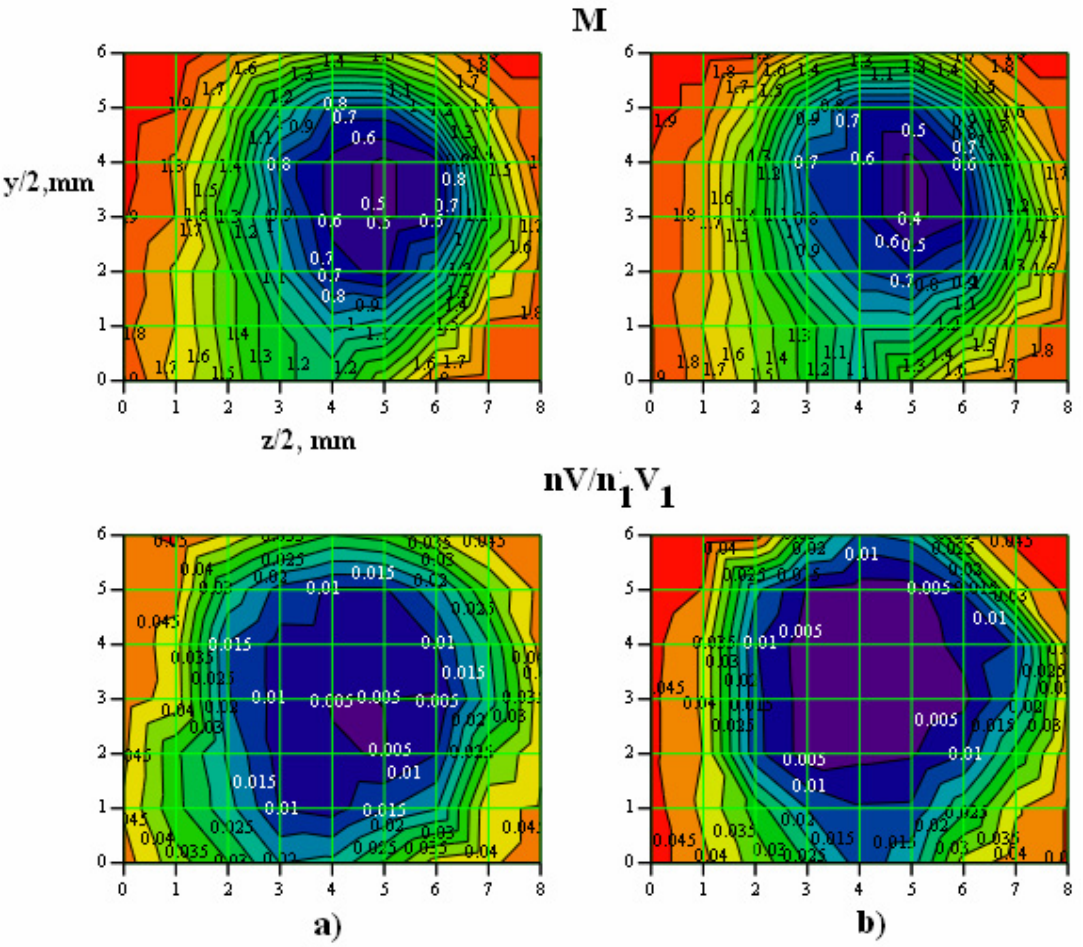

Fig.7.3. Distributions of a Mach number and a mass flow density calculated with a help of Eq.(7.1) – Eq.(7.5): a) air is injected through the mixer to the discharge area; b propane-air mixture is injected to the discharge area.

Then the static temperature is determined using Bernoulli law (at that we suppose that measurements were undertaken in the flow cross section where there is no external heating)

$$T = \frac{T_{stag}}{1 + \frac{\gamma - 1}{2} \cdot M^2} \qquad . \qquad (7.3)$$

A velocity and a density are determined using evident relations

$$V = M \cdot \sqrt{\gamma \cdot T} \qquad (7.4)$$

$$n = \frac{p_{st}}{T} \qquad (7.5)$$

Distributions of static temperature, a concentration and velocity of the flow calculated using Eq.(7.1) – Eq.(7.5) are represented in Fig.7.2. (the value $v1 = (p_1/\rho_1)^{1/2}$ is used as a unit of a velocity). The corresponding distributions of a Mach number and a density of mass flow nV are represented in Fig.7.3.

7.2. A wake structure

The mixer fore part is a truncated cone with a flat fore part with an inlet hole. A radius of a flat part is r_t=2 mm, an inlet hole radius is r_{in}=0.75 mm. A face part of a mixer forms bow shock wave in a supersonic flow with a stand off from the flat part equal to d_{sw}=1.3 r_t=2.6 mm at the Mach number M=1.95. The radius of the inlet hole is substantially smaller than the bow shock wave stand off. This allows to consider that air mass flow rate in the inlet hole is determined by the stagnation pressure of the incident flow and a pressure inside the mixer. An internal channel of the mixer works as a nozzle at an inlet pressure equal to a stagnation pressure and at room temperature. A pressure inside the mixer is certainly smaller than a critical pressure in the inlet hole. So a supersonic air stream is formed inside the mixer behind the inlet hole. Air mass flow rate is equal to $F_a=6.4\cdot10^{21}$ 1/s or 0.3 g/s in indicated conditions.

The inlet nozzle forms a submerged supersonic stream, which set against a tube of propane injection creates a shock wave. A ratio of the distance between the mixer walls and a tube of propane injection and the full cross section is determined by the following relation

$$s = \frac{2}{\pi}\left(\varepsilon^2 \cdot \arccos(\varepsilon) - \varepsilon \cdot \sqrt{1-\varepsilon^2}\right), \qquad (7.6)$$

here **ε** is a ratio of the propane injection tube radius and the mixer internal radius. ε = 0.4 in the applied design, so s = 0.5. A shock wave is formed before a tube of injection at this narrowing of the channel cross section. It drags all the flow in the mixer to the subsonic velocity and it rises a gas temperature to a value close to the stagnation temperature 300 K. A static pressure close to the pressure in the working chamber 105 Topp is maintained at the outlet of the mixer. These data determine a mixture injection velocity from the mixer at known mass flow rate. Propane delivery (or air in the control experiments) to air flow of the mixer through the propane injection tube practically do not change flow gasdynamic characteristics at the outlet from the mixer since a concentration and a mass portion of propane are small. Trivial calculations give a following value of the mixture injection velocity V_{out} = 38 m/s.

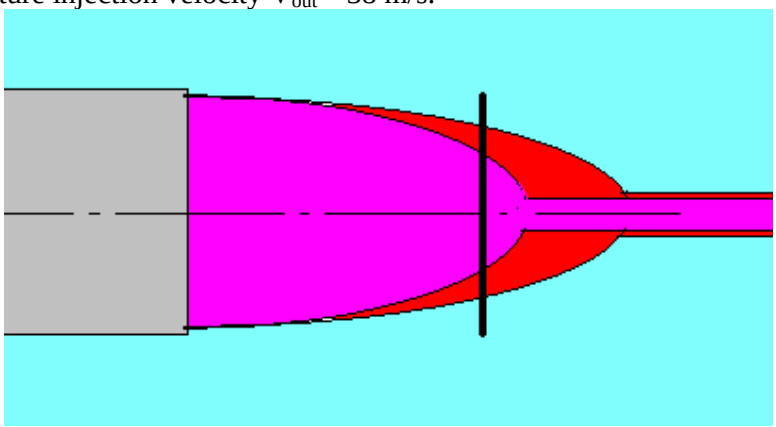

Fig.7.4. Injected gas flow regions after the mixer base: violet color- at air injection, violet and red colors at flammable mixture injection.

Turbulent friction appearing at the boundary separating the supersonic and subsonic flows behind the mixer (in the result of Helmholtz instability) speeds up the subsonic flow forming a structure represented in Fig.7.4. Here a zone of cold supersonic flow is indicated by the bleu color, and by the violet and red colors is indicated a zone of injected mixture for cases of injection of air and propane air mixture at MW discharge presence. A vertical black line indicates a cross section of measurements of stagnation temperature and stagnation. Switching

on of energy release source to a flow at the mixer outlet (due to MW discharge or due to combustion of the mixture) leads to changing of a contact boundary separating cold supersonic and hot subsonic flows

Calculations made using measurement results represented in Fig.7.3 show that integrals of mass flow rates through the measuring area are naturally differ (more than for 5%). This circumstance has to be accounted in energy balance.

7.3. Determination of combustion power

Power putted into a flow in general case can be determined as a difference between integrals of flow energy in a wake at an energy put and without it. An integration area at that has to correspond to the same set of fluid tubes. In other words mass flow integrals have to be the same in the both cases. The measuring area in the measured cross section covers the contact surface in all the cases. This allows to consider that the stagnation temperature equals to initial one 300 K in the periphery part of the measured flow since it corresponds to internal part of the flow, which is not heated. Combustion power of the mixture in this supposition can be determined by the equation

$$P_{burn} = C_p \left(\iint_S n_m V_m T_{stag_m} ds - \iint_S n_a V_a T_{stag_a} ds + \iint_S \left(n_a V_a - n_m V_m \right) T_0 ds \right) \qquad (7.7)$$

Where subscripts **m** and **a** correspond to injection of the mixture and air at switched on discharge. S is a measuring area, T_o = 1. A last term accounts changing of contact surface boundaries.

The formulae Eq.(7.7) can be represented in the form

$$P_{burn} = C_p \left(\iint_S n_m V_m \left(T_{stag_m} - 1 \right) ds - \iint_S n_a V_a \left(T_{stag_a} - 1 \right) ds \right) \qquad (7.8)$$

Analogous argumentations lead us to a conclusion that each of a summand has its own sense in Eq.(7.8). The second summand is a heating power at air injection to a discharge

$$P_a = C_p \left(\iint_S n_a V_a \left(T_{stag_a} - 1 \right) ds \right) \quad , \qquad (7.9)$$

And the first one is a heating power at a mixture injection to a discharge

$$P_m = C_p \left(\iint_S n_m V_m \left(T_{stag_m} - 1 \right) ds \right) \quad . \qquad (8.10)$$

Integration made with using of Eq.(7.8) – Eq.(7.10) with an application of data from Fig.7.2 and Fig.7.3 gave the following values:

P_a = 714 W,

P_m = 1414 W and

P_{burn} = 700 W.

The combustion power is limited by the value 800 W without air admixture from the supersonic flow in which the mixer is located. This can mean that propane-air mixing in the mixer takes place with insufficient quality. By this fact one can explain an exceeding of the stoichiometric value by the optimal portion of injected propane.

The maximum flow temperature in the measuring cross section is 1000 K. Ignition time at this temperature is 0,45 s and it is much greater then the flight time through the discharge area. In spite of it the combustion reaction has enough time to take place. This circumstance can be

reliable evidence of the MW discharge plasma defining role in the combustion process of the gas mixture.

8. Calculations of MW field distribution near vibrator sharpenings

MW electric field distribution was calculated in a vicinity of vibrator base sharpenings. The design of the vibrator is represented in Fig.6.1. The calculation method is described in the work Ref.[4]. Real vibrator was simulated by a set of thin rods located on the cylindrical surface symmetrically with respect to azimuth, they were directed along the cylinder axis coinciding with the axis z. A number of rods equals to a number of sharpenings on a real vibrator. In calculations we accounted influence of reflection current in metallic screen and distributed load of the vibrator by the discharge. The radiation propagates towards the axis y.

Calculation results of electric field amplitude distribution in the cross section $z = z_{end}$ (z_{end} is the coordinate of the initiator metallic base end cross section) are represented in Fig.8.1 and Fig.8.2. Vibrator sharpenings create increase of the field amplitude sufficient for discharge initiation in the mixture delivered through the internal channel of the mixer.

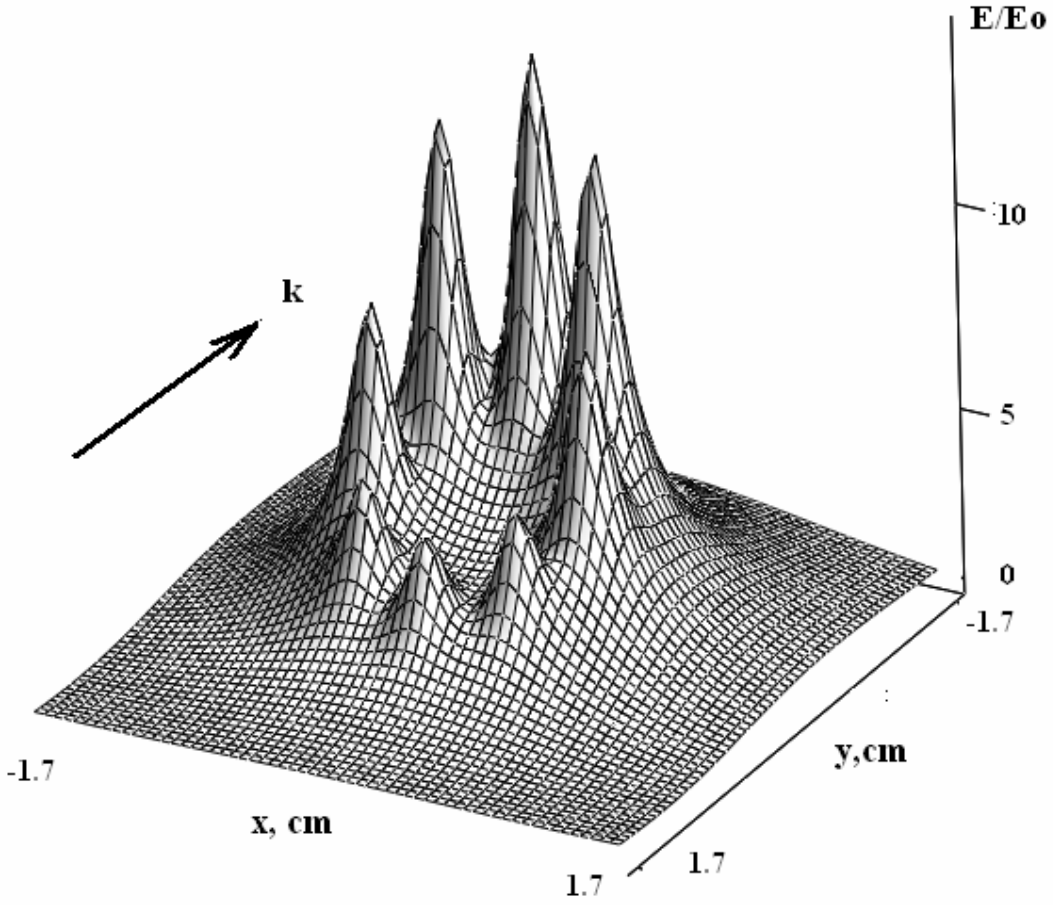

Fig.8.1.Electric field amplitude distribution in the transversal cross section corresponding to the vibrator end with sharpenings.

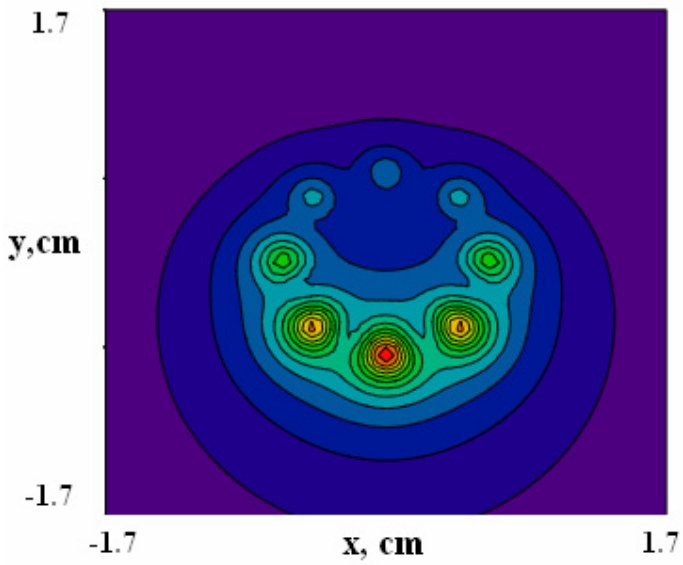

Fig.8.2.Equal level lines of the electric field amplitude in the transversal cross section corresponding to the vibrator end with sharpenings.

Strong non-uniformity of the amplitude distribution over the sharpenings attracts attention. Highest amplitude is realized on the sharpenings most distant from the radiation source. Manifestation of this effect is clearly seen on discharge photos represented in Fig.5.4.2. Asymmetry in greater or smaller extent is revealed in all the discharge photos. The screen presence emphasizes this asymmetry and increases the maximum amplitude at the vibrator end by about two times. At that it insures reliable discharge initiation.

Non uniformity of the amplitude distribution near sharpenings means that the most gas heating power density is realizes in the discharge in the lower part of the injected flow. Rest part is heated due to thermal conductivity and turbulent mixing. This circumstance has to be taken into account at interpretation of experimental results described in section 7 of the report.

9. The elementary model of combustible mix initiation in the mixer

For understanding of processes in the mixer and interpretation of results of supervision it is useful to carry out researches on the elementary model simulating area of the discharge in a aftt of the mixer. As it was specified, the discharge is raised inside the cylindrical chamber along which axis the mix with the known mass fluxes of air and propane proceeds. Pressure upon an output of the mixer is supported at a level of pressure in the system, equal to static pressure in a stream overflowing the mixer. Inside the cylindrical «combustion chamber» of mixer with necessary clauses can be supposed a stream homogeneous and be accepted for modeling one-dimensional stationary approximation. The discharge is simulated by the given area of energy addition (near to the end of a metal part of the vibrator) with known total power. The propane content is near stoichiometric values. The propane and air fluxes correspond to experimental values. The discharge power is varied.

For one-dimensional stationary stream of reacting gas the following ratios are fair

$$\frac{\partial w}{\partial x} = \frac{q(x)}{v_0 \cdot n_0} \tag{9.1}$$

$$\frac{\partial h}{\partial x} = -\frac{h}{\tau(n,T)} \tag{9.2}$$

$$v = \frac{C_p \cdot \left(v_0 + \frac{p_0}{n_0 \cdot v_0}\right) - \sqrt{\left(C_p \cdot \left(v_0 + \frac{p_0}{n_0 \cdot v_0}\right)\right)^2 - 4 \cdot \left(C_p - \frac{1}{2}\right) \cdot (w - h)}}{2 \cdot \left(C_p - \frac{1}{2}\right)} \tag{9.3}$$

$$n = \frac{n_0 \cdot v_0}{v} \tag{9.4}$$

$$T = \left(v_0 + \frac{p_0}{n_0 \cdot v_0}\right) \cdot v - v^2 \tag{9.5}$$

$$p = n \cdot T \tag{9.6}$$

$$w = C_p \cdot T + \frac{v^2}{2} + h \tag{9.7}$$

Here **v, n, T, w, h** - dimensionless speed, density, temperature, thermal function and chemical potential of a mix, Cp - a thermal capacity of a mix at constant pressure.

As units the values are used: for pressure - $\mathbf{p_1}$, for temperatures - $\mathbf{T_1}$ and for density - $\boldsymbol{\rho_1}$ corresponding to a normal atmosphere, for speed - $v_1 = (p_1/\rho_1)^{1/2}$, for distances - r_1 = 1 cm and for time - $t_1 = r_1/v_1$.

Function for characteristic combustion time $\boldsymbol{\tau}$

$$\tau(n,T) = \frac{1.362 \cdot 10^{-10}}{t_1} \cdot \frac{\exp\left(\frac{T_{act}}{T}\right)}{p^{3/2}}, \tag{10.8}$$

where T_{act}= 20000/T_1, is approximation of calculated data published in Ref.[5].

The spatial distribution of specific power of MW discharge is accepted in view

$$q(x) = Q \cdot 2 \cdot \frac{x}{x_h} \cdot \exp\left(-\left(\frac{x}{x_h}\right)^2\right), \quad x>0 \tag{9.9}$$

Coefficient Q is proportional to total power of discharge

$$Q = \frac{P_W \cdot 10^7 \cdot t_1}{p_1 \cdot \pi \cdot a_{out}{}^2 \cdot x_h \cdot r_1} \tag{9.10}$$

P_W –total power of discharge, W, a_{out} = 0.4 cm – outlet radius of the mixer.

Parameters of the task are outlet boundary values:
p_0 = 0.138, T_0 = 1, n_0 = 0.138, v_0 = 0.131, corresponding to experimental values, described in chapters 7 and 8. The value of total power P_W is varied..

The modeling results are presented in Fig.9.1.

Modeling has shown:

- The mix has burned in boundaries of calculation zone (1 cm), if power P, including into discharge, is more 350 W.
- At that case combustion power is 600 W, which is lower measured value (700 Вт).
- Static pressure and stagnation pressure are changed insignificantly, being on the level of static pressure of external flow.
- Velocity of the burned mix is equal (or more a little) to velocity of external flow, overflowing the mixer.

- Mach number of burned mix is less than 0,5

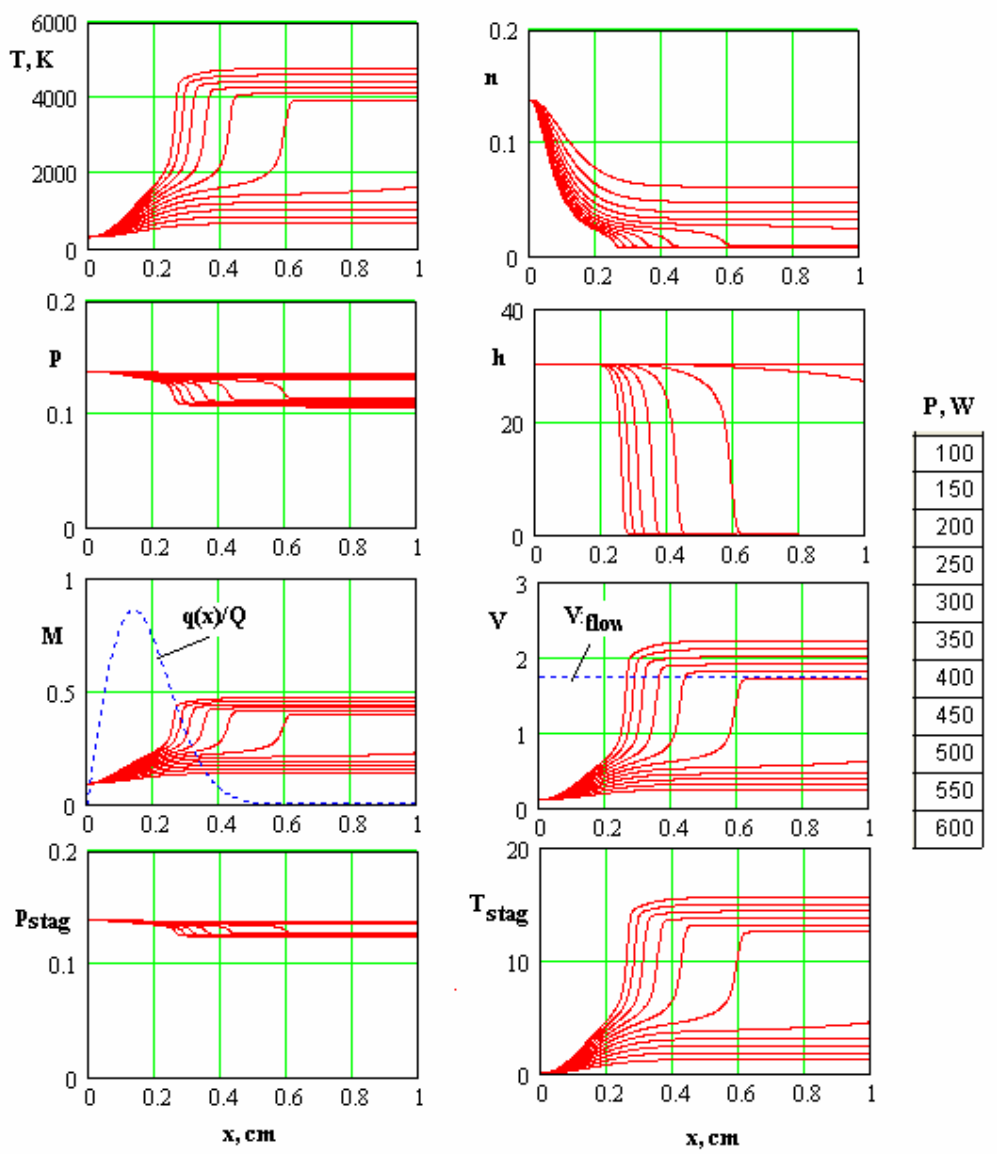

Fig.9.1. The mix temperature **T**, density **n**, static pressure **p**, chemical potential **h**, Mach number **M**, flow velocity **V**, stagnation pressure $\mathbf{p}_{stag}$ and stagnation temperature $\mathbf{T}_{stag}$ in dependence on distance **x** at different values of total power **P**, including into discharge.

Comparison of the obtained modeling results to the data of processing of the measurement results (chapters 7 and 8) allows to draw a conclusion that in trail behind the mixer aft the addition of air from external stream in the trail takes place, providing additional combustion of superfluous (in relation to stoichiometric values) quantities of propane.

10. Conclusions

Works reflected in the present Report close investigation cycle made in frames of three year ICTS Project №2429p with the title “Investigations of flammable gas mixture ignition possibility with a help of undercritical microwave streamer gas discharge”. These works were carried out from August 2002 till July 2005. In Conclusions we will in short enumerate results of first two stages of these works and in details we will describe scientific results obtained in a course of works during final reported third stage.

In frames of the present Report we investigated properties of deeply undercritical microwave (MW) discharge in quasi optical beam of electromagnetic (EM) radiation of centimeter range of wavelength λ.. The discharge was realized in air at comparably high pressure p values of hundreds Torr. We used exclusive means of MW discharge initiation in EM field with initial level of its electrical component E_0 by ten or hundred times smaller than the critical breakdown level E_{cr}. The discharge is initiated by linear electrical "antenna" vibrator. in the discharge is realized in a streamer form in indicated range of pressure p and E_0, and its streamer channel are attached to an initiator during a whole time of EM radiation existence.

We showed in works executed during the stage that plasma channels of this discharge can be low temperature and high temperature as well. We experimentally determined typical times of physical processes development that determine high temperature quality of the discharge plasma. At that we mostly used a method of flammable propane-air mixture ignition by this discharge. Obtained results allow to develop adequate models of high temperature streamer deeply undercritical MW discharge.

Physical principles were developed in executed works; they allow to ignite this MW discharge in high-speed air flow including SS flow velocities. At that applied comparably thin linear electrical vibrator is weakly disturbing initial gas flow. It was experimentally shown that the discharge plasma is high-temperature also at MW discharge ignition in SS flow. This plasma is capable to ignite propane-air flammable mixture. Propane during experiments of first two stages was injected to SS flow through internal area of "thin" vibrator initiating the discharge to the vibrator base part. MW discharge was burning in this area then propane –air mixing took place. Created flammable mixture ignition and its combustion took place.

Obvious determination method of EM field energy (that excites the discharge) efficiency put and propane burn-out level in air high-speed flow was developed during the second stage of these works. It uses spatial distributions of flow stagnation pressure p_{stag} and flow stagnation temperature O T_{stag} in a wake of discharge burning area and combustion area of the flammable mixture. A corresponding theoretical analysis of experimental p_{stag} and T_{stag} distributions showed that about of 10% of EM beam (exciting the discharge) energy can be putted to air (flowing around the initiator) heating. It also showed high efficiency of burning out of propane injected to the discharge area.

At the same time we did not succeed in experimental formulation of pure propane amount combustion control at it injection directly to the discharge area. Combustion power P_{com} firstly rose with increase of its injection rate, and then it was stabilized at comparably low level. In these experiments we managed to realize maximum propane combustion power P_{com} only of 100-200 W.

Following main results were obtained during third stage.

We experimentally have determined resonance features of unique "thick" electrical antenna vibrators. It was shown that these properties are manifested at first resonance mode at vibrator's length $2L \leq \lambda/2$ only at vibrator diameter $2a$ and λ ratio smaller than 0.1: $2a/\lambda < 0.1$. These results were compared with numerical experiment results obtained with a help of specially developed theoretical model.

Deeply undercritical MW discharge was realized with an application of thick tube-type electrical initiating vibrators in SS air flow. The discharge burns in a base area of this vibrator. We experimentally demonstrated experimental possibility of required gasdynamic vibrator shaping in SS flow with an application of radio transparent nose and bas nozzles. At that the vibrator feature to initiate a discharge is conserved.

We experimentally determined that undercritical MW discharge burns at initial flow velocity of v_{fl} = 500 m/s (corresponding to the Mach number M = 2) over the whole initiator perimeter only at its diameter $2a \leq 6$ mm. We experimentally selected a geometry of a vibrator base end that allowed to realize relatively uniform zone of MW discharge in transversal direction to air flow at $2a \leq 12$ mm. Experiments showed that the transversal size of uniform discharge area does not exceed 10 mm in the given experimental formulation.

We have developed a design of a vibrator initiating MW discharge that allows realizing in the vibrator internal region a preliminary air and propane mixing to the flammable mixture with required proportion of propane. At that air comes to a mixing zone directly from SS air flow.

Developed design allowed to effectively combust preliminary prepared flammable mixture in the plasma area of MW discharge. Combustion efficiency was insured by dielectric "combustion chamber" presence in the vibrator base area. Experimentally we demonstrated a possibility to vary an amount of effectively combusted propane in sufficiently wide range. Obtained spatial p_{stag} and T_{stag} distributions in energy release wake and their corresponding analysis showed that it is in principle possible to set a required combustion power in this experimental formulation. We managed to realize total energy release power higher than 1 kW.

Detected length of propane-air combusting area and measured flow velocity spatial distribution allow to suppose that hard optical radiation of deeply undercritical MW discharge plays a vital part in physical processes governing propane combustion velocity in air.

Three year cycle of fundamental investigations of plasma dynamic processes with microwave discharge participation showed availability of principally new scientific direction that blends together electrodynamics, physics of electrical gas discharge and combustion physics.

Investigations in this direction can be continued with a help of modernized set up with an application of additional and already developed diagnostic means.

Main tasks of the set up modernizing are:

- Realization of propane-air flammable mixture SS submerged stream of round cross section.
- Realization of SS submerged stream with "flat" geometry.
- Realization of fan-type quasi-optical beam of EM waves for feeding of multi vibrator initiation system.
- Realization of SS air flow with higher temperature.

To main supposed additional diagnostic means we can attribute an equipment for high-speed frame by frame photo detection with exposure time up 10^{-7} s and shadow method of gasdynamic processes recording.

In the result we can execute experiments, which schemes are conditionally represented in Fig.10.1, and we expect the following results:

- Spatial and temporary structure of deeply undercritical initiated MW discharge in SS flow will be determined.
- Influence of deeply undercritical MW discharge plasma on propane-air mixture combustion with respect to its propagation velocity over a plasma area will be investigated.
- Influence of deeply undercritical MW discharge plasma in high-speed propane-air flammable mixture on concentration ignition limits will be determined.
- Influence of deeply undercritical MW discharge plasma on combustion completeness of propane-air mixture with respect to its over a plasma area will be investigated.
- Flame propagation velocity over high-speed flow of propane – air mixture at its ignition by deeply undercritical MW discharge.
- Resonance excitation capability of linear electrical vibrator by fan-type beam of EM radiation will be studied.
- Mutual electrodynamic influence of initiating vibrators system when MW undercritical MW discharges burn in their base areas will be studied.
- A possibility of propane-air flammable mixture spatially-multiple ignition with a help of a system of electrodynamically connected deeply undercritical discharges initiated by vibrators will be determined.
- Control experiment on switching on of initiated deeply undercritical MW discharge in high temperature submerged SS air stream will be undertaken.

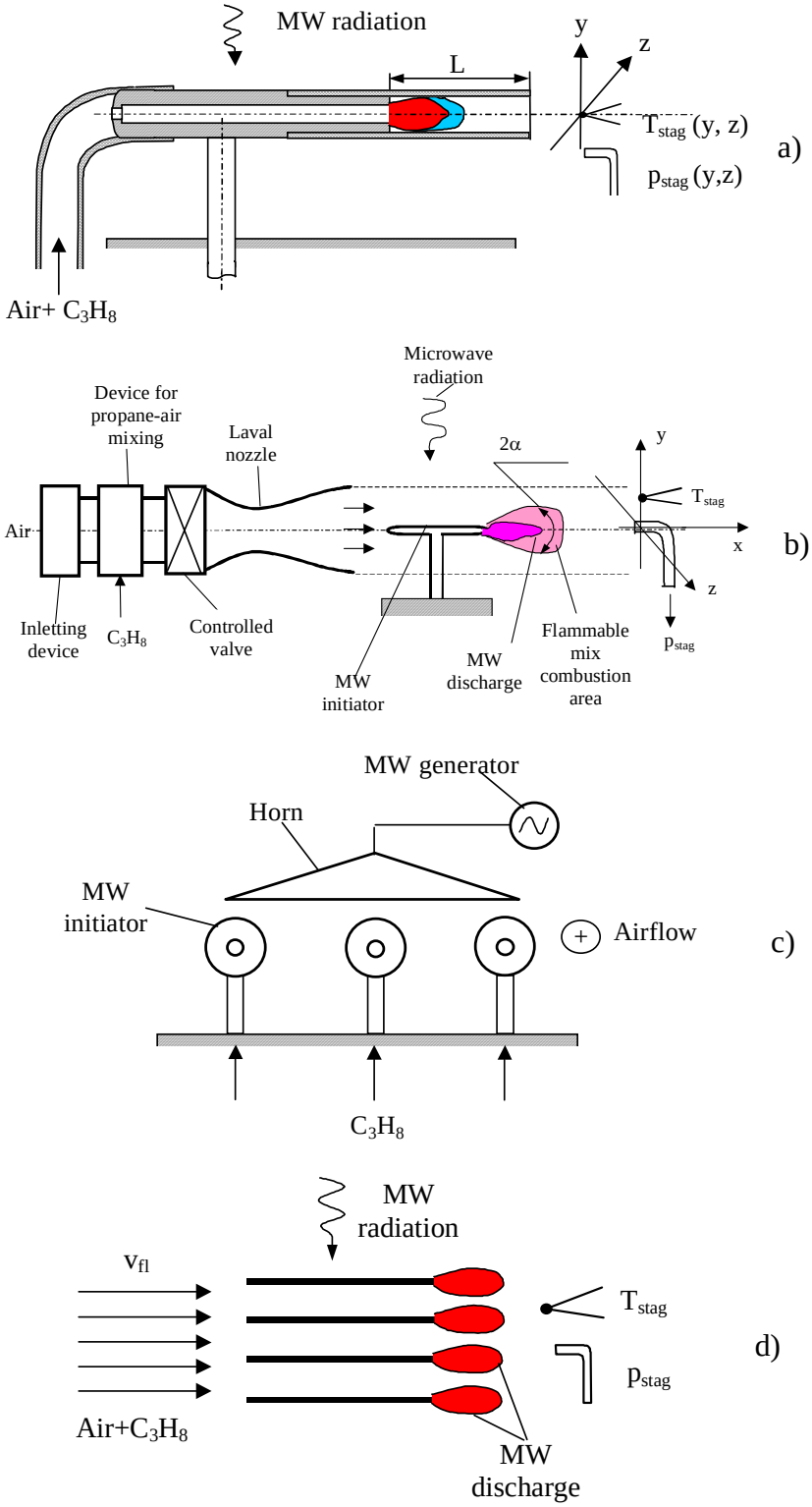

Fig.10.1. Schemes of planned experiments

Enumerated information will allow determining real prospective of gas mixtures combustion modes optimization with a help of MW discharge technology in wide range of conditions.

List of illustrations

References

1 *The study of possibility of ignition of a combustible gas mix by the undercritical СВЧ streamer discharge*. Annual Technical Report on Project ISTC #2429. 2003.

2 *The study of possibility of ignition of a combustible gas mix by the undercritical СВЧ streamer discharge*. Annual Technical Report on Project ISTC #2429. 2004.

3. *Investigation of the possibility of the application of the under-critical microwave streamer gas discharge for the ignition of a fuel in the jet engine*. Annual Technical Report on Project ISTC #1840p. 2001.

4 Kirill V. Khodataev. *The physical basis of the high ability of the streamer MW discharge to a resonant absorption of MW radiation*. 42nd AIAA Aerospace Sciences Meeting 5-8 January 2004, Reno, NV. Paper AIAA-2004-0180.

5. M.V.Petrova, B.Varatharjan and F.A.Williams. *Theory of propane autoignition*. 42nd AIAA Aerospace Sciences Meeting 5-8 January 2004, Reno, NV. Paper AIAA-2004 -1325